

Role of protein-protein interactions on protein aggregation and emulsion flocculation

Roy J.B.M. Delahaije

Thesis committee

Promotor

Prof. Dr H. Gruppen
Professor of Food Chemistry
Wageningen University

Co-promotor

Dr P.A. Wierenga
Assistant Professor, Laboratory of Food Chemistry
Wageningen University

Other members

Dr K. Broersen, University of Twente, The Netherlands
Prof. Dr S.D. Stoyanov, Wageningen University & Unilever R&D Vlaardingen
Prof. Dr E. van der Linden, Wageningen University
Dr T.J. Wooster, Nestlé Research Center, Switzerland

This research was conducted under the auspices of the Graduate School VLAG (Advanced studies in Food Technology, Agrobiotechnology, Nutrition and Health Sciences).

Role of protein-protein interactions on protein aggregation and emulsion flocculation

Roy J.B.M. Delahaije

Thesis

submitted in fulfilment of the requirements for the degree of doctor
at Wageningen University
by the authority of the Rector Magnificus
Prof. Dr M.J. Kropff,
in the presence of the
Thesis Committee appointed by the Academic Board
to be defended in public
on Friday 19 September 2014
at 1.30 p.m. in the Aula.

Roy J.B.M. Delahaije

Role of protein-protein interactions on protein aggregation and emulsion flocculation

166 pages

PhD thesis, Wageningen University, Wageningen, NL (2014)

With references, with summaries in English and Dutch

ISBN: 978-94-6257-005-4

Abstract

In this thesis, the effect of molecular properties on the aggregation and flocculation behaviour is studied. The aggregation behaviour was thought to be mainly affected by the structural stability of the protein. A decreased structural stability results in unfolded proteins which are more prone to aggregation. The flocculation behaviour was shown to be affected by the adsorbed amount at saturation and the adsorption rate. These parameters have been combined in a surface coverage model, which describes the stabilization of emulsions away from the iso-electric point (pI) to be affected by excess protein in the continuous phase. In addition, a model was proposed for the prediction of the adsorbed amount at saturation. This is influenced by the protein charge and radius and system conditions (i.e. pH and ionic strength). The adsorption rate, which is a measure for the affinity of the protein towards the adsorption to the interface, was shown to increase with increasing relative exposed hydrophobicity and a decrease of the electrostatic repulsion (i.e. decrease of ionic strength or the protein charge). Close to the pI, the applicability of protein-stabilized emulsions is limited. Hence, a steric interaction was introduced to stabilize the emulsion. It was shown that glycation of the protein with a trisaccharide was sufficient to sterically stabilize the emulsions against pH-induced flocculation.

Table of contents

Abstract		
Chapter 1	General introduction	1
Chapter 2	Comparison of heat-induced aggregation of globular proteins	17
Chapter 3	Protein concentration and protein exposed hydrophobicity as dominant parameters determining flocculation of protein-stabilized oil-in-water emulsions	35
Chapter 4	Effect of glycation on the flocculation behaviour of protein-stabilized oil-in-water emulsions	55
Chapter 5	Improved emulsion stability by succinylation of patatin is caused by partial unfolding rather than charge effects	73
Chapter 6	Quantitative description of the parameters affecting the adsorption behaviour of globular proteins	95
Chapter 7	Quantitative description of the parameters resulting in stability of protein-stabilized emulsions	113
Chapter 8	General discussion	127
Summary		141
Samenvatting		145
Acknowledgements		149
About the author		153

Chapter 1

General introduction

Protein-protein interactions play an important role in biological systems (e.g. formation of amyloid fibrils associated with diseases like Alzheimer's disease)¹⁻³ as well as food systems (e.g. desired clustering of proteins for texture formation)⁴. In such systems, protein aggregation is typically described based on the balance between attractive and repulsive interactions between the proteins. Similar to protein aggregation, protein-protein interactions are also of importance for the flocculation of emulsion droplets which are stabilized by adsorbed protein layers⁵. Qualitatively, the interactions between protein molecules in the continuous phase (i.e. protein aggregation) and between adsorbed protein layers at the oil-water interface (i.e. emulsion flocculation) have been described extensively under different system parameters (e.g. pH, I, T)^{6, 7}. Quantitatively, however, the interactions and the importance of the various parameters have not been studied in detail. Lack of knowledge about the importance of the various parameters makes it difficult to control the interactions and compare the functionality of different proteins. Moreover, most studies generally focussed on a single protein, in one state (i.e. in the continuous phase or adsorbed at the interface) at different system parameters. Therefore, there is little information on how the existing knowledge can be extrapolated to different proteins (e.g. novel protein sources) and how the behaviour of bulk proteins relates to that of adsorbed protein layers.

The present work focuses on a description of the effect of (system) parameters and protein properties on the interactions between the protein molecules. It aims to compare the role of these parameters on the aggregation of proteins and the flocculation of protein-stabilised emulsion droplets. This will provide insights in the key parameters determining the protein-protein interactions and the correlation between the behaviour of proteins in the bulk and at the interface. Moreover, it will enable control over the interactions, which may for instance be achieved by directed modification of the proteins (e.g. glycation).

Protein aggregation

Protein aggregation is a process in which proteins cluster as a result of an attractive interaction between the protein molecules which dominates the repulsive forces. The origin of this increased attractive interaction can, for instance, be an opposite surface charge of the protein molecules involved⁸⁻¹⁰, charge anisotropy¹¹⁻¹³ or (partial) unfolding and the consequent exposure of hydrophobic amino acid residues^{2, 14, 15}. In the case of heat-induced aggregation of a system of only one type of protein, aggregation is caused by an increase of the hydrophobic attraction due to the exposure of hydrophobic amino acids.

A schematic overview of heat-induced aggregation, which involves (partial) unfolded protein as intermediates in the aggregation process, has been proposed by Lumry and Eyring¹⁶ (figure 1A). The transitions and equilibria between the different states (native,

unfolded, refolded and aggregated) depend on the structural stability of the protein and system conditions (e.g. pH and T). After unfolding, the (partially) unfolded protein can either refold or irreversibly aggregate. In the case of aggregation, the (partially) unfolded protein aggregates with another (partially) unfolded protein (figure 1B, number 1), or with an already formed aggregate (figure 1B, number 2). Furthermore, aggregated proteins can also aggregate with other aggregates (figure 1B, number 3).

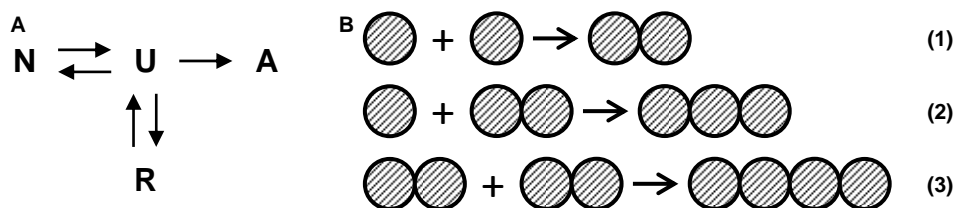


Figure 1. Schematic overview of the (ir)reversible transitions in heat-induced protein unfolding and aggregation (A) and a schematic overview of first steps of protein aggregation (B). N, U, R and A in figure A represent the native, (partially) unfolded, refolded and aggregated protein, respectively.

For the description of the aggregation behaviour of globular proteins, studies typically focus on (1) the aggregation kinetics (rate and order) and/or (2) the aggregate properties (size and structure).

Aggregation rate and order

Generally, the aggregation rate and order are determined from the decrease of native, non-aggregated protein in time. This decrease is affected by two parameters; (1) the equilibrium between native and unfolded protein and (2) the consequent aggregation of non-aggregated protein (figure 1B, numbers 1 and 2)¹⁷. Both processes are affected by the temperature, pH and ionic strength. In diluted systems, the protein concentration only influences the aggregation step.

Temperature has been described to be the dominant parameter affecting the decay of non-aggregated protein and thereby the aggregation rate¹⁸⁻²¹. Protein unfolding is considered to be fast compared to the subsequent aggregation step. Therefore, this effect of temperature is explained based on the equilibrium between native (folded) protein and unfolded protein. At increased temperatures, this equilibrium shifts towards the unfolded protein^{2, 22}. As a consequence, the probability that two unfolded proteins meet increases, resulting in faster aggregation. In addition, the diffusion of proteins, which is described by the Stokes-Einstein equation (equation 1)²³, also increases with increasing temperature (i.e. increase of $\pm 8.5\%$ from 70 to 75 °C). This results in an increased probability for different molecules to meet, collide and aggregate^{14, 24}. In contrast to the aggregation rate, the reaction order is not influenced by temperature^{18, 25}.

$$D = \frac{k_B T}{6\pi\eta R} \quad (1)$$

in which D is the diffusion coefficient [$\text{m}^2 \text{s}^{-1}$], k_B is Boltzmann's constant [$1.38 \times 10^{-23} \text{ J K}^{-1}$], T is the absolute temperature [K], η is the viscosity of the solution [Pa s] and R is the radius of the protein molecule [m].

Besides temperature, pH and ionic strength also influence the aggregation rate and order. This has been ascribed to their effect on the electrostatic repulsion within and between the protein molecules¹⁷. A decrease of the electrostatic repulsion results in stabilization of the protein structure due to more intramolecular interactions. At the same time, the lower repulsion promotes the formation of intermolecular bonds (i.e. aggregation)²⁶⁻²⁸. These two processes do not affect all proteins similarly. The aggregation rate of β -lactoglobulin for instance increases with ionic strength, whereas that of ovalbumin is not affected at all^{18, 29}. In addition to the effect on the electrostatic repulsion, a decrease of the pH has been described to be accompanied by an decrease of the reactivity of disulphide bonds^{27, 30}. The combined effect of the electrostatic repulsion and the reactivity of the disulphide bonds resulted in a lower aggregation rate of β -lactoglobulin with decreasing pH¹⁹.

Another factor which may affect the aggregation rate is the protein concentration. An increase of the number of protein molecules in a constant volume increases the likelihood for collisions. In contrast to the expectations, the effect of protein concentration also varies among proteins. Whereas the aggregation rate of β -lactoglobulin increases with increasing concentration, the aggregation of ovalbumin is not affected by temperature. This is attributed to the monomer-dimer equilibrium for β -lactoglobulin. In contrast to the aggregation rate, the aggregation order is concentration independent for all proteins^{18, 25}.

Aggregate size and structure

In addition to the aggregation kinetics derived from the decrease of non-aggregated protein in time, protein aggregation is also described by the size and structure of the formed aggregates. These are typically determined from the angular dependence of the scattered intensity (e.g. light and neutron scattering). Some systems with different aggregation kinetics may still result in similar aggregates, showing that the aggregation kinetics do not relate to the size and structure of the aggregates. This is explained by the fact that the aggregate formation only depends on the attraction and repulsion between the proteins, whereas the aggregation kinetics are also affected by protein unfolding. Theoretically, the growth kinetics can be derived from the increase of the aggregate size in time. This has been qualitatively applied to show that the size of the aggregates increases with increasing heating time³¹, but the growth kinetics have not been quantitatively determined.

Temperature affects the aggregation rate, while it does not influence the aggregate formation^{20, 21}. This shows the purely kinetic effect of temperature on the aggregation behaviour.

In contrast to temperature, electrostatic repulsion does affect the aggregate size and structure. As indication for the aggregate structure, the fractal dimension is used. At conditions with high electrostatic repulsion (i.e. low ionic strength and pH far from the iso-electric point (pI)), the repulsion between the protein molecules results in the formation of small, linear aggregates (e.g. ovalbumin aggregates with a fractal dimension of 1.7) (figure 2)^{32, 33}. When the electrostatic repulsion is decreased (i.e. at high ionic strength), different proteins (i.e. ovalbumin^{34, 35}, β -lactoglobulin^{30, 36}, BSA³⁷ and patatin³⁸) were observed to form larger aggregates than at low ionic strength. Moreover, the structure of these aggregates was more branched compared to the aggregates formed at low ionic strength (i.e. fractal dimension of 2.0 at 100 mM for β -lactoglobulin and ovalbumin)^{31, 33, 39}. Close to the pI, the low electrostatic repulsion leads to the formation of even larger, denser aggregates with a fractal dimension approaching 3.0 (i.e. compact spheres)¹¹.

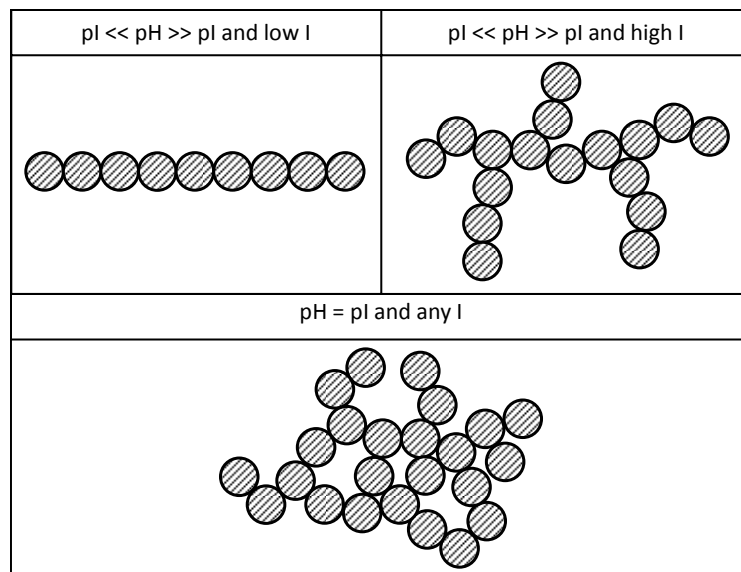


Figure 2. Schematic overview of the effect of electrostatic repulsion on the aggregate size and structure.

The aggregate structure of β -lactoglobulin has been described to be independent of the concentration (i.e. fractal dimension of 2.0 at pH 7, 100-150 mM, 70-80 °C and 0.4-110 g L⁻¹ for β -lactoglobulin)^{21, 39}. The aggregate size, on the other hand, increases with increasing concentration^{20, 40, 41}. In addition, disulphide bond formation has been described to be important for the morphology of ovalbumin aggregates (i.e. from a linear, fibrillar

aggregate to a highly branched, random aggregate with increasing number of reactive sulfhydryl groups)⁴².

Emulsion flocculation

Flocculation of emulsion droplets is, similar to protein aggregation, a process of clustering. It is also caused by the fact that attractive interactions (e.g. van der Waals and hydrophobic) dominate over the repulsive interactions (e.g. electrostatic). Another cause for flocculation are external factors, not related to the (adsorbed) protein (e.g. depletion effect by other molecules)^{7, 43-45}. The external factors, which for instance include depletion flocculation by a polysaccharide, are generally not important for pure protein-stabilized emulsions. In contrast to protein aggregation in the continuous phase, the interactions resulting in emulsion flocculation are due to the adsorbed protein layers at the oil-water interface rather than the proteins in the bulk.

The description of the flocculation behaviour of protein-stabilized emulsion can, in contrast to aggregation, not be based on the decrease of non-flocculated droplets in time. Therefore, flocculation is described by the formation of aggregated droplets (i.e. an increase of the droplet size).

Interactions affecting emulsion flocculation

The main cause for flocculation is the domination of attractive interactions (i.e. van der Waals, hydrophobic) between the adsorbed protein layers over the repulsive interactions (i.e. electrostatic and steric)^{45, 46}. The balance between the attractive and repulsive interactions is determined by the adsorbed layer (e.g. pI of the protein and layer thickness) and the system parameters (e.g. pH and I).

In general terms, ionic strength and pH influence the electrostatic repulsion between the emulsion droplets. At high electrostatic repulsion (i.e. pH far from the pI and low ionic strength), the repulsion between the droplets is sufficient to limit flocculation. With decreasing electrostatic repulsion (i.e. pH approaching the pI and increasing ionic strength), the strength and range of the repulsive interactions decrease and the attractive interactions may dominate, resulting in flocculation^{7, 47}. This is generally described with a barrier which, within relevant time scales, demarcates a system stable against flocculation from a system unstable against flocculation.

The exposure of hydrophobic amino acid residues, originating from (partial) unfolding of the protein after adsorption to the interface, has been described to increase the hydrophobic attraction between the droplets^{47, 48}. This increase was postulated to promote flocculation. In general, however, the hydrophobic residues of a protein are thought to arrange towards the oil rather than the water phase. Thereby, it prevents an increase of the hydrophobic attraction between the adsorbed layers.

Steric repulsion has also been described to increase the stability of protein-stabilized emulsions against flocculation⁴⁹. However, it must be noted that a typical adsorbed protein layer has a thickness of only several nanometers⁴⁹. Hence, steric repulsion seems of less importance for the flocculation behaviour of emulsions stabilized by a protein. Protein polysaccharide-complexes^{49, 50} or multilayer adsorption of proteins with oppositely charged polysaccharides^{51, 52}, on the other hand, result in thicker adsorbed layers (> 5-10 nm) which can stabilize emulsions against flocculation.

Theoretical description of protein-protein aggregation

Theoretically, protein aggregation and emulsion flocculation are qualitatively described by the combination of a repulsive electrostatic interaction (U_e) and an attractive van der Waals (U_{vdW}) interaction as described in the DLVO theory (equation 2)^{48, 53, 54}. A representative curve of the electrostatic, van der Waals and total interaction energies (U_{tot}) with the secondary minimum (S), primary maximum (P') and primary minimum (P) between two emulsion droplets with a radius of 1 μm far from the iso-electric point (pI) and at high ionic strength (i.e. 100 mM) is shown in figure 3A.

$$U_{tot}(h) = U_{vdW}(h) + U_e(h) \quad (2)$$

The van der Waals and electrostatic interactions are generally described by equations 3 and 4⁵⁵, respectively.

$$U_{vdW}(h) = -\frac{A}{6} \left(\frac{2R_1R_2}{(2R_1 + 2R_2 + h)h} + \frac{2R_1R_2}{(2R_1 + h)(2R_2 + h)} + \ln \frac{(2R_1 + 2R_2 + h)h}{(2R_1 + h)(2R_2 + h)} \right) \quad (3)$$

$$U_e(h) = 2\pi\epsilon_0\epsilon_r \left(\frac{2R_1R_2}{R_1 + R_2} \right) (\Psi_{0,1}\Psi_{0,2}) e^{-\kappa h} \quad (4)$$

in which the reciprocal Debye length (κ [m^{-1}]) for a monovalent electrolyte is described by equation 5^{55, 56}.

$$\kappa = \sqrt{\frac{2N_a e^2 I}{\epsilon_0 \epsilon_r k_B T}} \quad (5)$$

in which h is the separation distance [m], A is the Hamaker constant [5.35×10^{-21} J]⁵⁷, R_n is the radius of protein/droplet n [m], ϵ_0 is the dielectric constant of a vacuum [8.85×10^{-12} C² J⁻¹ m⁻¹], ϵ_r is the relative dielectric constant of the medium [80], $\Psi_{0,n}$ is the surface potential of protein/droplet n [V], N_a is the Avogadro constant [6.022×10^{23} mol⁻¹], e is the elementary charge [1.602×10^{-19} C], I is the ionic strength [mol m⁻³], k_B is the Boltzmann constant [1.38×10^{-23} J K⁻¹] and T is the temperature [K].

For protein aggregation, two situations are distinguished. In the first situation, the aggregating protein molecules are identical (e.g. aggregation of non-aggregated proteins or aggregates with the same size) (figure 1B, numbers 1 and 3). In this case, the radius and the surface potential of both protein molecules is equal (i.e. $R_1 = R_2$ and $\Psi_{0,1} = \Psi_{0,2}$). In the second situation, the aggregating protein molecules are different (figure 1B, number 2). Consequently, the radius and surface potential of both protein molecules is also different (i.e. $R_1 \neq R_2$ and $\Psi_{0,1} \neq \Psi_{0,2}$). For emulsion flocculation, only the first situation (i.e. identical droplets) is considered. Hence, the radius and surface potential of the interacting droplets is equal (i.e. $R_1 = R_2$ and $\Psi_{0,1} = \Psi_{0,2}$).

Based on equation 4, the strength of the electrostatic repulsion depends on pH and the type of protein (i.e. surface charge density), and the range of the repulsion is influenced by the ionic strength (i.e. charge screening)⁵⁵ (figure 4). Temperature and concentration do not influence the electrostatic repulsion.

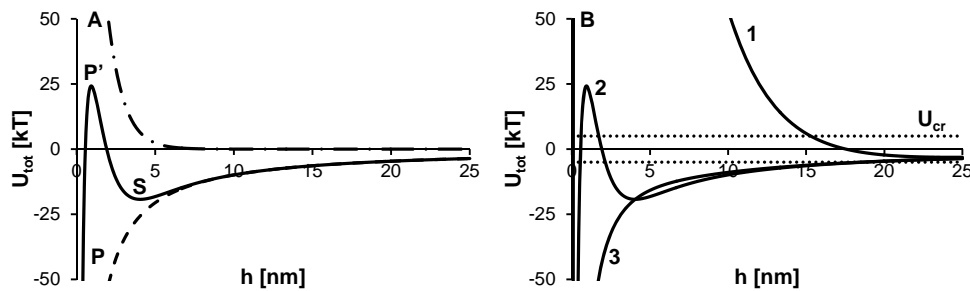


Figure 3. Representative curve for the van der Waals (dashes), electrostatic (dash dots) and total interaction energy (solid) between two droplets (A) and the total interaction energy at three different conditions (B) as function of separation distance. S, P' and P in A represent the secondary minimum, the primary maximum and the primary minimum, respectively. Lines 1-3 in B represent a situation far from the pI and low ionic strength, far from the pI and high ionic strength and close to the pI at any ionic strength, respectively. The dotted line in B corresponds with the critical barrier (U_{cr}) of 5 kT. Calculations were performed using equation 2 and the following parameters; (A) $R_1 = R_2 = 1 \times 10^{-6}$ m, $\Psi_0 = 2 \times 10^{-2}$ V and $I = 100$ mol m^{-3} , (B) $R_1 = R_2 = 1 \times 10^{-6}$ m, (line 1) $\Psi_0 = 4 \times 10^{-2}$ V, (line 2) $\Psi_0 = 2 \times 10^{-2}$ V, (line 3) $\Psi_0 = 5 \times 10^{-3}$ V and (lines 1 and 3) $I = 10$ mol m^{-3} and (line 2) $I = 100$ mol m^{-3} .

Protein molecules are expected aggregate when the total interaction energy (U_{tot}) exceeds the critical barrier (i.e. decreased electrostatic interactions). An interaction energy of 5 kT is used as a critical barrier, which is the demarcation between systems stable and unstable against aggregation or flocculation^{58,59}. Hence, aggregation or flocculation occurs when the primary maximum decreases below 5 kT, or when the secondary minimum decreases below -5 kT (U_{cr}). At high electrostatic repulsion (i.e. pH far from pI and low ionic strength), the repulsive interaction between the protein molecules prevents protein-protein interaction (i.e. protein aggregation and emulsion flocculation)^{47, 60, 61}. This is also indicated by the steep

increase of the interaction energy (figure 3B, line 1). At low electrostatic repulsion (i.e. high ionic strength (figure 3B, line 2) and close to the pI (figure 3B, line 3)), on the other hand, the net interactions between the proteins become net attractive, resulting in aggregation or flocculation. At increased ionic strength, this results in aggregation in the secondary minimum (S), as the primary maximum (P') prevents aggregation in the primary minimum (P). Close to the pI, the primary maximum is absent, resulting in interactions between the protein molecules in the primary minimum.

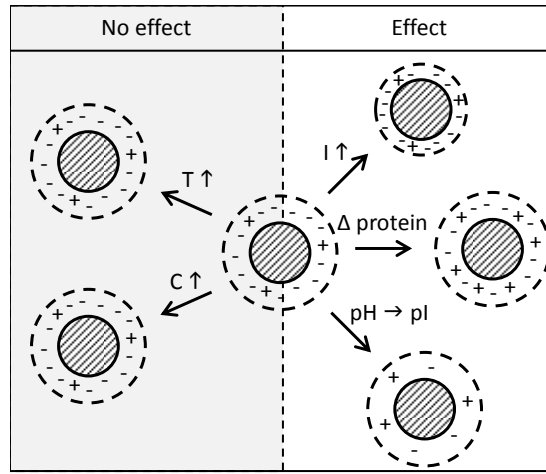


Figure 4. Schematic overview of the effect of various factors on the range and strength of the protein charge.

Emulsion flocculation

Besides the DLVO interactions, steric (U_s) and hydrophobic (U_h) interactions (equations 6^{48, 62} and 7⁴⁸, respectively) are commonly incorporated into the DLVO theory (i.e. extended DLVO theory) to describe the flocculation behaviour of protein-stabilized emulsion^{7, 47}.

$$U_s = \left(\frac{2\delta}{h} \right)^\infty \quad (6)$$

$$U_h = -2\pi R\gamma\phi\lambda e^{-h/\lambda} \quad (7)$$

in which δ is the layer thickness of the adsorbed layer [m], h is the separation distance between the droplets [m], R is the radius of the droplet [m], γ is the interfacial tension at the oil-water interface [J m^{-1}], ϕ is the fractional hydrophobicity of the droplet surface and λ is the decay length of the hydrophobic interaction [m].

Based on equation 6, the repulsive steric interaction increases steeply at $h \leq 2\delta$. As a protein monolayer has a thickness of several nanometers⁴⁹, this interaction acts only over a short

separation distance, and does therefore not prevent flocculation in the secondary minimum. In the case of larger polymers (e.g. polysaccharides), complexes (e.g. protein-polysaccharide complex or protein aggregates) or protein multilayers, the layer thickness can significantly increase^{49, 63}, resulting in steric stabilization against flocculation. The hydrophobic interaction depends on the fractional hydrophobicity of the droplet surface, which was described to depend on the extent of protein unfolding at the interface⁴⁸.

Aggregation and flocculation; similarities and differences

From the above, it is clear that there are many similarities between the process of protein aggregation and emulsion droplet flocculation. Both processes are determined by the molecular properties of the protein and system conditions and occur when the attractive interactions dominate the repulsive interactions. Despite these seemingly clear similarities, a comparison between these processes has not been described in literature. In addition, differences which may arise from the physico-chemical properties have also not been addressed.

Despite the differences in the molecular properties, no intrinsic differences in the behaviour of the different proteins are expected.

Proteins

Four globular proteins are studied in order to test the importance of the protein properties (table 1). In addition to the similarities, some distinct properties are identified.

β -Lactoglobulin β -Lactoglobulin is the most abundant whey protein from bovine milk. It has a molecular mass of 18.3 kDa, and naturally occurs as dimer in solution (pH = 7.0, I = 10 mM, T = 25 °C).

Ovalbumin Ovalbumin is the major protein in avian egg white. It is a glycoprotein with a molecular mass of 44.5 kDa^{64, 65}.

Patatin Patatin is the main protein from potato tubers. It has a molecular mass of 40-42 kDa, dependent on the extent of glycosylation⁶⁶. Similar to β -lactoglobulin, it naturally occurs as a dimer⁶⁷. Compared to the other proteins, the thermostability is relatively low compared to the other proteins ($T_d = 60$ °C⁶⁸), which may be attributed to the absence of disulphide bonds.

Lysozyme Lysozyme is a minor protein from avian egg white (~3-4 %(w/v)). It has a molecular mass of 14.3 kDa. In contrast to the other proteins, it has a positive charge at neutral pH due to its relatively high iso-electric point⁶⁵.

Table 1. Protein properties obtained from literature (<http://www.expasy.org>)

Protein	Expasy code	Origin	M _w [kDa]	pI	#COOH/ #NH ₂ ^a	σ _w ^b [mC m ⁻²]	#S-S/ #S-H	D _s ^c [x 10 ⁻¹⁰ m ² s ⁻¹]	T _d ^d [°C]
β-Lactoglobulin	P02754	Cow milk	18.3	4.83	26/18	-21.9	2/1	1.40/1.11	73.8 ^e
Ovalbumin	P01012	Hen egg white	42.8	5.19	47/35	-24.2	1/4	1.05	78.3 ^f
Patatin	P07745	Potato	40.0	5.25	43/32	-17.9	0/1	1.08	60.0 ^g
Lysozyme	P00698	Hen egg white	14.3	9.32	9/17	25.8	4/0	1.52	72.3 ^h

^a#COOH and #NH₂ are the maximum number of negatively charged (aspartic and glutamic acid) and positively charged (arginine and lysine) groups in the primary sequence, respectively.

^btheoretical net charge density at pH 7.0.

^ctheoretical diffusion coefficient calculated from the radius using the Stokes-Einstein equation ($D_s = k_b T / 6\pi\eta R$). R was calculated from the M_w ($R = (3vM_w/4\pi N_a)^{1/3}$)⁶⁹ assuming a partial specific volume of $0.73 \times 10^{-6} \text{ m}^3 \text{ g}^{-1}$.

^ddenaturation temperature at pH 7.0 and I ≤ 15 mM.

^{e,f,g,h}literature values^{18, 68, 70, 71}, respectively.

Aim and outline of the thesis

This thesis aims at increasing the understanding of protein-protein interactions in protein aggregation (i.e. in the bulk) and in emulsion flocculation (i.e. at the interface). This knowledge can then be used to control the processes. In addition, the behaviour of proteins in the continuous phase and adsorbed at the interface are linked. Therefore, the aggregation (**chapter 2**) and flocculation behaviour (**chapter 3**) of various globular proteins is compared to obtain insights in the extent to which the physico-chemical properties (e.g. charge, exposed hydrophobicity) affect these phenomena. To correlate the protein properties to the aggregation and flocculation behaviour, both properties and behaviour are analysed in detail. In **chapter 4**, patatin is modified by glycation with mono- and oligosaccharides to introduce a steric repulsive interaction between the protein molecules and thereby changing the flocculation behaviour. In **chapter 5**, patatin is modified by succinylation to change the electrostatic repulsion and as a consequence the flocculation behaviour. In **chapter 6**, the effect of system conditions and the protein properties on the adsorption behaviour is compared for three proteins. In **chapter 7**, the insights from **chapters 3-6** are combined and extended to develop a theory to predict the flocculation behaviour of protein-stabilized emulsions. The general discussion (**chapter 8**) evaluates to which extent protein aggregation in the continuous phase and emulsion flocculation compare. Also, the effect of protein properties on the aggregation behaviour is discussed.

References

1. Krebs, M. R. H.; Devlin, G. L.; Donald, A. M., Protein particulates: another generic form of protein aggregation? *Biophys. J.* **2007**, 92, (4), 1336-1342.
2. Wang, W.; Nema, S.; Teagarden, D., Protein aggregation - pathways and influencing factors. *Int. J. Pharm.* **2010**, 390, (2), 89-99.
3. Ross, C. A.; Poirier, M. A., Protein aggregation and neurodegenerative disease. *Nat. Med.* **2004**, 10, S10-S17.
4. Donald, A. M., Aggregation in β -lactoglobulin. *Soft Matter* **2008**, 4, 1147-1150.
5. Dickinson, E., Milk protein interfacial layers and the relationship to emulsion stability and rheology. *Colloids Surf., B* **2001**, 20, (3), 197-210.
6. Wang, W., Protein aggregation and its inhibition in biopharmaceutics. *Int. J. Pharm.* **2005**, 289, (1-2), 1-30.
7. Dickinson, E., Flocculation of protein-stabilized oil-in-water emulsions. *Colloids Surf., B* **2010**, 81, (1), 130-140.
8. Desfougères, Y.; Croguennec, T.; Lechevalier, V.; Bouhallab, S.; Nau, F., Charge and size drive spontaneous self-assembly of oppositely charged globular proteins into microspheres. *J. Phys. Chem. B* **2010**, 114, (12), 4138-4144.
9. Salvatore, D. B.; Duraffourg, N.; Favier, A.; Persson, B. A.; Lund, M.; Delage, M.-M.; Silvers, R.; Schwalbe, H.; Croguennec, T.; Bouhallab, S.; Forge, V., Investigation at residue level of the early steps during the assembly of two proteins into supramolecular objects. *Biomacromolecules* **2011**, 12, (6), 2200-2210.
10. Persson, B. A.; Lund, M., Association and electrostatic steering of α -lactalbumin-lysozyme heterodimers. *Phys. Chem. Chem. Phys.* **2009**, 11, (39), 8879-8885.
11. Yan, Y.; Seeman, D.; Zheng, B.; Kizilay, E.; Xu, Y.; Dubin, P. L., pH-dependent aggregation and disaggregation of native β -lactoglobulin in low salt. *Langmuir* **2013**, 29, (14), 4584-4593.
12. Giger, K.; Vanam, R. P.; Seyrek, E.; Dubin, P. L., Suppression of insulin aggregation by heparin. *Biomacromolecules* **2008**, 9, (9), 2338-2344.
13. Majhi, P. R.; Ganta, R. R.; Vanam, R. P.; Seyrek, E.; Giger, K.; Dubin, P. L., Electrostatically driven protein aggregation: β -lactoglobulin at low ionic strength. *Langmuir* **2006**, 22, (22), 9150-9159.
14. Chi, E. Y.; Krishnan, S.; Randolph, T. W.; Carpenter, J. F., Physical stability of proteins in aqueous solution: mechanism and driving forces in nonnative protein aggregation. *Pharm. Res.* **2003**, 20, (9), 1325-1336.
15. Pace, C. N., Conformational stability of globular proteins. *Trends Biochem. Sci.* **1990**, 15, (1), 14-17.
16. Lumry, R.; Eyring, H., Conformation changes of proteins. *J. Phys. Chem.* **1954**, 58, (2), 110-120.
17. Olsen, S. N.; Andersen, K. B.; Randolph, T. W.; Carpenter, J. F.; Westh, P., Role of electrostatic repulsion on colloidal stability of *Bacillus halmapalus* α -amylase. *Biochim. Biophys. Acta, Proteins Proteomics* **2009**, 1794, (7), 1058-1065.
18. Weijers, M.; Barneveld, P. A.; Cohen Stuart, M. A.; Visschers, R. W., Heat-induced denaturation and aggregation of ovalbumin at neutral pH described by irreversible first-order kinetics. *Protein Sci.* **2003**, 12, (12), 2693-2703.
19. Verheul, M.; Roefs, S. P. F. M., Structure of particulate whey protein gels: effect of NaCl, concentration, pH, heating temperature, and protein composition. *J. Agric. Food Chem.* **1998**, 46, (12), 4909-4916.

20. Baussay, K.; Le Bon, C.; Nicolai, T.; Durand, D.; Busnel, J. P., Influence of the ionic strength on the heat-induced aggregation of the globular protein β -lactoglobulin at pH 7. *Int. J. Biol. Macromol.* **2004**, 34, (1-2), 21-28.
21. Gimel, J. C.; Durand, D.; Nicolai, T., Structure and distribution of aggregates formed after heat-induced denaturation of globular proteins. *Macromolecules* **1994**, 27, (2), 583-589.
22. Mahler, H.-C.; Friess, W.; Grauschopf, U.; Kiese, S., Protein aggregation: pathways, induction factors and analysis. *J. Pharm. Sci.* **2009**, 98, (9), 2909-2934.
23. Walstra, P., *Physical chemistry of foods*. Marcel Dekker, Inc.: New York, NY, USA, 2003.
24. Speed, M. A.; King, J.; Wang, D. I. C., Polymerization mechanism of polypeptide chain aggregation. *Biotechnol. Bioeng.* **1997**, 54, (4), 333-343.
25. Le Bon, C.; Nicolai, T.; Durand, D., Kinetics of aggregation and gelation of globular proteins after heat-induced denaturation. *Macromolecules* **1999**, 32, (19), 6120-6127.
26. Verheul, M.; Roefs, S. P. F. M.; de Kruif, K. G., Kinetics of heat-induced aggregation of β -lactoglobulin. *J. Agric. Food Chem.* **1998**, 46, (3), 896-903.
27. Creighton, T. E., *Proteins: structure and molecular properties*. 2 ed.; W.H. Freeman: New York, NY, USA, 2002.
28. Velev, O. D.; Kaler, E. W.; Lenhoff, A. M., Protein interactions in solution characterized by light and neutron scattering: comparison of lysozyme and chymotrypsinogen. *Biophys. J.* **1998**, 75, (6), 2682-2697.
29. Broersen, K.; Weijers, M.; de Groot, J.; Hamer, R. J.; de Jongh, H. H. J., Effect of protein charge on the generation of aggregation-prone conformers. *Biomacromolecules* **2007**, 8, (5), 1648-1656.
30. Hoffmann, M. A. M.; van Mil, P. J. J. M., Heat-induced aggregation of β -lactoglobulin as a function of pH. *J. Agric. Food Chem.* **1999**, 47, (5), 1898-1905.
31. Le Bon, C.; Nicolai, T.; Durand, D., Growth and structure of aggregates of heat-denatured β -lactoglobulin. *Int. J. Food Sci. Technol.* **1999**, 34, (5-6), 451-465.
32. Weijers, M.; Broersen, K.; Barneveld, P. A.; Cohen Stuart, M. A.; Hamer, R. J.; De Jongh, H. H. J.; Visschers, R. W., Net charge affects morphology and visual properties of ovalbumin aggregates. *Biomacromolecules* **2008**, 9, (11), 3165-3172.
33. Weijers, M.; Visschers, R. W.; Nicolai, T., Light scattering study of heat-induced aggregation and gelation of ovalbumin. *Macromolecules* **2002**, 35, (12), 4753-4762.
34. Mine, Y., Laser light scattering study on the heat-induced ovalbumin aggregates related to its gelling property. *J. Agric. Food Chem.* **1996**, 44, (8), 2086-2090.
35. Choi, S. J.; Moon, T. W., Influence of sodium chloride and glucose on the aggregation behavior of heat-denatured ovalbumin investigated with a multiangle laser light scattering technique. *J. Food Sci.* **2008**, 73, (2), C41-C49.
36. Durand, D.; Gimel, J. C.; Nicolai, T., Aggregation, gelation and phase separation of heat denatured globular proteins. *Phys. A* **2002**, 304, (1-2), 253-265.
37. Yohannes, G.; Wiedmer, S. K.; Elomaa, M.; Jussila, M.; Aseyev, V.; Riekkola, M.-L., Thermal aggregation of bovine serum albumin studied by asymmetrical flow field-flow fractionation. *Anal. Chim. Acta* **2010**, 675, (2), 191-198.
38. Pots, A. M.; ten Grotenhuis, E.; Gruppen, H.; Voragen, A. G. J.; de Kruif, K. G., Thermal aggregation of patatin studied in situ. *J. Agric. Food Chem.* **1999**, 47, (11), 4600-4605.
39. Pouzot, M.; Durand, D.; Nicolai, T., Influence of the ionic strength on the structure of heat-set globular protein gels at pH 7. β -lactoglobulin. *Macromolecules* **2004**, 37, (23), 8703-8708.
40. Roefs, S. P. F. M.; de Kruif, K. G., A model for the denaturation and aggregation of β -lactoglobulin. *Eur. J. Biochem.* **1994**, 226, (3), 883-889.
41. Hoffmann, M. A. M.; van Mil, P. J. J. M., Heat-induced aggregation of β -lactoglobulin: role of the free thiol group and disulfide bonds. *J. Agric. Food Chem.* **1997**, 45, (8), 2942-2948.

42. Broersen, K.; Van Teeffelen, A. M. M.; Vries, A.; Voragen, A. G. J.; Hamer, R. J.; De Jongh, H. H. J., Do sulfhydryl groups affect aggregation and gelation properties of ovalbumin? *J. Agric. Food Chem.* **2006**, *54*, (14), 5166-5174.
43. van Aken, G. A.; Blijdenstein, T. B. J.; Hotrum, N. E., Colloidal destabilisation mechanisms in protein-stabilised emulsions. *Curr. Opin. Colloid Interface Sci.* **2003**, *8*, (4-5), 371-379.
44. McClements, D. J., Protein-stabilized emulsions. *Curr. Opin. Colloid Interface Sci.* **2004**, *9*, (5), 305-313.
45. Damodaran, S., Protein stabilization of emulsions and foams. *J. Food Sci.* **2005**, *70*, (3), R54-R66.
46. Dalglish, D. G., Adsorption of protein and the stability of emulsions. *Trends Food Sci. Technol.* **1997**, *8*, (1), 1-6.
47. McClements, D. J., *Food emulsions: Principles, practices and techniques*. Second ed.; CRC Press: Boca Raton, FL, USA, 2005.
48. Kim, H. J.; Decker, E. A.; McClements, D. J., Impact of protein surface denaturation on droplet flocculation in hexadecane oil-in-water emulsions stabilized by β -lactoglobulin. *J. Agric. Food Chem.* **2002**, *50*, (24), 7131-7137.
49. Wooster, T. J.; Augustin, M. A., The emulsion flocculation stability of protein-carbohydrate diblock copolymers. *J. Colloid Interface Sci.* **2007**, *313*, (2), 665-675.
50. Dickinson, E., Hydrocolloids as emulsifiers and emulsion stabilizers. *Food Hydrocolloids* **2009**, *23*, (6), 1473-1482.
51. Dickinson, E., Mixed biopolymers at interfaces: competitive adsorption and multilayer structures. *Food Hydrocolloids* **2011**, *25*, (8), 1966-1983.
52. Surh, J.; Decker, E. A.; McClements, D. J., Influence of pH and pectin type on properties and stability of sodium-caseinate stabilized oil-in-water emulsions. *Food Hydrocolloids* **2006**, *20*, (5), 607-618.
53. Kulmyrzaev, A. A.; Schubert, H., Influence of KCl on the physicochemical properties of whey protein stabilized emulsions. *Food Hydrocolloids* **2004**, *18*, (1), 13-19.
54. Tcholakova, S.; Denkov, N. D.; Sidzhakova, D.; Ivanov, I. B.; Campbell, B., Effects of electrolyte concentration and pH on the coalescence stability of β -lactoglobulin emulsions: experiment and interpretation. *Langmuir* **2005**, *21*, (11), 4842-4855.
55. Israelachvili, J. N., *Intermolecular and surface forces*. Third ed.; Academic Press: New York, NY, USA, 2011.
56. Hermansson, M., The DLVO theory in microbial adhesion. *Colloids Surf., B* **1999**, *14*, (1-4), 105-119.
57. Silvestre, M. P. C.; Decker, E. A.; McClements, D. J., Influence of copper on the stability of whey protein stabilized emulsions. *Food Hydrocolloids* **1999**, *13*, (5), 419-424.
58. Hesselink, F. T.; Vrij, A.; Overbeek, J. T. G., Theory of the stabilization of dispersions by adsorbed macromolecules. II. Interaction between two flat particles. *J. Phys. Chem.* **1971**, *75*, (14), 2094-2103.
59. Wiese, G. R.; Healy, T. W., Effect of particle size on colloid stability. *Trans. Faraday Soc.* **1970**, *66*, 490-499.
60. Tsai, A. M.; van Zanten, J. H.; Betenbaugh, M. J., II. Electrostatic effect in the aggregation of heat-denatured RNase A and implications for protein additive design. *Biotechnol. Bioeng.* **1998**, *59*, (3), 281-285.
61. Chi, E. Y.; Krishnan, S.; Kendrick, B. S.; Chang, B. S.; Carpenter, J. F.; Randolph, T. W., Roles of conformational stability and colloidal stability in the aggregation of recombinant human granulocyte colony-stimulating factor. *Protein Sci.* **2003**, *12*, (5), 903-913.
62. Vincent, B.; Young, C. A.; Tadros, T. F., Equilibrium aspects of heteroflocculation in mixed sterically-stabilised dispersions. *Faraday Discuss. Chem. Soc.* **1978**, *65*, 296-305.

63. Wooster, T. J.; Augustin, M. A., β -Lactoglobulin–dextran Maillard conjugates: their effect on interfacial thickness and emulsion stability. *J. Colloid Interface Sci.* **2006**, 303, (2), 564-572.
64. Nisbet, A. D.; Saundry, R. H.; Moir, A. J. G.; Fothergill, L. A.; Fothergill, J. E., The complete amino-acid sequence of hen ovalbumin. *Eur. J. Biochem.* **1981**, 115, (2), 335-345.
65. Mine, Y., Recent advances in the understanding of egg white protein functionality. *Trends Food Sci. Technol.* **1995**, 6, (7), 225-232.
66. Pots, A. M.; Gruppen, H.; Hessing, M.; van Boekel, M. A. J. S.; Voragen, A. G. J., Isolation and characterization of patatin isoforms. *J. Agric. Food Chem.* **1999**, 47, (11), 4587-4592.
67. Pots, A. M.; Gruppen, H.; de Jongh, H. H. J.; van Boekel, M. A. J. S.; Walstra, P.; Voragen, A. G. J., Kinetic modeling of the thermal aggregation of patatin. *J. Agric. Food Chem.* **1999**, 47, (11), 4593-4599.
68. van Koningsveld, G. A.; Gruppen, H.; de Jongh, H. H. J.; Wijngaards, G.; van Boekel, M. A. J. S.; Walstra, P.; Voragen, A. G. J., Effects of pH and heat treatments on the structure and solubility of potato proteins in different preparations. *J. Agric. Food Chem.* **2001**, 49, (10), 4889-4897.
69. Erickson, H. P., Size and shape of protein molecules at the nanometer level determined by sedimentation, gel filtration, and electron microscopy. *Biol. Proced. Online* **2009**, 11, (1), 32-51.
70. Haug, I. J.; Skar, H. M.; Vegarud, G. E.; Langsrud, T.; Draget, K. I., Electrostatic effects on β -lactoglobulin transitions during heat denaturation as studied by differential scanning calorimetry. *Food Hydrocolloids* **2009**, 23, (8), 2287-2293.
71. van der Veen, M.; Norde, W.; Cohen Stuart, M., Effects of succinylation on the structure and thermostability of lysozyme. *J. Agric. Food Chem.* **2005**, 53, (14), 5702-5707.

Chapter 2

Comparison of heat-induced aggregation of globular proteins

Abstract

The heat-induced aggregation has been extensively studied focussing on a single protein. Consequently, there is limited information on the exact relation between the molecular properties and aggregation behaviour of different proteins. To improve this, the heat-induced aggregation of ovalbumin, β -lactoglobulin and patatin is systematically studied under various conditions (i.e. pH, ionic strength, concentration and temperature). This study indicates that the behaviour of one protein can only partly be extrapolated to that of another protein. In general, the aggregation rate of β -lactoglobulin is significantly slower (i.e. > 10 times) than that of ovalbumin and patatin. This is postulated to be caused by the higher structural stability of β -lactoglobulin, as it could not be related to the basic molecular properties (surface charge and exposed hydrophobicity). In addition, β -lactoglobulin aggregation is affected by the system conditions (pH, I and C), whereas ovalbumin and patatin aggregation are not. Furthermore, the formed aggregates of all proteins become larger and/or denser with decreasing electrostatic repulsion. This effect of electrostatic repulsion was, however, smaller for ovalbumin than for the other two proteins. Hence, it was concluded that the behaviour of proteins cannot be described simply based on their molecular properties.

Introduction

Heat-induced aggregation of globular proteins is generally described to be caused by the exposure of the internal hydrophobic amino acids due to unfolding^{1,2}. After unfolding of the protein and exposure of the hydrophobic amino acid residues, the (partially) unfolded protein either refolds or irreversibly aggregate with other (partially) unfolded proteins^{3,4}. The likelihood of refolding or aggregation depends on the balance between the increased hydrophobic attraction due to unfolding and the mainly electrostatic barrier for aggregation. Qualitatively, aggregation has been investigated extensively, mainly in terms of (1) aggregation kinetics⁵⁻⁷, (2) aggregate size^{8,9} and (3) aggregate structure^{10,11}. These studies typically investigate the effect of conditions (e.g. ionic strength) on the aggregation of a single protein (e.g. β -lactoglobulin). A detailed comparison of the aggregation of different proteins, on the other hand, is still missing. Exactly such information may advance the understanding of the aggregation process of globular proteins, especially with respect to an overall description of the effect of parameters influencing the aggregation process. Hence, the aim of the present paper is to determine the effect of the properties of three proteins on the aggregation behaviour under various conditions.

The aggregation kinetics (i.e. order (n) and rate (k)) are generally derived from the decrease of the concentration non-aggregated protein in time. Therefore, they provide information on the kinetics of protein unfolding and integration of non-aggregated proteins in aggregates, whereas it does not contain information on the size and structure of the formed aggregates.

Aggregation order

To determine the order of aggregation, two approaches have been described: (A) determination of the concentration dependence of the initial aggregation rate⁵⁻⁷ and (B) fitting the decrease of the concentration non-aggregated protein in time with the specific reaction equations. These are equations 1 and 2 for 1st and nth order kinetics, respectively¹².

$$C_t = C_0 e^{-kt} \quad \text{for } n = 1 \quad (1)$$

$$C_t = (C_0^{1-n} + (n-1)kt)^{\frac{1}{1-n}} \quad \text{for } n \neq 1 \quad (2)$$

in which C_t and C_0 is the concentration of non-aggregated protein at time t and time 0 [g L⁻¹], respectively, n is the aggregation order [-] and k is the aggregation rate [L g⁻¹ s⁻¹].

Discrepancies between the two approaches originate from the fact that the aggregation process becomes more complex at longer heating times. This is due to aggregation of non-aggregated protein with other non-aggregated protein, non-aggregated with aggregated proteins, and aggregated proteins with other aggregated proteins.

For ovalbumin, the initial aggregation rate was shown to be concentration independent. Hence, the aggregation process has been described as a first-order reaction⁶. The aggregation rate of β -lactoglobulin, on the other hand, increases with increasing

concentration, indicating concentration dependence. This resulted in an aggregation order of 1.5^{5, 7, 13}. In addition, the aggregation orders of ovalbumin and β -lactoglobulin were shown to be independent of temperature^{6, 14, 15}, pH^{8, 14} and ionic strength^{6, 16}.

Aggregation rate

For all proteins, the fraction unfolded protein and the diffusion rate of the protein molecules increase upon increasing the temperature^{17, 18}. The fraction unfolded proteins depends on the heating temperature relative to the denaturation temperature (T_d). For a more fundamental comparison of the aggregation properties of different proteins, the proteins are studied at a fixed temperature relative to T_d , rather than an absolute temperature. This results in a constant fraction unfolded protein. An increase of the diffusion rate results in an increased likelihood of the proteins to meet, collide and aggregate^{19, 20}. The aggregation rate is also affected by electrostatic repulsion. However, a clear link is difficult to make, since the main factors (i.e. ionic strength and pH) can have several effects. Increasing the electrostatic repulsion increases both the intra- and intermolecular repulsion. The increased intramolecular repulsion decreases the denaturation temperature^{21, 22}. The increase of intermolecular repulsion, on the other hand, increases the electrostatic barrier for aggregation²³. While the first effect would (when heating at given temperature) result in an increase of the aggregation rate, the second would decrease the rate of aggregation. In addition, a pH change does not only affect the electrostatic interactions, but also changes the reactivity of the disulphide bonds. While changes in the electrostatic repulsion (i.e. ionic strength and pH) do not affect the aggregation rate of ovalbumin^{6, 24}, the aggregation rate of β -lactoglobulin increases with increasing ionic strength (< 0.1 M)¹⁶ and pH^{8, 14}. This difference indicates that the electrostatic repulsion affects both proteins differently. The enhancing effect of ionic strength on the aggregation rate of β -lactoglobulin showed that the increase of the denaturation temperature was less important than the decrease of the electrostatic barrier for aggregation¹⁶. At the same time, a higher denaturation temperature and a decrease of the reactivity of the disulphide bonds were described to reduce the aggregation rate of β -lactoglobulin with decreasing pH¹⁴.

Aggregate formation

To describe the aggregate formation, the size and structure of the aggregates are typically determined by scattering techniques (i.e. neutron, x-ray and light scattering). The structure of the aggregates is described by the fractal dimension. The fractal dimension was found to be independent of the heating temperature^{15, 25}. As temperature only affects the aggregation kinetics and not the formation of aggregates, the effect of temperature has been described as a purely kinetic effect¹⁵. Electrostatic repulsion, however, strongly affects the aggregate formation (size as well as structure). A decrease of the electrostatic repulsion (i.e. increase of the ionic strength and/or a shift of the pH towards the iso-electric point (pI)) resulted in the formation of larger aggregates of ovalbumin^{26, 27}, β -lactoglobulin^{8, 28}, BSA⁹ and

patatin²⁹, based on light scattering. At conditions with high electrostatic repulsion (i.e. low ionic strength and pH far from the pI), linear aggregates with a fractal dimension of 1.7 were formed by ovalbumin³⁰ and β -lactoglobulin^{31,32}. When the electrostatic repulsion was decreased (i.e. by increasing the ionic strength from 10 to 100 mM), the β -lactoglobulin and ovalbumin aggregates become more branched. This was indicated by a fractal dimension of 2.0^{15, 30, 33-35}, and confirmed by cryo-TEM³⁰. When the electrostatic repulsion is minimal (i.e. close to the pI), β -lactoglobulin forms even more compact aggregates with a fractal dimension of 3.0³⁶. The effect of electrostatic repulsion on the aggregate size and structure is explained by the electrostatic barrier for aggregation^{30, 32, 35}. Furthermore, the size of β -lactoglobulin and BSA aggregates increased with increasing concentration^{9, 15, 33, 37}. This concentration dependence has been postulated to be a result of an increase of the ionic strength due to the counter ions of the protein.

Since β -lactoglobulin has most often been used to study the aggregation process, its aggregation behaviour is quite well understood. However, little is known on how this knowledge can be extrapolated to describe the aggregation of other proteins. To extend the understanding on the effect of protein properties on the aggregation of globular proteins, this study focusses on the comparison of the aggregation process of different proteins. Hence, the differences in the kinetics and factors influencing the aggregation of three proteins (β -lactoglobulin, ovalbumin and patatin) under various conditions (pH, ionic strength, temperature and protein concentration) are studied.

Materials and methods

Materials

Ovalbumin (A-5503, Lot n° 031M7008V; protein content 92 % (N x 6.22)³⁸ of which ≥ 98 % ovalbumin (based on agarose gel electrophoresis)) and β -lactoglobulin (L-0130, Lot n° SLBC2933V ; protein content of 94 % (N x 6.38)³⁸ of which 99 % β -lactoglobulin (based on PAGE)) were purchased from Sigma-Aldrich (St. Louis, MO, USA). Potatoes were provided by AVEBE BA (Veendam, The Netherlands). Patatin was isolated from potato juice as described previously³⁹, except that gel filtration was performed on a Superdex 200 column (52 x 10 cm). The obtained patatin fraction (purity ≥ 90 % based on analytical size-exclusion chromatography) was dialysed against demineralized water, freeze-dried and stored at -20 °C. All other chemicals were of analytical grade and purchased from either Sigma-Aldrich or Merck.

Differential scanning calorimetry (DSC)

The denaturation temperature of the proteins was determined using a VP-DSC MicroCalorimeter (MicroCal Inc., Northampton, MA, USA). The proteins were dissolved in 10 mM sodium phosphate buffer pH 7.0 at a concentration of 2 g L⁻¹. Subsequently, thermograms were recorded from 20 to 100 °C at a heating rate of 1 °C min⁻¹. The denaturation temperatures (T_d) of ovalbumin, β -lactoglobulin and patatin were found to be 77.5, 75.0 and 60.0 °C, respectively. This is in close agreement with the denaturation temperatures reported in literature^{6, 21, 39}.

Heat-induced aggregation

Heat-induced aggregation was performed in a water bath. Aliquots of 1 mL were heated for different time intervals (0, 1, 2, 5, 10, 20, 30, 40, 50, 60, 100, 200, 300, 400, 500, 1500, 1800, 3000, 4500 and 10080 min) in Kimax tubes. After heating, the samples were cooled on ice-water. Four different sets of experiments were performed:

Effect of temperature Proteins were dissolved in 10 mM sodium phosphate buffer pH 7.0 at a concentration of 2 g L⁻¹. Subsequently, these solutions were heated at temperatures at the same distance from the denaturation temperature (T_d): $T_d - 10$ °C, $T_d - 5$ °C, T_d and $T_d + 5$ °C. This was chosen to ensure as well as possible a similar rate of unfolding for all proteins. The reason is that at T_d , for all proteins, the native and unfolded protein are present in equal amounts^{12, 17}. This equilibrium between native and unfolded protein shifts towards the native protein with decreasing and towards unfolded protein with increasing temperature (figure 1). This equilibrium is, at a certain temperature from T_d (e.g. $T_d - 5$ °C), assumed to be equal for all proteins. For the incubations at the two highest temperatures, additional time intervals (i.e. 0.5, 1.5, 2.5, 3, 4, 7.5, 12.5, 15, 17.5 and 25 min) were included.

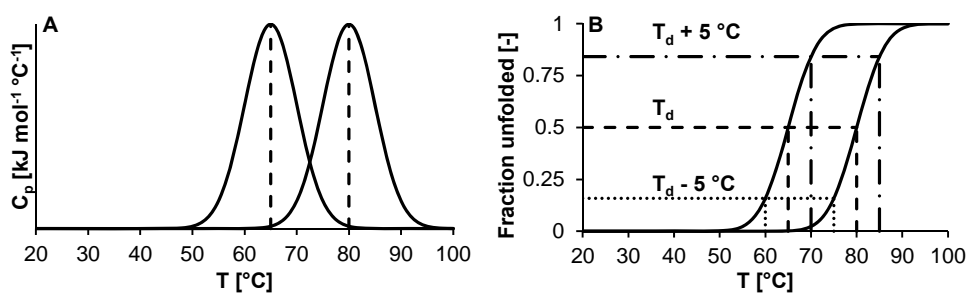


Figure 1. Schematic DSC thermograms (A) and the derived fraction unfolded protein (B) for two proteins with a T_d of 65 and 80 °C, respectively. The dotted, dashed and dash dotted lines represent temperatures of $T_d - 5$ °C, T_d and $T_d + 5$ °C, respectively.

The aggregation rate was determined based on the decrease of the concentration non-aggregated protein in time using equation 1 or 2. From the temperature dependence of

the aggregation rate (k), the activation energy (E_a) was calculated by the Arrhenius equation.

Effect of pH Proteins were dissolved in 10 mM sodium phosphate buffer pH 7.0, pH 6.0 and pH 5.0 at a concentration of 2 g L^{-1} . Subsequently, the solutions were heated at $T_d - 5 \text{ }^\circ\text{C}$.

Effect of ionic strength Proteins were dissolved in 10 mM sodium phosphate buffer pH 7.0 in the presence of absence of 10, 40 and 90 mM NaCl at a concentration of 2 g L^{-1} , resulting in a final ionic strength of 10, 20, 50 and 100 mM. Subsequently, the solutions were heated at $T_d - 5 \text{ }^\circ\text{C}$.

Effect of protein concentration Proteins were dissolved in 10 mM sodium phosphate buffer pH 7.0 at concentrations of 1, 2, 5 and 10 g L^{-1} . Subsequently, the solutions were heated at $T_d - 5 \text{ }^\circ\text{C}$.

Size-exclusion chromatography (SEC)

The concentration non-aggregated protein (i.e. monomer concentration for ovalbumin and dimer concentration for β -lactoglobulin and patatin) was determined using SEC on an Äkta Micro equipped with a Superdex 200 PC 3.2/30 column (GE Healthcare, Uppsala, Sweden). Samples ($20 \text{ } \mu\text{L}$) were injected and eluted with 10 mM sodium phosphate buffer pH 7.0 at a flow rate of 0.06 mL min^{-1} . The elution was monitored at 214 nm. The calibration was performed with globular proteins with a mass range of 13.7-67 kDa (GE Healthcare).

Determination of the aggregation kinetics

The aggregation kinetics are determined in several ways: (1) concentration dependence of the time required to aggregate half of the protein (i.e. t_h as indication of the aggregation rate), (2) fitting the decrease of the concentration non-aggregated protein in time using equations 1 and 2 and (3) fitting the natural logarithm of concentration ($n = 1.0$), reciprocal of the square root of concentration ($n = 1.5$) and the reciprocal of the concentration ($n = 2.0$) against time with a linear function, fixing the intercept with the y-axis corresponding to the initial concentration (C_0). The first approach only includes the datapoints $C_t \geq 0.5C_0$, whereas the other two approaches are applied to the regime $C_t \geq 0.05C_0$.

Static light scattering (SLS)

The scattered light intensity was determined in time using a Malvern Zetasizer Nano ZS (Malvern Instruments, Worcestershire, UK). The protein solutions (as described in the section heat-induced aggregation) were filtered over a $0.1 \text{ } \mu\text{m}$ PTFE filter (Puradisc 13; Whatman, Kent, UK). Subsequently, the filtered solutions were heated at the temperatures described in the section on *heat-induced aggregation*. The scattered light intensity was

measured every 30 seconds for 7200 seconds. The intensity of the scattered light is generally described by equation 3^{13,40}.

$$I(q) \propto KcM_w P(q)S(q) \quad (3)$$

in which $I(q)$ is the intensity of the scattered light at angle q (i.e. 173°), K is an optical constant, c is the concentration [g L^{-1}], M_w is the molar mass of the particles [g mol^{-1}], $P(q)$ is the particle form factor which describes the shape and size of the particles and $S(q)$ is the structure factor that describes the spatial arrangement of the particles.

As the concentration (c) and the optical constant (K) are constant during and between the measurements equation 3 can be simplified to:

$$I(q) \propto M_w P(q)S(q) \quad (4)$$

This shows that an increase of the scattered light intensity relates to an increase of the aggregate size and/or a more dense aggregate structure.

Results and discussion

Aggregation order

The first parameter used to compare the aggregation behaviour of different proteins is the aggregation order (n). To obtain information whether the aggregation order is affected by the conditions, the decrease of the concentration non-aggregated protein is plotted against the time divided by the time required to aggregate half of the proteins (t_h) (figures 2A-C). All curves of one protein superimpose onto one master curve, indicating that the aggregation order is not affected by temperature, concentration, pH and ionic strength. Hence, the aggregation process of each protein can be described by a single aggregation order at the different conditions applied.

Table 1. Aggregation order of ovalbumin, β -lactoglobulin and patatin determined by different methods.

Determination of the aggregation order	Ovalbumin	β -Lactoglobulin	Patatin
(1) Concentration dependence of the t_h ($C_t \geq 0.5C_0$)	1.0	1.5	1.0
(2) Fit concentration in time using equations 1 and 2 ($C_t \geq 0.05C_0$)	2.1	2.5	2.9
(3.1) Linear fit of $\ln(C_t)$ in time ($n = 1.0$) ($C_t \geq 0.05C_0$)	$R^2 = 0.28 \pm 0.32$	$R^2 = 0.85 \pm 0.13$	$R^2 = 0.28 \pm 0.30$
(3.2) Linear fit of $1/\sqrt{C}$ in time ($n = 1.5$) ($C_t \geq 0.05C_0$)	$R^2 = 0.80 \pm 0.13$	$R^2 = 0.96 \pm 0.04$	$R^2 = 0.83 \pm 0.09$
(3.3) Linear fit of $1/C$ in time ($n = 2.0$) ($C_t \geq 0.05C_0$)	$R^2 = 0.95 \pm 0.04$	$R^2 = 0.93 \pm 0.07$	$R^2 = 0.97 \pm 0.01$

The aggregation order was determined using three approaches. The first approach derives the aggregation order from the concentration dependence of t_h (figure 3 and table 1). The t_h is concentration independent for ovalbumin and patatin, indicating a first order reaction. For ovalbumin, this is in line with previous data⁶, whereas for patatin no previous data is present. For β -lactoglobulin, on the other hand, t_h depends on the concentration. The slope of the concentration dependence of t_h is -0.5 , showing that, within the experimental error, t_h scales with \sqrt{C} . This implies an order of $1.5^{5,7}$, which is in line with literature^{15,16}.

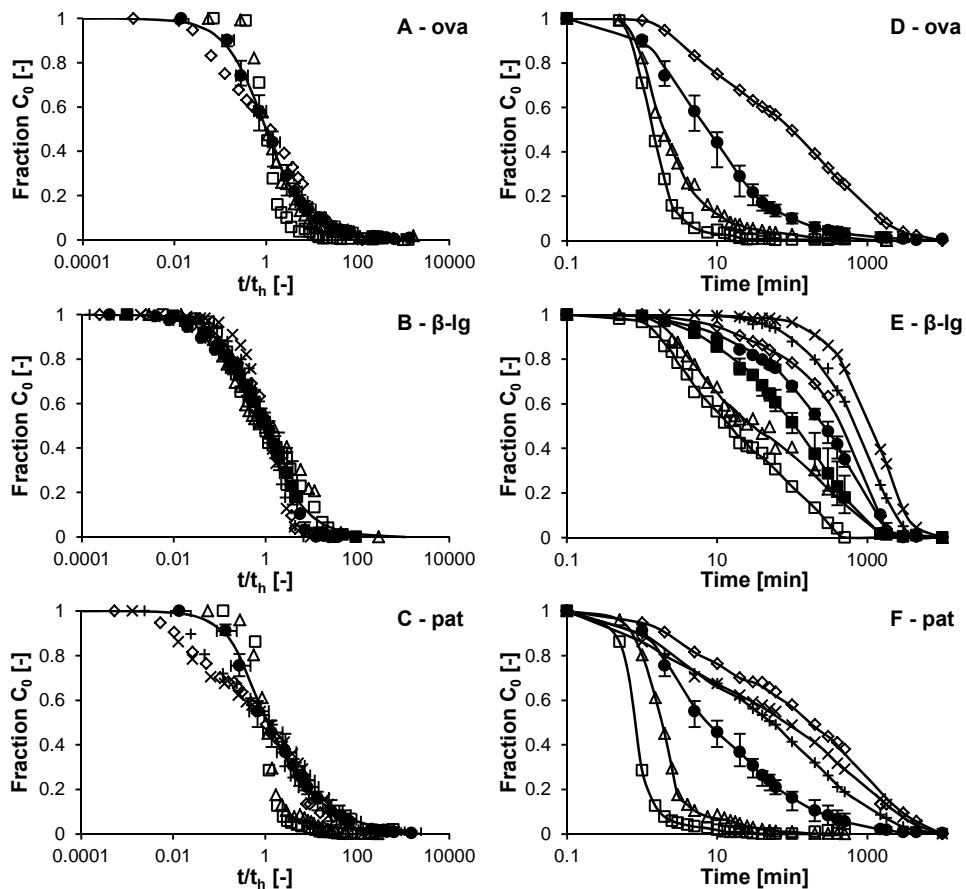


Figure 2. Fraction of non-aggregated protein (C_0) as function of the time normalized by t_h (A-C) and as function of the time (D-F) for ovalbumin (A and D), β -lactoglobulin (B and E) and patatin (C and F). The markers represent the different conditions: $T_d - 10$ °C (\diamond), T_d (\triangle), $T_d + 5$ °C (\square), pH 5.0 (\times), pH 6.0 ($+$), 5 g L⁻¹, 10 g L⁻¹, 40 mM NaCl and 90 mM NaCl (\blacksquare) and the average of all remaining conditions ($T_d - 5$ °C, 2 g L⁻¹, 10 mM NaCl and all not indicated by the other markers), with error bars indicating the variation (\bullet). Solid lines in D-F are guides to the eye. The solid lines in A-C represent the best fits ($n = 2.1$ for ovalbumin, $n = 2.5$ for β -lactoglobulin, and $n = 2.9$ for patatin).

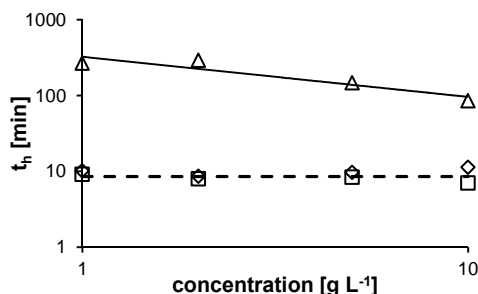


Figure 3. Concentration dependence of the time required to aggregate half of the proteins (t_h) for ovalbumin (□), β -lactoglobulin (△) and patatin (◇) heated at $T_d - 5$ °C. The solid line has a slope of -0.5 . The dashed line is a guide to the eye.

The second approach is based on fitting the decrease of the concentration non-aggregated protein in time using equations 1 and 2. For all proteins, the order of the aggregation process is higher than second order kinetics (i.e. $n = 2.5, 2.1$ and 2.9 for β -lactoglobulin, ovalbumin and patatin, respectively) (table 1). This indicates a complex aggregation process, in which non-aggregated proteins for instance aggregate with other non-aggregated proteins and aggregated proteins. The third approach is based on fitting the decrease of $\ln C_t$, $1/\sqrt{C_t}$ and $1/C_t$ in time to a linear function. This resulted in the best fit (i.e. R^2) of an aggregation order of 2.0 for ovalbumin and patatin ($R^2 = 0.95 \pm 0.04$ and 0.97 ± 0.01 for ovalbumin and patatin, respectively) (table 1). Moreover, it showed that the first order kinetics for ovalbumin and patatin, as determined by the first approach, the low R^2 (i.e. $R^2 = 0.28$) disqualifies the first order kinetics. Hence, their aggregation can well be described based on second order kinetics. The best for β -lactoglobulin was an aggregation order of 1.5 ($R^2 = 0.96 \pm 0.04$). The fit of the data of β -lactoglobulin for a second order reaction is, however, not significantly different from that of an order of 1.5. Although the aggregation process of β -lactoglobulin can overall be described by an aggregation order of 1.5 or 2.0, the aggregation process at pH 5.0 shows a better fit with first order kinetics (i.e. $R^2 = 0.99$ and 0.84 for $n = 1.0$ and 1.5 , respectively).

Summarizing, the aggregation process of all tested proteins, β -lactoglobulin, ovalbumin and patatin, is described by an order of 2.0 ($R^2 > 0.90$ for all proteins). The aggregation process of β -lactoglobulin at pH 5.0 is a first order process.

Aggregation rate

The aggregation rate (k) is determined by fitting the decrease of the concentration non-aggregated protein with equation 2. To allow quantitative comparison of the aggregation rates, the data of all proteins is fitted with an aggregation order of 2.0 ($R^2 > 0.90$ for all proteins) (table 1).

Effect of temperature (2 g L⁻¹ in 10 mM buffer pH 7.0)

Quantitatively, the effect of temperature on the aggregation rate varies significantly between the proteins (figures 2D-F and table 2). Whereas the decrease of the concentration non-aggregated protein for ovalbumin and patatin at $T_d - 5^\circ\text{C}$ (pH = 7.0, I = 10 mM and C = 2 g L⁻¹) is in the same order of magnitude (i.e. $t_h \sim 10$ min), the decrease of non-aggregated β -lactoglobulin is significantly slower (i.e. $t_h \sim 220$ min) (table 2). In addition, the temperature dependence of the aggregation rate varies significantly between the proteins. This is reflected in the activation energy (E_a), calculated using the Arrhenius equation, which was found to be 343, 295 and 221 kJ mol⁻¹ for patatin, ovalbumin and β -lactoglobulin, respectively. These activation energies are lower than reported in literature (i.e. ~ 260 -300 kJ mol⁻¹ for β -lactoglobulin^{41, 42} and 338 kJ mol⁻¹ for ovalbumin²⁴) under similar conditions (i.e. pH 6.5-7.0). As these differences between the proteins cannot be explained based on the relative exposed hydrophobicity or the net surface charge density reported previously⁴³, they are postulated to be caused by a difference in the structural stability of the proteins. β -Lactoglobulin, which has 2 disulphide bonds, is expected to unfold to a lower extent than ovalbumin and patatin. Consequently, less hydrophobic amino acids become exposed for β -lactoglobulin than for the other two proteins, leading to less non-covalent interactions.

Effect of pH (2 g L⁻¹ in 10 mM buffer heated at $T_d - 5^\circ\text{C}$)

The aggregation rate of ovalbumin is not affected by the pH in the range from pH 5 to pH 7 (figure 2D and table 2). The aggregation rates of β -lactoglobulin and patatin, on the other hand, are slower at a pH closer to the iso-electric point (pI) (i.e. t_h of 223 and 10.8 min at pH 7.0 to t_h of 1052 and 73 min at pH 5.0 for β -lactoglobulin and patatin, respectively) (figures 2E and F and table 2).

For patatin, the effect of pH seems to be due to a difference in the denaturation temperature. When the aggregation rates of patatin at pH 5 and pH 6 are compared to pH 7 at different temperatures, they are similar to pH 7 at a temperature between $T_d - 5^\circ\text{C}$ and $T_d - 10^\circ\text{C}$ (table 2). This corresponds with a theoretical increase of T_d of $\sim 4^\circ\text{C}$, which is in close agreement with literature (i.e. 3°C increase of T_d from pH 7 to pH 6⁴⁴). For β -lactoglobulin, the aggregation rate at pH 5 and pH 6 is slower than at pH 7 and $T_d - 10^\circ\text{C}$ (table 2). The observed decrease of the aggregation rate by shifting the pH towards the pI is in line with literature^{5, 7, 8, 14}. However, based on the temperature dependence of the aggregation rate (table 2), the T_d should increase by 7-10 $^\circ\text{C}$ to explain this decrease in aggregation rate. Experimentally, the T_d of β -lactoglobulin was only reported to increase by 2°C when the pH was decreased from pH 7 to pH 5¹⁶. Consequently, another factor also has to be influenced by the pH change. The association state of β -lactoglobulin, as measured by size-exclusion chromatography, was not affected by the pH changes (data not

shown). The thiol groups, on the other hand, become less reactive with decreasing pH⁸. Therefore, the decreased reactivity of the thiol groups can explain the observed differences. Effect of ionic strength (2 g L⁻¹ in buffer pH 7.0 heated at T_d - 5 °C) and concentration (10 mM buffer pH 7.0 heated at T_d - 5 °C)

For β -lactoglobulin, the aggregation rate increases with increasing ionic strength (i.e. t_h decreases from 223 min at 10 mM to 87 min at 100 mM) and protein concentration (i.e. t_h decreases from 255 min at 1 g L⁻¹ to 84 min at 10 g L⁻¹) (figure 2E and table 2). The effect of ionic strength is explained by a decrease of the electrostatic repulsion within and between the protein molecules. This was described to result in an increase of the denaturation temperature (i.e. 2 and 5 °C from 0 to 100 mM for β -lactoglobulin and BSA, respectively)^{21, 22}. In addition, it also results in a decrease of the electrostatic barrier for aggregation²³. As in this case the aggregation rate increases rather than decreases, the enhancing effect of electrostatics was more important than the observed increase of the denaturation temperature. The effect of concentration on the aggregation rate is line with previous data⁷. The effect is postulated to be caused by the fact that at higher protein concentrations the absolute number of unfolded protein increases, resulting in an increased likelihood of proteins to meet, collide and aggregate. In contrast to the observation for β -lactoglobulin, the aggregation rates of ovalbumin and patatin are neither affected by the ionic strength nor by the protein concentration (figures 2D and F). These results show that it is important to use different proteins, as the behaviour of proteins cannot be extrapolated from one protein to another.

Formation of aggregates

Whereas some protein solutions remained transparent after heating, others became translucent or opaque. These clear visual differences between the heated protein solutions are also reflected in the ionic strength dependence of the aggregated protein in time determined by SEC (figure 4).

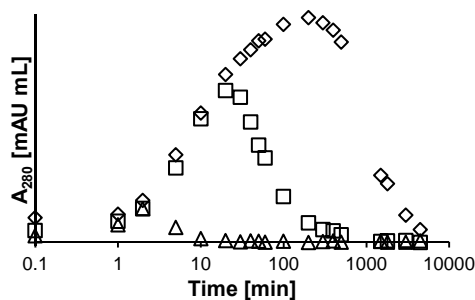


Figure 4. UV peak area of aggregated patatin (10 mM sodium phosphate buffer pH 7.0, 2 g L⁻¹, T_d - 5 °C) in time determined by size-exclusion chromatography. The markers represent samples heated at different NaCl concentrations: 0 mM NaCl (◇), 10 mM NaCl (□) and 90 mM NaCl (△).

At all ionic strengths, the UV peak area corresponding to the aggregates initially increases and subsequently decreases. This decrease shifted to shorter heating times with increasing ionic strength. This decrease at increased ionic strength and longer times is due to the formation of larger aggregates, which are removed by centrifugation prior to analysis.

Table 2. Half times (t_h) and aggregation rate (k) of the ovalbumin, β -lactoglobulin and patatin at different heating conditions.

Var.	C [g L ⁻¹]	pH	I [mM]	T [°C]	t_h [min]			k [L g ⁻¹ s ⁻¹] (n = 2) ^a		
					Ova	β -Lg	Pat	Ovalbumin	β -Lactoglobulin	Patatin
Ref	2	7	10	$T_d - 5$	8.7	223	10.8	9.64E-04	3.74E-05	7.71E-04
T	2	7	10	$T_d - 10$	8.1	330	144	1.02E-04	2.52E-05	5.78E-05
	2	7	10	T_d	2.0	29.2	1.5	4.21E-03	2.85E-04	5.66E-03
	2	7	10	$T_d + 5$	1.1	16.0	0.5	7.87E-03	5.20E-04	1.60E-02
I	2	7	20	$T_d - 5$	7.8	188	10.7	1.07E-03	4.42E-05	7.76E-04
	2	7	50	$T_d - 5$	8.7	93	9.9	9.63E-04	8.94E-05	8.38E-04
	2	7	100	$T_d - 5$	6.8	87	7.2	1.22E-03	9.63E-05	1.16E-03
C	1	7	10	$T_d - 5$	9.9	255	11.1	1.69E-03	6.53E-05	1.50E-03
	5	7	10	$T_d - 5$	8.9	128	10.8	3.75E-04	2.59E-05	3.07E-04
	10	7	10	$T_d - 5$	8.0	84	13.3	2.08E-04	1.99E-05	1.26E-04
pH	2	6	10	$T_d - 5$	7.1	621	49.1	1.17E-03	1.34E-05	1.70E-04
	2	5	10	$T_d - 5$	4.8	1052	73	1.72E-03	7.92E-06	1.14E-04

^aaggregation rate determined based on n = 2.

To obtain insights in the effect of the conditions (e.g. pH) on the formation of aggregates, the scattered light intensity is monitored in time (figures 5A-C). According to equation 4, an increase in the scattered light intensity is caused by an increase of the aggregate size and/or alterations of the aggregate shape. Based on the aggregation kinetics (table 2), the time is recalculated into the fraction aggregated protein (figures 5D-F). This provides insights in the aggregation mechanism (e.g. preference towards the formation of small or large aggregates).

For ovalbumin and β -lactoglobulin, the scattered light intensity does not significantly increase when the proteins are heated at $T_d - 5$ °C in a concentration of 2 g L⁻¹. For patatin, on the other hand, the intensity of the scattered light increases significantly (i.e. $I/I_0 = 8$ after 7200 seconds). This indicates that the patatin aggregates are larger and/or denser than the ovalbumin and β -lactoglobulin aggregates. These differences cannot be explained based

on the aggregation kinetics (i.e. t_h of ovalbumin and patatin is similar). This shows that for patatin, the formation of less, but larger aggregates is favored over more, smaller aggregates as is the case for ovalbumin and β -lactoglobulin under these conditions.

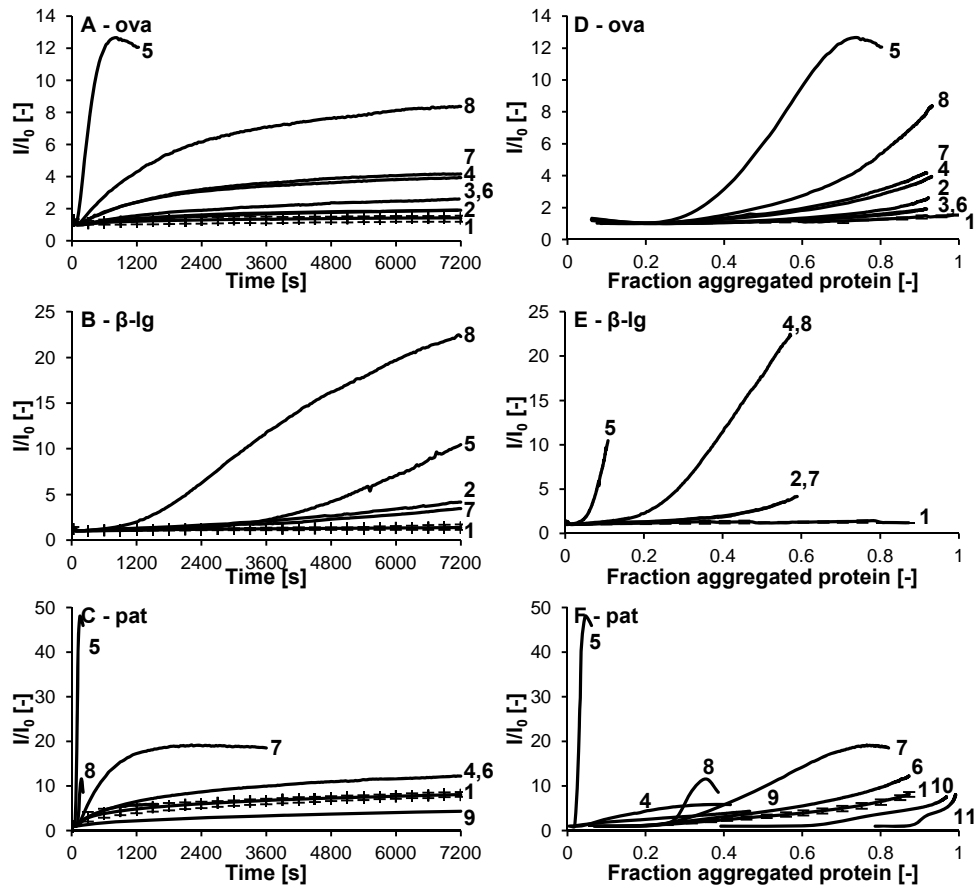


Figure 5. Normalized intensity (I/I_0) of heated ovalbumin (A and D), β -lactoglobulin (B and E) and patatin (C and F) in time (A-C) and as a function of the fraction aggregated protein (D-F). The numbers represent the different conditions: (1) T_d - 5 °C and 2 g L⁻¹ (and all conditions not indicated by the other numbers), with error bars indicating the variation, (2) 10 g L⁻¹, (3) 5 g L⁻¹, (4) pH 6.0, (5) pH 5.0, (6) 10 mM NaCl, (7) 40 mM NaCl, (8) 90 mM NaCl, (9) T_d - 10°C, (10) T_d and (11) T_d + 5 °C.

Effect of pH and ionic strength

For β -lactoglobulin, a lag phase precedes the intensity increase (figure 5B). Moreover, the intensity of the scattered light in time increases for all three proteins (i.e. ovalbumin, β -lactoglobulin and patatin) with increasing ionic strength or a shift of the pH towards the

pI (figures 5A-C). The intensity, however, increases more strongly for patatin (i.e. $I/I_0 = 47$ and 12 after 200 seconds for pH 5 and 100 mM, respectively) compared to β -lactoglobulin (i.e. $I/I_0 = 10$ and 22 after 7200 seconds for pH 5 and 100 mM, respectively) and ovalbumin (i.e. $I/I_0 = 12$ after 900 seconds and 8 after 7200 seconds for pH 5 and 100 mM, respectively). The observed lag phase for β -lactoglobulin has also been reported in literature where it is ascribed to the monomer-dimer equilibrium⁴⁵ or the formation of small aggregates¹⁶. Furthermore, it was concluded that a decrease of the electrostatic repulsion results in the formation of larger and/or denser aggregates. This is explained by a lower electrostatic repulsion between the aggregates. Consequently, aggregates can continue to grow to larger sizes and/or the formed aggregates are denser. In literature, the molecular mass and size of β -lactoglobulin aggregates were also described to increase when the pH shifts towards the pI and/or the ionic strength increases^{8, 46, 47}. However, as shown, this effect is not the same for all proteins. The difference among the proteins indicates that the magnitude by which the aggregate size/structure in time is affected by electrostatics is dependent on the protein.

Recalculating time into the fraction aggregated protein provides information on the mechanism of aggregation (figures 5D-F). Close to the pI (i.e. pH 5), for patatin and β -lactoglobulin, the intensity increases with the incorporation of even a minor fraction of the protein into the aggregates (i.e. $\sim 5\%$) (figures 5E and F). For ovalbumin, the intensity increases after $\sim 25\%$ of the protein aggregated (figure 5D). At a pH away from the pI or at lower ionic strength, a larger fraction aggregated protein is required for the intensity to increase. These results show that for patatin and β -lactoglobulin at low electrostatic repulsion (i.e. pH 5) even in the initial stages (i.e. $< 10\%$ aggregated protein) large and/or dense aggregates are formed. For ovalbumin, on the other hand, the lag phase indicates that initially (i.e. $< 25\%$ aggregated protein) smaller and/or more open aggregates are formed. Subsequently, at a higher fraction of aggregated protein, large and/or denser aggregates are formed. Similarly, also at higher electrostatic repulsion initially smaller and/or more open aggregates are formed, followed by the formation of larger and/or denser aggregates. The differences between the proteins show that patatin has the highest tendency to form larger and/or denser aggregates.

Effect of concentration and temperature

In general, changes in temperature or concentration resulted only in minor changes of the intensity as function of heating time (figures 5A-C). This shows that these two parameters do not affect the aggregate formation (i.e. size and structure) as strongly as ionic strength or pH. For patatin, the intensity is concentration independent, whereas it decreases with decreasing temperature (i.e. $I/I_0 = 4$ after 7200 seconds) (figure 5C). For β -lactoglobulin and ovalbumin, the intensity in time increases slightly with increasing concentration (i.e. $I/I_0 = 4$ and 3 at 10 g L^{-1} after 7200 seconds for β -lactoglobulin and ovalbumin,

respectively) (figures 5A and B). This increase is in line with literature, as the mass and size of β -lactoglobulin aggregates have been described to increase with concentration (at higher concentrations until 110 g L^{-1})^{7, 28, 48}. The effect of temperature on the aggregation of patatin is expected to be purely determined by kinetics, as a consequence the aggregate formation in time is decelerated.

From the intensity as function of the fraction aggregated protein it can be observed that, even at large fractions of aggregated protein, the intensity is not affected by concentration and temperature. This confirms that, also after correcting for the aggregation kinetics, the aggregate size and structure are independent of temperature and concentration. Hence, at high electrostatic repulsion (i.e. pH 7.0 and 10 mM), relatively small and/or open aggregates are formed.

In summary, the aggregate formation is limited by the electrostatic repulsion between the protein (aggregates) due to the protein charge. In case of screening of the charge (i.e. increased ionic strength) or a decreased surface charge (i.e. pH closer to pI), this electrostatic barrier decreases and larger and/or denser aggregates are formed. Concentration and temperature, on the other hand, did not strongly affect the aggregate size and/or structure. Although for all proteins aggregate formation was qualitatively similar, quantitatively the behaviour was significantly different. This shows that the information on one protein cannot directly be related to another protein. In general, ovalbumin showed to have the least tendency to form larger and/or denser aggregates, followed by β -lactoglobulin. Patatin, on the other hand, directly forms large and/or dense aggregates.

Conclusion

The aggregation rate of β -lactoglobulin was found to be more than 10 times slower than that for patatin and ovalbumin. This difference was postulated to be caused by a difference in structural stability as it could not be explained based on differences in the basic molecular properties, such as surface charge and exposed hydrophobicity. In addition, the aggregation rate of β -lactoglobulin was affected by pH, ionic strength and concentration, while the aggregation rate of patatin and ovalbumin was not affected by these parameters. Furthermore, the aggregation order can neither be applied as a descriptor for the aggregation behaviour nor for the aggregate formation. Moreover, a decrease of the electrostatic repulsion resulted in the formation of larger and/or denser aggregates for all proteins. In contrast to the expectations based on the similar surface charge, the quantitative effect of the electrostatic interactions varied among the proteins. Ovalbumin showed the least tendency to form larger, denser aggregates, followed by β -lactoglobulin and patatin. These results show that the behaviour of one protein can only be partly extrapolated to that of another protein.

References

1. Pauling, L., Protein interactions: aggregation of globular proteins. *Discuss. Faraday Soc.* **1953**, 13, 170-176.
2. Creighton, T. E., *Proteins: structure and molecular properties*. 2 ed.; W.H. Freeman: New York, NY, USA, 2002.
3. Lumry, R.; Eyring, H., Conformation changes of proteins. *J. Phys. Chem.* **1954**, 58, (2), 110-120.
4. Mahler, H.-C.; Müller, R.; Frieß, W.; Delille, A.; Matheus, S., Induction and analysis of aggregates in a liquid IgG1-antibody formulation. *Eur. J. Pharm. Biopharm.* **2005**, 59, (3), 407-417.
5. Roefs, S. P. F. M.; de Kruijff, K. G., A model for the denaturation and aggregation of β -lactoglobulin. *Eur. J. Biochem.* **1994**, 226, (3), 883-889.
6. Weijers, M.; Barneveld, P. A.; Cohen Stuart, M. A.; Visschers, R. W., Heat-induced denaturation and aggregation of ovalbumin at neutral pH described by irreversible first-order kinetics. *Protein Sci.* **2003**, 12, (12), 2693-2703.
7. Le Bon, C.; Nicolai, T.; Durand, D., Kinetics of aggregation and gelation of globular proteins after heat-induced denaturation. *Macromolecules* **1999**, 32, (19), 6120-6127.
8. Hoffmann, M. A. M.; van Mil, P. J. J. M., Heat-induced aggregation of β -lactoglobulin as a function of pH. *J. Agric. Food Chem.* **1999**, 47, (5), 1898-1905.
9. Yohannes, G.; Wiedmer, S. K.; Elomaa, M.; Jussila, M.; Aseyev, V.; Riekkola, M.-L., Thermal aggregation of bovine serum albumin studied by asymmetrical flow field-flow fractionation. *Anal. Chim. Acta* **2010**, 675, (2), 191-198.
10. Weijers, M.; Visschers, R. W.; Nicolai, T., Influence of the ionic strength on the structure of heat-set globular protein gels at pH 7. Ovalbumin. *Macromolecules* **2004**, 37, (23), 8709-8714.
11. Krebs, M. R. H.; Devlin, G. L.; Donald, A. M., Protein particulates: another generic form of protein aggregation? *Biophys. J.* **2007**, 92, (4), 1336-1342.
12. van Boekel, M. A. J. S., *Kinetic modeling of reactions in foods*. CRC Press: Boca Raton, FL, USA, 2009.
13. Hoffmann, M. A. M.; Roefs, S. P. F. M.; Verheul, M.; van Mil, P. J. J. M.; de Kruijff, K. G., Aggregation of β -lactoglobulin studied by in situ light scattering. *J. Dairy Res.* **1996**, 63, (3), 423-440.
14. Verheul, M.; Roefs, S. P. F. M., Structure of particulate whey protein gels: effect of NaCl, concentration, pH, heating temperature, and protein composition. *J. Agric. Food Chem.* **1998**, 46, (12), 4909-4916.
15. Le Bon, C.; Nicolai, T.; Durand, D., Growth and structure of aggregates of heat-denatured β -lactoglobulin. *Int. J. Food Sci. Technol.* **1999**, 34, (5-6), 451-465.
16. Verheul, M.; Roefs, S. P. F. M.; de Kruijff, K. G., Kinetics of heat-induced aggregation of β -lactoglobulin. *J. Agric. Food Chem.* **1998**, 46, (3), 896-903.
17. Mahler, H.-C.; Friess, W.; Grauschopf, U.; Kiese, S., Protein aggregation: pathways, induction factors and analysis. *J. Pharm. Sci.* **2009**, 98, (9), 2909-2934.
18. Wang, W.; Nema, S.; Teagarden, D., Protein aggregation - pathways and influencing factors. *Int. J. Pharm.* **2010**, 390, (2), 89-99.
19. Chi, E. Y.; Krishnan, S.; Randolph, T. W.; Carpenter, J. F., Physical stability of proteins in aqueous solution: mechanism and driving forces in nonnative protein aggregation. *Pharm. Res.* **2003**, 20, (9), 1325-1336.
20. Speed, M. A.; King, J.; Wang, D. I. C., Polymerization mechanism of polypeptide chain aggregation. *Biotechnol. Bioeng.* **1997**, 54, (4), 333-343.
21. Haug, I. J.; Skar, H. M.; Vegarud, G. E.; Langsrud, T.; Draget, K. I., Electrostatic effects on β -lactoglobulin transitions during heat denaturation as studied by differential scanning calorimetry. *Food Hydrocolloids* **2009**, 23, (8), 2287-2293.

22. Giancola, C.; De Sena, C.; Fessas, D.; Graziano, G.; Barone, G., DSC studies on bovine serum albumin denaturation. Effects of ionic strength and SDS concentration. *Int. J. Biol. Macromol.* **1997**, *20*, (3), 193-204.
23. De Young, L. R.; Fink, A. L.; Dill, K. A., Aggregation of globular proteins. *Acc. Chem. Res.* **1993**, *26*, (12), 614-620.
24. Broersen, K.; Weijers, M.; de Groot, J.; Hamer, R. J.; de Jongh, H. H. J., Effect of protein charge on the generation of aggregation-prone conformers. *Biomacromolecules* **2007**, *8*, (5), 1648-1656.
25. Mehalebi, S.; Nicolai, T.; Durand, D., The influence of electrostatic interaction on the structure and the shear modulus of heat-set globular protein gels. *Soft Matter* **2008**, *4*, 893-900.
26. Mine, Y., Laser light scattering study on the heat-induced ovalbumin aggregates related to its gelling property. *J. Agric. Food Chem.* **1996**, *44*, (8), 2086-2090.
27. Choi, S. J.; Moon, T. W., Influence of sodium chloride and glucose on the aggregation behavior of heat-denatured ovalbumin investigated with a multiangle laser light scattering technique. *J. Food Sci.* **2008**, *73*, (2), C41-C49.
28. Durand, D.; Gimel, J. C.; Nicolai, T., Aggregation, gelation and phase separation of heat denatured globular proteins. *Phys. A* **2002**, *304*, (1-2), 253-265.
29. Pots, A. M.; ten Grotenhuis, E.; Gruppen, H.; Voragen, A. G. J.; de Kruif, K. G., Thermal aggregation of patatin studied in situ. *J. Agric. Food Chem.* **1999**, *47*, (11), 4600-4605.
30. Weijers, M.; Visschers, R. W.; Nicolai, T., Light scattering study of heat-induced aggregation and gelation of ovalbumin. *Macromolecules* **2002**, *35*, (12), 4753-4762.
31. Mehalebi, S.; Nicolai, T.; Durand, D., Light scattering study of heat-denatured globular protein aggregates. *Int. J. Biol. Macromol.* **2008**, *43*, (2), 129-135.
32. Mahmoudi, N.; Mehalebi, S.; Nicolai, T.; Durand, D.; Riaublanc, A., Light-scattering study of the structure of aggregates and gels formed by heat-denatured whey protein isolate and β -lactoglobulin at neutral pH. *J. Agric. Food Chem.* **2007**, *55*, (8), 3104-3111.
33. Baussay, K.; Le Bon, C.; Nicolai, T.; Durand, D.; Busnel, J. P., Influence of the ionic strength on the heat-induced aggregation of the globular protein β -lactoglobulin at pH 7. *Int. J. Biol. Macromol.* **2004**, *34*, (1-2), 21-28.
34. Gimel, J. C.; Durand, D.; Nicolai, T., Structure and distribution of aggregates formed after heat-induced denaturation of globular proteins. *Macromolecules* **1994**, *27*, (2), 583-589.
35. Pouzot, M.; Durand, D.; Nicolai, T., Influence of the ionic strength on the structure of heat-set globular protein gels at pH 7. β -lactoglobulin. *Macromolecules* **2004**, *37*, (23), 8703-8708.
36. Yan, Y.; Seeman, D.; Zheng, B.; Kizilay, E.; Xu, Y.; Dubin, P. L., pH-dependent aggregation and disaggregation of native β -lactoglobulin in low salt. *Langmuir* **2013**, *29*, (14), 4584-4593.
37. Hoffmann, M. A. M.; Sala, G.; Olieman, C.; de Kruif, K. G., Molecular mass distributions of heat-induced β -lactoglobulin aggregates. *J. Agric. Food Chem.* **1997**, *45*, (8), 2949-2957.
38. Creusot, N.; Wierenga, P. A.; Laus, M. C.; Giuseppin, M. L. F.; Gruppen, H., Rheological properties of patatin gels compared with β -lactoglobulin, ovalbumin, and glycinin. *J. Sci. Food Agric.* **2011**, *91*, (2), 253-261.
39. van Koningsveld, G. A.; Gruppen, H.; de Jongh, H. H. J.; Wijngaards, G.; van Boekel, M. A. J. S.; Walstra, P.; Voragen, A. G. J., Effects of pH and heat treatments on the structure and solubility of potato proteins in different preparations. *J. Agric. Food Chem.* **2001**, *49*, (10), 4889-4897.
40. Podzimek, S., *Light scattering, size exclusion chromatography and asymmetric flow field flow fractionation*. John Wiley: Hoboken, NJ, USA, 2011.
41. Anema, S. G.; McKenna, A. B., Reaction kinetics of thermal denaturation of whey proteins in heated reconstituted whole milk. *J. Agric. Food Chem.* **1996**, *44*, (2), 422-428.

42. Dannenberg, F.; Kessler, H.-G., Reaction kinetics of the denaturation of whey proteins in milk. *J. Food Sci.* **1988**, *53*, (1), 258-263.
43. Delahaije, R. J. B. M.; Wierenga, P. A.; van Nieuwenhuijzen, N. H.; Giuseppin, M. L. F.; Gruppen, H., Protein concentration and protein-exposed hydrophobicity as dominant parameters determining flocculation of protein-stabilized oil-in-water emulsions. *Langmuir* **2013**, *29*, (37), 11567-11574.
44. Pots, A. M.; de Jongh, H. H. J.; Gruppen, H.; Hessing, M.; Voragen, A. G. J., The pH dependence of the structural stability of patatin. *J. Agric. Food Chem.* **1998**, *46*, (7), 2546-2553.
45. Elofsson, U. M.; Dejmek, P.; Paulsson, M. A., Heat-induced aggregation of β -lactoglobulin studied by dynamic light scattering. *Int. Dairy J.* **1996**, *6*, (4), 343-357.
46. Bauer, R.; Carrotta, R.; Rischel, C.; Øgendal, L., Characterization and isolation of intermediates in β -lactoglobulin heat aggregation at high pH. *Biophys. J.* **2000**, *79*, (2), 1030-1038.
47. Zúñiga, R.; Tolkach, A.; Kulozik, U.; Aguilera, J., Kinetics of formation and physicochemical characterization of thermally-induced β -lactoglobulin aggregates. *J. Food Sci.* **2010**, *75*, (5), E261-E268.
48. Ako, K.; Nicolai, T.; Durand, D., Salt-induced gelation of globular protein aggregates: Structure and kinetics. *Biomacromolecules* **2010**, *11*, (4), 864-871.

Chapter 3

Protein concentration and protein exposed hydrophobicity as dominant parameters determining flocculation of protein-stabilized oil-in-water emulsions

Abstract

The DLVO theory is often considered applicable for the description of flocculation of protein-stabilized oil-in-water emulsions. To test this, emulsions made with different globular proteins (β -lactoglobulin, ovalbumin, patatin and two variants of ovalbumin) were compared under different conditions (pH and electrolyte concentration). As expected, flocculation was observed under conditions in which the zeta potential is decreased (around the iso-electric point and at high ionic strength). However, the extent of flocculation at higher ionic strength (> 50 mM NaCl) decreased with increasing protein exposed hydrophobicity. A higher exposed hydrophobicity resulted in a higher zeta potential of the emulsion droplets, and consequently in increased stability against flocculation. Furthermore, the addition of excess protein strongly increased the stability against salt induced flocculation, which is not described by the DLVO theory. In the protein poor regime, emulsions showed flocculation at high ionic strength (> 100 mM NaCl), whereas the emulsions were stable against flocculation if excess protein was present. This research shows that the exposed hydrophobicity of the proteins, and the presence of excess protein affect the flocculation behaviour.

Based on: Delahaije, R.J.B.M.; Wierenga, P.A.; van Nieuwenhuijzen, N.H.; Giuseppin, M.L.F.; Gruppen, H. Protein concentration and protein-exposed hydrophobicity as dominant parameters determining flocculation of protein-stabilized oil-in-water emulsions. *Langmuir* **2013**, 29, (37), 11567-11574.

Introduction

Proteins are an important class of emulsifiers in food products. Proteins can facilitate the formation and increase the stability of oil-in-water emulsions due to their ability to adsorb to the interface and to lower the surface tension^{1, 2}. In addition, the presence of adsorbed protein layers can help to protect the emulsion against destabilization mechanisms, such as creaming, coalescence and flocculation^{3, 4}. In literature, flocculation, which can also lead to coalescence, is attributed to attractive interactions between the droplets^{5, 6}. To overcome the attractive interactions and prevent flocculation, repulsive interactions (e.g. electrostatic, or steric interactions) should be of sufficient range and strength².

The stabilizing effect of electrostatic repulsion has been shown for β -lactoglobulin and whey protein isolate (WPI)⁷⁻¹⁰. Under conditions of low electrostatic repulsion (i.e. around the iso-electric point (pI) or at high ionic strength) flocculation was observed, while it is prevented under conditions of high electrostatic repulsion (i.e. pH away from the pI or at low ionic strength). Model systems with thin liquid oil-water-oil films of β -lactoglobulin and BSA in combination with modelling showed that a combination of electrostatic repulsion and van der Waals attraction (which are combined in the DLVO theory) with an additional steric like repulsion can explain the interactions between two adsorbed protein interfaces¹¹⁻¹³. However, these steric repulsive interactions only act over short length scale (twice the layer thickness) and therefore do not affect the flocculation behaviour of emulsion stabilized by globular proteins^{14, 15}. In addition to the DLVO interactions and steric repulsion, exposed hydrophobicity and the associated attractive hydrophobic interactions are postulated to promote flocculation¹⁴.

Despite the research on emulsion destabilization, no quantitative relation has been reported to describe flocculation. This study aims to provide generic insights in the extent to which emulsion flocculation is determined by typical properties of the proteins, or by physical properties of the emulsion droplets. To achieve this, emulsions are prepared with five different globular proteins (β -lactoglobulin, ovalbumin, patatin and two types of modified ovalbumin), that vary in their exposed hydrophobicity^{16, 17}. Hence they can be used to modulate the strength of the hydrophobic interactions. In addition, the factors affecting the strength of the DLVO forces (i.e. Debye screening length, zeta potential and droplet radius) are studied. Therefore, the stability against flocculation is studied under different pH's and electrolyte concentrations to modulate the electrostatic interactions (zeta potential and Debye screening length). Next to this, different protein concentrations are used to study the effect of droplet radius. The occurrence of flocculation is characterized by the average droplet size and droplet mobility, which are respectively determined by laser diffraction and diffusing wave spectroscopy (DWS).

Materials and methods

Materials

Ovalbumin (Ova; A-5503) and β -lactoglobulin (β -lg; L-0130) were purchased from Sigma-Aldrich (St. Louis, MO, USA). Patatin Rich Fraction (PRF; Solanic 206P, ref n° 485882) was provided by AVEBE/Solanic (Foxhol, The Netherlands). Patatin from cv. Elkana was isolated as described previously¹⁷. Ovalbumin from hen egg white were isolated described previously¹⁶. From this ovalbumin, two variants were produced, that have increased hydrophobicity: A heat stable S-ovalbumin¹⁸ and a variant obtained by chemical modification with caprylic acid, Lipo. ovalbumin¹⁶. All chemicals were of analytical grade and purchased from either Sigma-Aldrich or Merck (Darmstadt, Germany).

Protein solutions

All proteins were dissolved overnight at 4 °C in 10 mM sodium phosphate buffer with varying pH (3.0, 4.0, 4.5, 5.0, 5.5, 6.0 and 7.0) at a concentration of 10 g L⁻¹. In addition, one set of samples was prepared by dissolving in 10 mM sodium phosphate buffer pH 7.0 and subsequently adjusting the ionic strength by addition of NaCl to final concentrations of 10, 20, 30, 60, 110 and 210 mM.

Determination of zeta potential

Zeta potentials of the protein solutions (10 g L⁻¹) were determined using a Zetasizer 2000 (Malvern Instruments, Worcestershire, UK). Measurements were performed at 25 °C and averaged from five sequential runs. Zeta potentials were calculated with Henry's equation¹⁹ (equation 1).

$$\zeta = \frac{3\eta \cdot \mu_e}{2\varepsilon F(\kappa\alpha)} \quad (1)$$

in which ζ is the zeta potential [V], η is the viscosity [Pa s], μ_e is the electrophoretic mobility [m² V⁻¹ s⁻¹], ε is the dielectric constant of the medium [C² J⁻¹ m⁻¹] and $F(\kappa\alpha)$ is Henry's function [-], which equals 1.5 by using the Smoluchowski approximation¹⁹.

Quantification of exposed hydrophobicity

Protein exposed hydrophobicity was determined by a fluorescence assay using 8-anilino-1-naphthalenesulfonic acid (ANSA) as fluorescent probe. The increase in fluorescence intensity upon binding of the probe to the accessible hydrophobic regions of the protein is used as a measure of protein surface hydrophobicity²⁰. The measurements were performed as described elsewhere¹⁶. The protein solutions (0.1 g L⁻¹) and ANSA solution (2.4 mM) were dissolved in 10 mM sodium phosphate buffer pH 7.0. Aliquots of 10 μ L ANSA solution were titrated to 1 mL of protein solution. The solution was excited at

385 nm, and the emission spectrum was measured from 400-650 nm using a Varian Cary Eclipse Fluorescence Spectrophotometer (Agilent Technologies, Santa Clara, CA, USA). The emission and excitation slits were set to 5 nm and the measurements were performed at 25 °C. The maximum area of the fluorescence spectrum was corrected with the area of the buffer. Subsequently the relative exposed hydrophobicity was expressed as the area of the sample relative to area of the sample with the maximum area.

Emulsion preparation

Emulsions were prepared by mixing 90 % (v/v) protein solution pH 7.0 and 0 mM NaCl with 10 % (v/v) sunflower oil. A pre-emulsion was prepared using an ultra turrax Type T-25B (IKA, Staufen, Germany) at 9500 rpm for 1 min. Subsequently, the pre-emulsion is passed 30 times through a Labhoscope 2.0 laboratory scale high-pressure homogenizer (Delta Instruments, Drachten, The Netherlands) operated at 15 MPa. Three different sets of experiments were performed;

Effect of pH and ionic strength To test the effects of the Debye screening length and/or zeta potential, emulsions were prepared with a protein solution (pH 7.0, 0 mM NaCl) of 5 g L⁻¹. After emulsification, the pH and the ionic strength were set with 0.1 M HCl or 2 M NaCl to the same pH or conductivity as the protein solutions.

Effect of protein concentration To test the effect of droplet radius, emulsions were prepared in 10 mM sodium phosphate buffer pH 7.0 at different protein concentrations. For β -lactoglobulin, concentrations of 1, 1.5, 2, 2.5, 5 and 10 g L⁻¹, and for ovalbumin and PRF, concentrations of 2.5, 5, 7.5, 10, 15 and 20 g L⁻¹ were studied. After emulsification, the ionic strength of the emulsions was adjusted by the addition of 2 M NaCl to final concentrations of 10, 20, 30, 60, 110 and 210 mM NaCl in the emulsion.

Effect of excess protein To determine the effect of excess protein, emulsions were prepared with (1) β -lactoglobulin (1.5, 2 and 2.5 g L⁻¹); (2) ovalbumin (5 and 7.5 g L⁻¹); and (3) PRF (7.5, 10 and 15 g L⁻¹) in 10 mM sodium phosphate buffer pH 7.0. After emulsification, the protein concentration was adjusted to a final concentration of 5 g L⁻¹ for β -lactoglobulin, and to 20 g L⁻¹ for ovalbumin and PRF. The ionic strength of these emulsions was then adjusted to 10 or 100 mM NaCl with 2 M NaCl.

Subsequently, the emulsions were stored for 24 hours at 20 °C prior to further analysis. For selected samples, it was confirmed that no significant changes occurred during this storage period.

Determination of flocculation

Laser diffraction

Droplet size distribution was measured using laser light diffraction (Mastersizer 2000, Malvern Instruments) equipped with a Hydro SM sample dispersion unit. The

volume-surface average diameter ($d_{3,2}$) (equation 2) was reported as an average of at least five runs.

$$d_{3,2} = \frac{\sum N_i d_i^3}{\sum N_i d_i^2} \quad (2)$$

in which N_i and d_i represent the number and diameter of droplets of size class i , respectively. The volume surface average diameter was expressed relative to the average diameter at pH 7.0 or 0 mM NaCl for the pH ($d_{3,2}/d_{3,2, \text{pH7}}$) and ionic strength ($d_{3,2}/d_{3,2, 0\text{mM}}$) range respectively.

Diffusing wave spectroscopy (DWS)

To determine droplet mobility as indication of droplet flocculation, DWS measurements were performed as described previously²¹. The correlation function was averaged from five sequential runs of 120 seconds. The correlation function was normalized by dividing the obtained $g_2(t)-1$ values by the maximum measured value. Normalized autocorrelation curves were fitted assuming that the equation used by Ruis et al.²¹ to describe the autocorrelation function can be simplified to equation 3.

$$g_2(t) - 1 \approx (e^{-\langle \Delta r^2(t) \rangle})^2 \approx e^{-\alpha t} \quad (3)$$

The decay time ($\tau_{1/2}$), which is defined as the time at which $g_2(t)-1$ decayed to half of its initial value, was determined using the fitted equation. An increase of the decay time is related to decreased droplet mobility^{22, 23}. To correct for differences in the initial droplet sizes, the decay time was expressed relative to the decay time at pH 7.0 and 10 mM NaCl for the pH ($\tau_{1/2}/\tau_{1/2, \text{pH7}}$) and ionic strength ($\tau_{1/2}/\tau_{1/2, 0\text{mM}}$) range, respectively.

Microscopy

The presence of flocculated droplets and absence of coalescence was verified by light microscopy using an Axioscope A01 (Carl Zeiss, Sliedrecht, The Netherlands) at a magnification of 40x. Moreover, SDS has been added to a final concentration of 0.3 % to show that the flocculates dissociate.

Determination of zeta potential of emulsion droplets

Zeta potentials of the emulsion droplets were determined with a Zetasizer Nano ZS (Malvern Instruments) using the laser Doppler velocimetry technique. The emulsions were diluted 500 times to prevent multiple scattering. The measurements were performed at 25 °C and 40 Volt. Five sequential runs were averaged to obtain the results. Zeta potentials were calculated with the equation 1.

Determination of surface load

The amount of protein adsorbed on the emulsion droplets (surface load, Γ [mg m^{-2}]) was estimated based on the surface area and the decrease in serum protein concentration using equation 4²⁴.

$$\Gamma = \frac{(C_{ini} - C_{serum}) \cdot V_{serum}}{A} \quad (4)$$

in which C_{ini} and C_{serum} [mg L^{-1}] are the initial and serum protein concentration respectively, V_{serum} is the volume of the serum [L]. The total oil-water interfacial area (A [m^2]) was calculated as $A = 3V_{oil} / 0.5d_{3,2}$, with V_{oil} the volume of oil in the emulsion [m^3] and $d_{3,2}$ the volume surface average diameter [m].

Emulsions were prepared with (1) β -lactoglobulin (1, 1.5, 2, 2.5, 5 and 10 g L^{-1}) and (2) ovalbumin (2.5, 5, 7.5, 10, 15, 20 g L^{-1}). The emulsions were centrifuged for 1 hour at 7000g to separate the cream from the serum phase. Subsequently, the serum phase was diluted with 10 mM sodium phosphate buffer pH 7.0 to a protein concentration of 1 g L^{-1} (based on the initial protein concentration) and the protein concentration in the serum phase (C_{serum}) was determined using the BCA protein assay (Pierce, Rockford, IL, USA).

Theoretical prediction of droplet flocculation

Theoretical predictions were based on the DLVO theory. This theory assumes that the overall interaction potential (U_{tot}) between two protein-stabilized emulsion droplets is the result of a combination of van der Waals (U_{vdw}) and electrostatic (U_e) interactions (equation 5)^{8, 12, 14}.

$$U_{tot}(h) = U_{vdw}(h) + U_e(h) \quad (5)$$

where h is the separation distance between the droplets.

To test the agreement between theory and experiment, theoretical calculations are performed to predict the magnitude of the colloidal interactions between the droplets. The van der Waals and electrostatic interactions are respectively described by equations 6 and 7^{8, 14}.

$$U_{vdw} = -\frac{A}{6} \left(\frac{2R^2}{4Rh + h^2} + \frac{2R^2}{4R^2 + 4Rh + h^2} + \ln \left(\frac{4Rh + h^2}{4R^2 + 4Rh + h^2} \right) \right) \quad (6)$$

$$U_e = 2\pi\epsilon_0\epsilon_r R\Psi_0^2 e^{-\kappa h} \quad (7)$$

where κ for a monovalent electrolyte is described by equation 8^{25, 26}.

$$\kappa = \sqrt{\frac{2N_a e^2 I}{\epsilon_0 \epsilon_r k_B T}} \quad (8)$$

in which A is the Hamaker constant [5.35×10^{-21} J]²⁷, R is the droplet radius [m], ϵ_0 is the dielectric constant of a vacuum [8.85×10^{-12} C² J⁻¹ m⁻¹], ϵ_r is the relative dielectric constant of the medium (80), Ψ_0 is the surface potential of the droplets [V], κ is the reciprocal of the Debye screening length [m⁻¹], N_a is the Avogadro constant [6.022×10^{23} mol⁻¹], e is the

elementary charge [1.602×10^{-19} C], I is the ionic strength [mol m^{-3}], k_B is the Boltzmann constant [1.38×10^{-23} J K $^{-1}$] and T is the temperature [K].

As a critical barrier, which is the demarcation between systems stable and unstable towards flocculation, an interaction potential of 5 kT is used^{28, 29}. Flocculation occurs when the primary maximum decreases below 5 kT or the secondary minimum decreases below -5 kT (U_{cr}). Subsequently, the theoretical calculations will be compared with theory to determine to which extent the DLVO theory coincides with the experimental data. The interaction potential is calculated using the droplet zeta potential³⁰, the average droplet size and Debye screening length.

Thin film exchange experiment

The effect of excess protein is further investigated in a controlled model experiment using a modified Sheludko-type thin film exchange cell³¹. β -Lactoglobulin solutions (1 g L^{-1}) are equilibrated in the cell for five minutes in order for the proteins to adsorb. Subsequently, liquid is removed to form a circular thin liquid film with a radius of 100 μm . The equilibrium film thickness is calculated with a Matlab routine based on the intensity of the reflected monochromatic light, calculated from the average light intensity of the pixels in a circle with a radius of 25 μm in the centre of film, using equation 9³².

$$h = \frac{\lambda}{n2\pi} \cdot \arcsin \left(\sqrt{\frac{I - I_{\min}}{I_{\max} - I_{\min}}} \right) \quad (9)$$

in which λ is the wavelength of the light ($\lambda = 546 \text{ nm}$), n is the refractive index of the film, I is the intensity of the reflected light and I_{\min} and I_{\max} are the minimum and maximum intensity, respectively.

Next, the bulk solution is exchanged and the subsequent equilibrium film thickness is determined as described above.

Results and discussion

Protein characteristics

The five proteins used in this study were characterized with respect to their physico-chemical properties in solution. The zeta potential of the proteins at pH 7 varies from -14 to -22 mV (figure 1A). This is in line with theoretical estimations of the net surface charge density (σ_w) based on the primary sequence of the proteins (table 1). With decreasing pH and increasing ionic strength, for all proteins a similar increase in zeta potential is observed (figure 2). While the zeta potentials were similar, significant differences between the relative exposed hydrophobicity of the proteins are observed (figure 1B). Since the differences in zeta potential are negligible, differences in the

flocculation behaviour of the different proteins are expected to be caused by the differences in hydrophobic rather than electrostatic interactions.

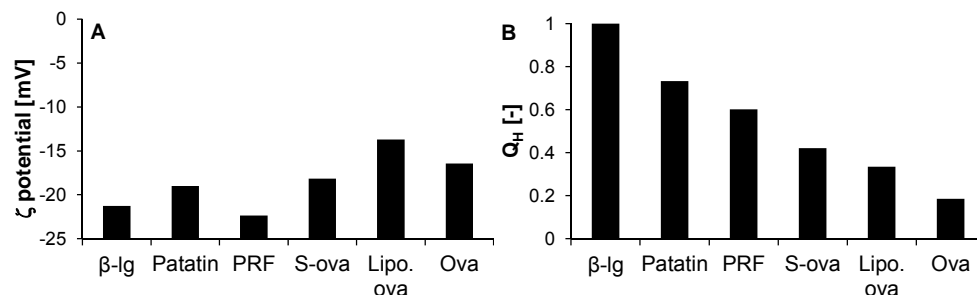


Figure 1. (A) Zeta potential of different globular proteins at pH 7.0. (B) Relative exposed hydrophobicity (Q_H) of different proteins (0.1 g L^{-1}) at pH 7.0 as determined by ANSA fluorescence.

Table 1. Protein parameters as obtained from the Swiss-Prot database (<http://www.expasy.org>)

Protein	Expsy Code	M _w [kDa]	pI	#COOH/ #NH ₂ ^a	σ _w ^b [mC m ⁻²]	Q _H [-]
β-lactoglobulin	P02754	18.4	4.83	26/18	-21.9	1.00
Patatin ^c	P07745	40.0	5.25	43/32	-17.9	0.73
Ovalbumin ^d	P01012	44.5	5.19	47/35	-24.2	0.19

^a#COOH and #NH₂ are the maximum number of negatively charged (aspartic and glutamic acid) and positively charged (arginine and lysine) groups in the primary sequence, respectively.

^bσ_w is the theoretical net surface charge density at pH 7.0.

^cPRF is assumed to have the same protein parameters as patatin.

^dLipo. ovalbumin and S-ovalbumin is assumed to have the same protein parameters as ovalbumin (except the relative exposed hydrophobicity (see figure 1B)).

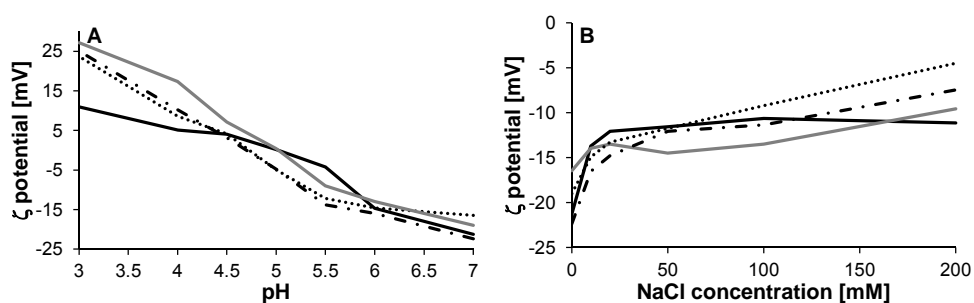


Figure 2. Zeta potential of ovalbumin (solid, grey), β-lactoglobulin (solid, black), patatin (dot, black) and PRF (dash dot, black) solutions as function of pH (A) and ionic strength at pH 7.0 (B).

Emulsion flocculation

The effect of pH on flocculation

The initial average droplet size of the emulsion droplets ($d_{3,2}$) stabilized by the different proteins varied between 0.5 and 3.3 μm (figure 3). In order to compare the different emulsions, the droplet size and decay time are expressed relative to the initial size or time. The effect of pH on the relative average droplet size and the relative decay time is shown in figure 3. A difference is observed between the data obtained by laser diffraction and DWS. Because the analysis by DWS does not require dilution, which might affect droplet flocculation, the DWS analysis is considered to be representative for the emulsion. For all proteins the droplet mobility decreases, and consequently the droplet size increases, around the iso-electric point (pI) indicating flocculation of the emulsion droplets.

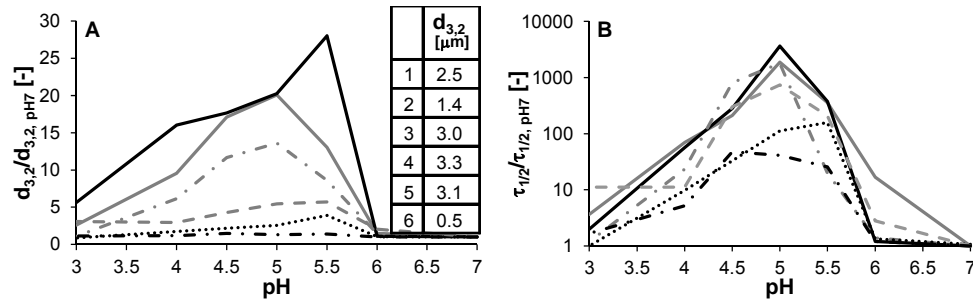


Figure 3. pH dependence of the relative average droplet size ($d_{3,2}/d_{3,2, \text{pH}7}$) (A) and the relative decay time ($\tau_{1/2}/\tau_{1/2, \text{pH}7}$) (B) of emulsions stabilized by ovalbumin (1; solid, grey), lipo. ovalbumin (2; dash dot, grey), S-ovalbumin (3; dash grey), patatin (4; dot, black), PRF (5; dash dot, black) and β -lactoglobulin (6; solid, black). In the insert the droplet size at pH 7.0 ($d_{3,2, \text{pH}7}$) are reported.

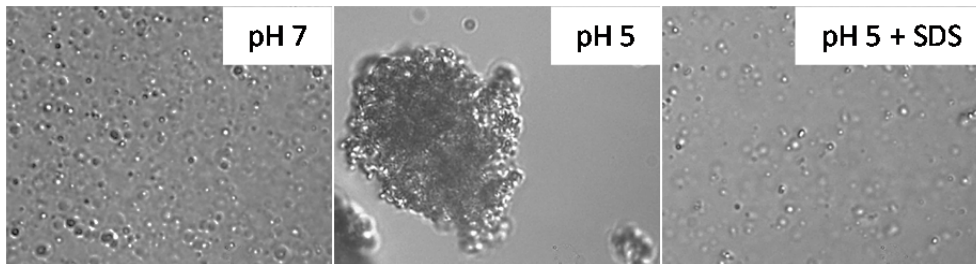


Figure 4. Microscopy pictures of emulsions of 1 % BLG (10% w/v oil) at pH 7, after adjustment to pH 5 and after addition of SDS to the flocculated emulsion at pH 5.

That the observed changes were indeed due to flocculation and not due to coalescence was confirmed by microscopy. Typical examples of normal (pH 7), and flocculated emulsions (pH 5) are shown in figure 4, where it was also shown that the flocculated emulsion at pH 5

could be dissociated by the addition of SDS. In this case, flocculation is caused by a decrease of the zeta potential if the pH approaches the pI (figure 2A). As a consequence, the electrostatic repulsion between the droplets, which forms a barrier against flocculation, decreases. Surprisingly, the variation of exposed hydrophobicity between the proteins does not affect pH induced flocculation as was suggested in literature¹⁴. Rather, the effect of pH seems to be dominated by electrostatic interactions.

The effect of ionic strength on flocculation

To confirm that the zeta potential is the only factor influencing droplet flocculation, the effect of ionic strength is investigated (figure 5). For ovalbumin, the extent of flocculation increases with increasing ionic strength, corresponding with the decreasing zeta potential. However, not all proteins behave this way towards changes in ionic strength. While for ovalbumin flocculation is strongly affected by ionic strength and is already initiated by the addition of only 10 mM NaCl, for patatin and especially β -lactoglobulin hardly any effects of ionic strength are observed.

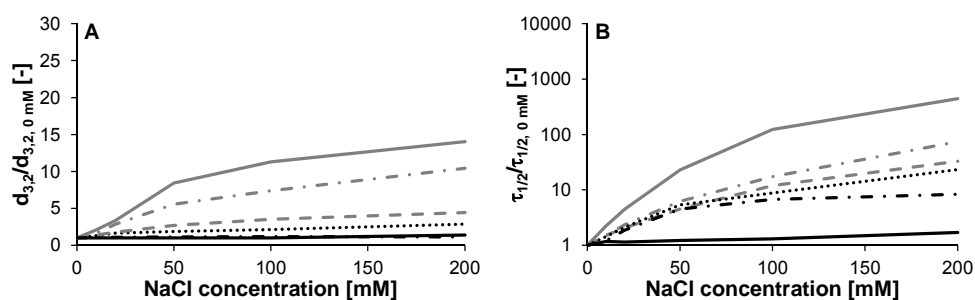


Figure 5. Ionic strength dependence of the relative average droplet size ($d_{3,2}/d_{3,2,0 \text{ mM}}$) (A) and the relative decay time ($\tau_{1/2}/\tau_{1/2,0 \text{ mM}}$) (B) of emulsions stabilized by ovalbumin (solid, grey), lipo. ovalbumin (dash dot, grey), S-ovalbumin (dash, grey), patatin (dot, black), PRF (dash dot, black) and β -lactoglobulin (solid, black) at pH 7.0.

These differences cannot be explained by means of electrostatic interactions as the zeta potential of the proteins in solution does not vary between the proteins (figure 2B). However, the zeta potential of the emulsion droplets varies significantly and is negatively correlated to the relative decay time (figure 6). In addition, the exposed hydrophobicity also shows a negative correlation to the relative decay time, and flocculation. This is in contrast to the expectations as in literature hydrophobic interactions were thought to act as an attractive force enhancing flocculation¹⁴. In our results, the decreased flocculation which was observed with increasing exposed hydrophobicity seems to correspond with an increase of the zeta potential of the emulsion droplets. A possible explanation could be that an increase of the exposed hydrophobicity results in an increase of the surface load. However, for ovalbumin and β -lactoglobulin, the surface load was estimated to be 2.5 ± 1

mg m⁻², indicating that there were no large differences in surface load. Furthermore, previous observations at the air-water interface also showed that the surface load did not depend on the exposed hydrophobicity of the protein¹⁶. More detailed characterization of the adsorbed layers will be needed to completely understand this phenomenon.

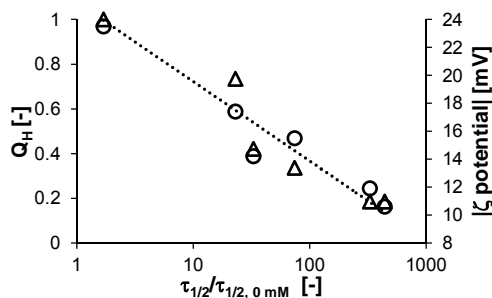


Figure 6. Relative exposed hydrophobicity (Δ , derived from figure 1B) and absolute zeta potential of the emulsion droplet at 200 mM NaCl (\circ) as function of the relative decay time ($\tau_{1/2}/\tau_{1/2, 0 \text{ mM}}$; derived from figure 5B).

Summarizing, although hydrophobic interactions seemed to be of minor importance for flocculation over the pH range, the relative exposed hydrophobicity indirectly affects flocculation over the range of ionic strength as it increases the zeta potential of the emulsion droplets. The influence of ionic strength on the flocculation behaviour correspond with the effect of pH as both suggest that the zeta potential is the only factor influencing droplet flocculation.

Quantitative description of droplet flocculation

The experimental data seemed to indicate that droplet flocculation was only dependent on the zeta potential of the emulsion droplets. This would mean that the flocculation behaviour could be predicted by the DLVO theory. Qualitatively flocculation was indeed observed when the ionic strength increases and when the pH approaches the pI^{8, 14}. The point from which flocculation is observed is expected to correspond to the point where the interaction potential between the droplets equals the critical interaction potential (U_{cr}). However, this relation between the experimental data and the DLVO theory was not quantitatively established. According to the DLVO theory, the interaction potential depends on three factors: (1) the zeta potential of the emulsion droplets, (2) the Debye screening length and (3) the droplet radius (equations 6 and 7). To study the flocculation in a systematic way, the flocculation behaviour of emulsions with different mean radii could be determined as function of ionic strength. If the zeta potential and the Debye screening length behave similar, independent of the droplet radius, the emulsions with smaller droplet radius are

expected to reach the critical interaction potential (U_{cr}) at a higher ionic strength and are therefore expected to be more stable against flocculation.

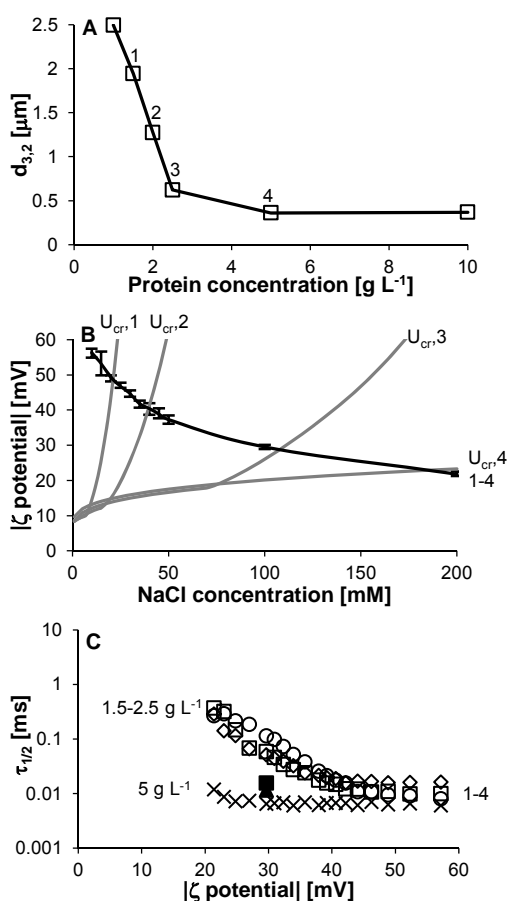


Figure 7. Average droplet size ($d_{3,2}$) of β -lactoglobulin stabilized emulsions as function of protein concentration (A). Average zeta potential of β -lactoglobulin stabilized emulsions with four different concentrations as a function of ionic strength (B). The decay time ($\tau_{1/2}$) of emulsions stabilized by β -lactoglobulin at different concentrations (1.5 g L^{-1} (\diamond), 2 g L^{-1} (\square), 2.5 g L^{-1} (\circ) and 5 g L^{-1} (\times) and all adjusted to 5 g L^{-1} (closed symbols)) as function of the absolute zeta potential (C). The grey lines in B represent the interaction potential of 5 kT (U_{cr}) given the radius of the droplets and the zeta potential and ionic strength of the solutions.

To test this, β -lactoglobulin emulsions with varying droplet radius are prepared by varying the protein concentration. Two regimes can be distinguished^{33, 34}. In the protein-poor regime ($< 5 \text{ g L}^{-1}$), the droplet radius decreases from 1.25 to 0.18 μm as there is insufficient protein to stabilize more surface area. In the protein-rich regime ($\geq 5 \text{ g L}^{-1}$), sufficient

protein is present to reach the minimal droplet radius (0.18 μm) (Figure 7A). In this regime the droplet size is determined by the system conditions (e.g. homogenization pressure, oil viscosity).

The flocculation behaviour of four of these emulsions (with radius ranging from 0.18 to 0.97 μm) was studied. The zeta potential of these emulsions was found to be independent of the droplet radius (figure 7B), and decreased similarly with increasing ionic strength. It can therefore be concluded that the observed flocculation behaviour should be solely due to the differences in droplet radius. The point from which flocculation is expected, i.e. the zeta potential reaches the critical interaction potential (U_{cr}), is plotted as function of ionic strength (figure 7B). Emulsions with smaller droplet radius reach the critical interaction potential (U_{cr}) at a higher ionic strength and are therefore expected to be more stable against flocculation. The experimental flocculation behaviour is shown in figure 7C. In contrast to the prediction, no difference in the flocculation behaviour is observed for the emulsions with the three largest droplet radii (0.31-0.97 μm), corresponding with the three lowest protein concentrations (1.5, 2 and 2.5 g L^{-1}). At the highest protein concentration (5 g L^{-1}), however, hardly any flocculation was observed (figure 7C). This is in contradiction with theory as the protein concentration rather than the droplet radius seems to be the determining factor for stability against flocculation.

To test whether the excess protein present at the highest protein concentration affects the flocculation behaviour, after emulsification additional protein is added to the emulsion in the protein-poor regime. This resulted in an increased stability towards flocculation at high ionic strength and therefore confirmed the stabilizing effect of the excess protein (figure 7C). This effect is also observed for ovalbumin and PRF stabilized emulsions (figure 8).

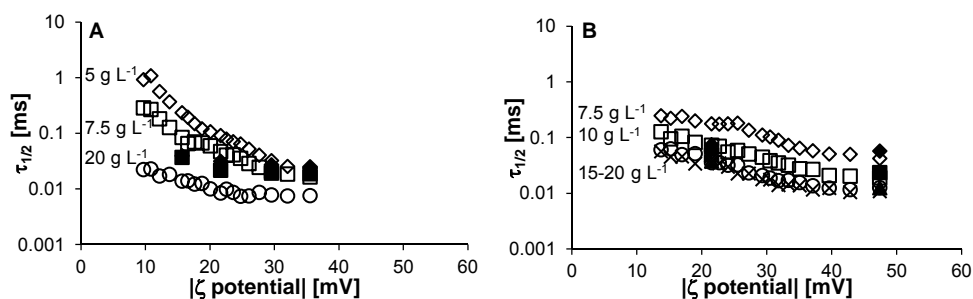


Figure 8. The decay time ($\tau_{1/2}$) of emulsions stabilized by ovalbumin at different concentrations (5 g L^{-1} (\diamond), 7.5 g L^{-1} (\square), 20 g L^{-1} (\circ) and adjusted to 20 g L^{-1} (closed symbols)) as function of the absolute zeta potential (A). The decay time ($\tau_{1/2}$) of emulsions stabilized by PRF at different concentrations (7.5 g L^{-1} (\diamond), 10 g L^{-1} (\square), 15 g L^{-1} (\circ) and 20 g L^{-1} (\times) and adjusted to 20 g L^{-1} (closed symbols)) as function of the absolute zeta potential (B).

However, for these proteins a higher protein concentration ($> 20 \text{ g L}^{-1}$) is needed to observe the effect of excess protein. This is caused by the fact that a higher concentration is required to reach the protein-rich regime (data not shown). In addition, it is observed that addition of protein to the PRF stabilized emulsions affects the flocculation behaviour less. This is thought to be caused by the addition of too little protein as at the lowest initial protein concentration (7.5 g L^{-1}) the effect is more pronounced than at higher protein concentrations (10 and 15 g L^{-1}) (figure 8B).

The significant effect of excess protein on the stabilization of emulsions against flocculation was not expected based on the DLVO theory. To explain the effect of excess protein, the differences between emulsions in the protein-poor and protein-rich regime should be addressed. At the lowest protein concentrations (i.e. protein-poor regime), the surface load is reported to be concentration independent and to correspond closely with the surface load of a monolayer^{1, 24, 35}. In the protein-rich regime, the remaining, excess protein present in the continuous phase can either adsorb onto the first monolayer to form a (reversibly bound) multilayer or remain in the continuous phase as non-adsorbed protein¹. As the surface load for ovalbumin and β -lactoglobulin at all protein concentrations was similar ($2.5 \pm 1 \text{ mg m}^{-2}$), the formation of multilayers is less likely. In both cases, a (reversible) multilayer or the presence of non-adsorbed proteins, there are two possible explanations for the effect of excess protein. The first explanation is that the excess protein adds a repulsive force. In case of a multilayer, steric repulsion due to a thicker adsorbed layer is expected²⁴. Non-adsorbed proteins could increase the electrostatic repulsion due to their equivalent charge or structure the continuous phase (similar to stratification observed for surfactants).

The second explanation for the stabilizing effect is based on the fact that the maximum adsorbed amount of protein increases with increasing ionic strength as is observed at the air-water interface³⁶. This increase is caused by screening of the Debye layer, which results in a decrease of the effective radius of the protein. As a consequence, in the absence of excess protein (i.e. protein-poor regime), the close packing configuration at low ionic strength (figure 9A) changes with increasing ionic strength into an interface which is not completely covered (figure 9B). The protein-poor interfaces, which are formed in the absence of excess protein, can approach to a closer distance resulting in flocculation^{24, 37}. This could be due to partial coalescence of the bare interface, or the result of the fact that proteins are shared by two droplets. This may result in bridging flocculation, which has been observed at low concentrations for emulsions stabilized by sodium caseinate³⁸. In the presence of excess protein, the excess proteins can adsorb, resulting in complete coverage with higher adsorbed amounts in the monolayer (figure 9C) and thereby prevent flocculation.

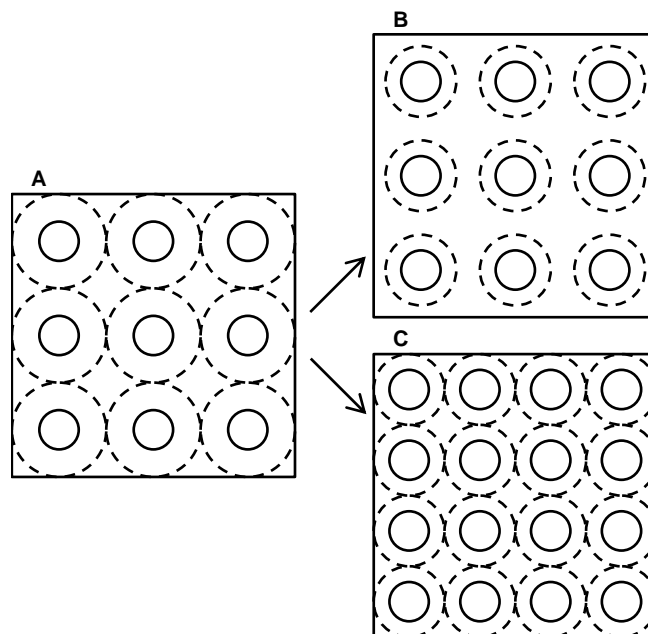


Figure 9. Schematic overview of the influence of increasing ionic strength on a protein-stabilized interface. The proteins in close packing configuration at low ionic strength (≤ 10 mM) with the solid circles representing adsorbed proteins and the dashed lines their Debye layer (A). The proteins at high ionic strength (> 50 mM) in the absence of excess protein (B) and in the presence of excess protein (C).

Verification of the effect of excess protein

To verify the unexpected effect of excess protein on droplet flocculation discussed above, thin liquid film experiments were performed. In the exchange cell the liquid between two adsorbed air-water interfaces can be exchanged by buffer to test whether a similar effect is observed. In literature it has been described that in the presence of electrostatic repulsion a black film (> 10 nm) is formed (also referred to as Common Black Film (CBF)). If the electrostatic repulsion decreased (i.e. at the pI or at high ionic strength), a thinner (< 10 nm) black film was formed (also referred to as Newton black film (NBF))^{39, 40}. In the absence of salt, β -lactoglobulin forms a film with an equilibrium thickness of around 40 nm (data not shown). In the presence of 100 mM NaCl, the equilibrium film thickness reduces to 15-20 nm (i.e. a CBF) (figure 10A). This reduction is caused by a decrease of the electrostatic repulsion between the adsorbed protein layers. However, when the solution containing excess protein between the two interfaces is exchanged by buffer with 100 mM NaCl and without excess protein, the film thins to a thickness of 5-9 nm (i.e. a NBF) (figure 10B). This effect of protein concentration was also described in literature, where excess protein

was related to the formation of a stable thick film⁴¹. Because removal of the excess protein results in a decrease of the thickness, it can be concluded that, if present, additional adsorbed layers, more than a single monolayer, are reversibly bound. However, exchange will also result in removal of the non-adsorbed proteins from the continuous phase. Therefore neither the formation of multilayers nor the effect of non-adsorbed proteins can be excluded.

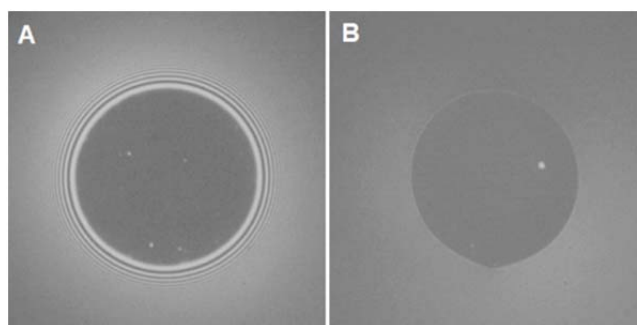


Figure 10. Pictures of thin films of β -lactoglobulin (1 g L^{-1} , 10 mM sodium phosphate buffer pH 7.0 + 100 mM NaCl) in the presence (A) and absence (B) of excess protein.

As in the emulsions, the thin film experiments show a significant difference in the behaviour in the presence and absence of excess protein. In both cases, the decrease in electrostatic repulsion between the adsorbed layers leads to a decrease of film thickness. However, only in the absence of excess protein this results in a Newton black film (in the thin film experiments), or flocculation (in the emulsion). This confirms that excess protein stabilizes the emulsion against flocculation.

Conclusion

By comparing the flocculation behaviour of emulsions stabilized by different proteins at different conditions, deviations from the expected behaviour were observed. These deviations were explained by two factors: protein exposed hydrophobicity and protein concentration. A higher exposed hydrophobicity of the protein results in a higher zeta potential of the emulsion droplets and consequently an increased stability against flocculation. So, differences observed in the stability of emulsions stabilized by different proteins as a function of ionic strength are due to the fact that the initial emulsion droplet has a different zeta potential, rather than on properties of the adsorbed proteins.

The other factor is the presence of excess protein. At low protein concentrations, the size of the emulsion droplets varies (depending on the protein concentration), but no excess protein is present. In this situation, the emulsions flocculate at the same ionic strength, regardless of droplet size. At higher protein concentrations, the presence of excess protein results in

stability against flocculation either due to the formation of a reversible multilayer or due to the presence of non-adsorbed protein in the continuous phase. This is supported by thin liquid film exchange experiments as the equilibrium film thickness is lower in the absence of excess protein, i.e. after exchange of the continuous phase by buffer.

References

1. McClements, D. J., Protein-stabilized emulsions. *Curr. Opin. Colloid Interface Sci.* **2004**, *9*, (5), 305-313.
2. Dickinson, E., Flocculation of protein-stabilized oil-in-water emulsions. *Colloids Surf., B* **2010**, *81*, (1), 130-140.
3. McClements, D. J., *Food emulsions: Principles, practices and techniques*. Second ed.; CRC Press: Boca Raton, FL, USA, 2005.
4. Narsimhan, G., Maximum disjoining pressure in protein stabilized concentrated oil-in-water emulsions. *Colloids Surf.* **1992**, *62*, (1-2), 41-55.
5. Dalgleish, D. G., Adsorption of protein and the stability of emulsions. *Trends Food Sci. Technol.* **1997**, *8*, (1), 1-6.
6. Damodaran, S., Protein stabilization of emulsions and foams. *J. Food Sci.* **2005**, *70*, (3), R54-R66.
7. Zhai, J.; Wooster, T. J.; Hoffmann, S. V.; Lee, T.; Augustin, M. A.; Aguilar, M., Structural rearrangement of β -lactoglobulin at different oil-water interfaces and its effect on emulsion stability. *Langmuir* **2011**, *27*, (15), 9227-9236.
8. Kulmyrzaev, A. A.; Schubert, H., Influence of KCl on the physicochemical properties of whey protein stabilized emulsions. *Food Hydrocolloids* **2004**, *18*, (1), 13-19.
9. Demetriades, K.; Coupland, J. N.; McClements, D. J., Physical properties of whey protein stabilized emulsions as related to pH and NaCl. *J. Food Sci.* **1997**, *62*, (2), 342-347.
10. Moreau, L.; Kim, H. J.; Decker, E. A.; McClements, D. J., Production and characterization of oil-in-water emulsions containing droplets stabilized by β -lactoglobulin-pectin membranes. *J. Agric. Food Chem.* **2003**, *51*, (22), 6612-6617.
11. Dimitrova, T. D.; Leal-Calderon, F.; Gurkov, T. D.; Campbell, B., Disjoining pressure vs thickness isotherms of thin emulsion films stabilized by proteins. *Langmuir* **2001**, *17*, (26), 8069-8077.
12. Tcholakova, S.; Denkov, N. D.; Sidzhakova, D.; Ivanov, I. B.; Campbell, B., Effects of electrolyte concentration and pH on the coalescence stability of β -lactoglobulin emulsions: experiment and interpretation. *Langmuir* **2005**, *21*, (11), 4842-4855.
13. Basheva, E. S.; Gurkov, T. D.; Christov, N. C.; Campbell, B., Interactions in oil/water/oil films stabilized by β -lactoglobulin; role of the surface charge. *Colloids Surf., A* **2006**, 282-283, 99-108.
14. Kim, H. J.; Decker, E. A.; McClements, D. J., Impact of protein surface denaturation on droplet flocculation in hexadecane oil-in-water emulsions stabilized by β -lactoglobulin. *J. Agric. Food Chem.* **2002**, *50*, (24), 7131-7137.
15. Vincent, B.; Young, C. A.; Tadros, T. F., Equilibrium aspects of heteroflocculation in mixed sterically-stabilised dispersions. *Faraday Discuss. Chem. Soc.* **1978**, *65*, 296-305.
16. Wierenga, P. A.; Meinders, M. B. J.; Egmond, M. R.; Voragen, A. G. J.; de Jongh, H. H. J., Protein exposed hydrophobicity reduces the kinetic barrier for adsorption of ovalbumin to the air-water interface. *Langmuir* **2003**, *19*, (21), 8964-8970.
17. Creusot, N.; Wierenga, P. A.; Laus, M. C.; Giuseppin, M. L. F.; Gruppen, H., Rheological properties of patatin gels compared with β -lactoglobulin, ovalbumin, and glycinin. *J. Sci. Food Agric.* **2011**, *91*, (2), 253-261.

18. Smith, M. B.; Back, J. F., Studies on ovalbumin II. The formation and properties of s-ovalbumin, a more stable form of ovalbumin. *Aust. J. Biol. Sci.* **1965**, 18, (2), 365-377.
19. Jachimska, B.; Wasilewska, M.; Adamczyk, Z., Characterization of globular protein solutions by dynamic light scattering, electrophoretic mobility, and viscosity measurements. *Langmuir* **2008**, 24, (13), 6866-6872.
20. Alizadeh-Pasdar, N.; Li-Chan, E. C. Y., Comparison of protein surface hydrophobicity measured at various pH values using three different fluorescent probes. *J. Agric. Food Chem.* **2000**, 48, (2), 328-334.
21. Ruis, H. G. M.; van Gruijthuisen, K.; Venema, P.; van der Linden, E., Transitions in structure in oil-in-water emulsions as studied by diffusing wave spectroscopy. *Langmuir* **2007**, 23, (3), 1007-1013.
22. Blijdenstein, T. B. J.; Hendriks, W. P. G.; van der Linden, E.; van Vliet, T.; van Aken, G. A., Control of strength and stability of emulsion gels by a combination of long- and short-range interactions. *Langmuir* **2003**, 19, (17), 6657-6663.
23. Vasbinder, A. J.; van Mil, P. J. J. M.; Bot, A.; de Kruijff, K. G., Acid-induced gelation of heat-treated milk studied by diffusing wave spectroscopy. *Colloids Surf., B* **2001**, 21, (1-3), 245-250.
24. Tcholakova, S.; Denkov, N. D.; Ivanov, I. B.; Campbell, B., Coalescence in β -lactoglobulin-stabilized emulsions: effects of protein adsorption and drop size. *Langmuir* **2002**, 18, (23), 8960-8971.
25. Hermansson, M., The DLVO theory in microbial adhesion. *Colloids Surf., B* **1999**, 14, (1-4), 105-119.
26. Israelachvili, J. N., *Intermolecular and surface forces*. Third ed.; Academic Press: New York, NY, USA, 2011.
27. Silvestre, M. P. C.; Decker, E. A.; McClements, D. J., Influence of copper on the stability of whey protein stabilized emulsions. *Food Hydrocolloids* **1999**, 13, (5), 419-424.
28. Hesselink, F. T.; Vrij, A.; Overbeek, J. T. G., Theory of the stabilization of dispersions by adsorbed macromolecules. II. Interaction between two flat particles. *J. Phys. Chem.* **1971**, 75, (14), 2094-2103.
29. Wiese, G. R.; Healy, T. W., Effect of particle size on colloid stability. *Trans. Faraday Soc.* **1970**, 66, 490-499.
30. Walstra, P., *Physical chemistry of foods*. Marcel Dekker, Inc.: New York, NY, USA, 2003.
31. Wierenga, P. A.; Basheva, E. S.; Denkov, N. D., Modified capillary cell for foam film studies allowing exchange of the film-forming liquid. *Langmuir* **2009**, 25, (11), 6035-6039.
32. Serway, R. A.; Jewett, J. W., *Physics for scientists and engineers*. Sixth ed.; Brooks/Cole: Belmont, PA, USA, 2003.
33. Tcholakova, S.; Denkov, N. D.; Sidzhakova, D.; Ivanov, I. B.; Campbell, B., Interrelation between drop size and protein adsorption at various emulsification conditions. *Langmuir* **2003**, 19, (14), 5640-5649.
34. Tcholakova, S.; Denkov, N. D.; Ivanov, I. B.; Campbell, B., Coalescence stability of emulsions containing globular milk proteins. *Adv. Colloid Interface Sci.* **2006**, 123-126, 259-293.
35. Gurkov, T. D.; Russev, S. C.; Danov, K. D.; Ivanov, I. B.; Campbell, B., Monolayers of globular proteins on the air/water interface: applicability of the Volmer equation of state. *Langmuir* **2003**, 19, (18), 7362-7369.
36. Wierenga, P. A.; Meinders, M. B. J.; Egmond, M. R.; Voragen, A. G. J.; De Jongh, H. H. J., Quantitative description of the relation between protein net charge and protein adsorption to air-water interfaces. *J. Phys. Chem. B* **2005**, 109, (35), 16946-16952.
37. Kim, H. J.; Decker, E. A.; McClements, D. J., Influence of free protein on flocculation stability of β -lactoglobulin stabilized oil-in-water emulsions at neutral pH and ambient temperature. *Langmuir* **2004**, 20, (24), 10394-10398.

Concentration and exposed hydrophobicity as parameters determining flocculation

38. Dickinson, E.; Golding, M.; Povey, M. J. W., Creaming and flocculation of oil-in-water emulsions containing sodium caseinate. *J. Colloid Interface Sci.* **1997**, 185, (2), 515-529.
39. van Aken, G. A.; Blijdenstein, T. B. J.; Hotrum, N. E., Colloidal destabilisation mechanisms in protein-stabilised emulsions. *Curr. Opin. Colloid Interface Sci.* **2003**, 8, (4-5), 371-379.
40. Marinova, K. G.; Gurkov, T. D.; Velev, O. D.; Ivanov, I. B.; Campbell, B.; Borwankar, R. P., The role of additives for the behaviour of thin emulsion films stabilized by proteins. *Colloids Surf., A* **1997**, 123-124, 155-167.
41. Yampolskaya, G.; Platikanov, D., Proteins at fluid interfaces: adsorption layers and thin liquid films. *Adv. Colloid Interface Sci.* **2006**, 128-130, 159-183.

Chapter 4

Effect of glycation on the flocculation behaviour of protein-stabilized oil-in-water emulsions

Abstract

Glycation of proteins by the Maillard reaction is often considered as a method to prevent flocculation of protein-stabilized oil-in-water emulsions. The effect has been suggested, but not proven, to be the result of steric stabilization, and to depend on the molecular mass of the carbohydrate moiety. To test this, the stability of emulsions of patatin glycated to the same extent with different mono- and oligosaccharides (xylose, glucose, maltotriose and maltopentaose) were compared under different conditions (pH and electrolyte concentration). The emulsions with non-modified patatin flocculate under conditions in which the zeta potential is decreased (around the iso-electric point and at high ionic strength). The attachment of monosaccharides (i.e. glucose) did not affect the flocculation behaviour. Attachment of maltotriose and maltopentaose ($M_w > 500$ Da), on the other hand, provided stability against flocculation at the iso-electric point. Since the zeta potential and the interfacial properties of the emulsion droplets are not affected by the attachment of the carbohydrate moieties, this is attributed to steric stabilization. Experimentally, a critical thickness of the adsorbed layer required for steric stabilization against flocculation was found to be 2.29-3.90 nm. The theoretical determination based on the DLVO interactions with an additional steric interaction coincides with the experimental data. Hence, it can be concluded that the differences in stability against pH-induced flocculation are caused by steric interactions.

Published as: Delahaije, R.J.B.M.; Gruppen, H.; van Nieuwenhuijzen, N.H.; Giuseppin, M.L.F.; Wierenga, P.A. Effect of glycation on the flocculation behavior of protein-stabilized oil-in-water emulsions. *Langmuir* **2013**, 29, (49), 15201-15208.

Introduction

The flocculation behaviour of protein-stabilized emulsions is often described using theoretical descriptions of colloidal interactions¹. In a previous study it was shown that patatin (molecular mass: 40 kDa; pI: 4.7), a globular plant protein isolated from potato, showed similar emulsifying properties as β -lactoglobulin and ovalbumin (chapter 3). For these pure globular proteins, flocculation typically occurs when the electrostatic repulsive interactions are low (around the iso-electric point and at high ionic strength (> 50 mM NaCl)) (chapter 3)^{2, 3}. To prevent flocculation under these conditions, the range and strength of the repulsive forces (e.g. steric repulsion) should be increased¹.

It was previously shown that the stability of silica particles against flocculation can be increased by steric repulsion as a result of coupling of synthetic polymers⁴. Similarly, glycation of proteins is described to result in steric stabilization of emulsions due to the covalent coupling of carbohydrate moieties to the protein⁵⁻⁷. This effect was also observed to improve the emulsifying properties of proteins, which are naturally glycosylated (e.g. ovalbumin and soy proteins)^{8, 9}.

To benefit from steric stabilization two factors are of importance: (1) the size/molecular mass of the carbohydrate moieties and (2) the density of the carbohydrate moieties coupled to the protein (i.e. the number of modified groups). It has been reported that the critical density of carbohydrate moieties coupled to the protein for steric repulsion decreases with the molecular mass of maltodextrins (i.e. average number of modified groups of 2.0 for 900 Da to 1.6 carbohydrate moieties per protein for 1900 Da)¹⁰. Moreover, the stabilizer (i.e. the carbohydrate moiety) should be of a minimum size in order to prevent the droplets to approach into the range of attractive van der Waals forces^{11, 12}. At a similar number of carbohydrate moieties attached to β -lactoglobulin, mono- and disaccharides have been shown to lack the ability to sterically stabilize against flocculation, whereas oligosaccharides (maltodextrins \geq 900 Da) and polysaccharides (dextrans \geq 18500 Da) do possess this ability^{10, 13}. This is related to the fact that the molecular mass correlates to the thickness of the adsorbed layer¹⁰.

However, in literature, no conclusive results regarding the critical molecular mass and/or density have been provided. This is caused by the fact that typically maltodextrins with a certain dextrose equivalent (DE) are attached to the protein. Hence, it has to be taken into account that (1) these maltodextrins consist of molecules with a range of molecular masses and (2) conjugation of smaller carbohydrates to proteins is faster than that of larger carbohydrates¹⁴. Therefore, when maltodextrin mixtures are used it is not exactly known which carbohydrate moieties are coupled to the protein. As a consequence the critical molecular mass and/or density for steric stabilization cannot be determined.

This study aims to provide insights in the critical adsorbed layer thickness (δ_{cr}) required to stabilize against flocculation (i.e. to prevent the droplets to approach into the range of van der Waals attraction). To assess this, the experimental data (i.e. flocculation behaviour after glycation of patatin with xylose, glucose, maltotriose and maltopentaose at the same number of modified groups) is combined with theoretical calculations based on the DLVO theory with additional steric repulsion (i.e. to determine the theoretical critical layer thickness).

Materials and methods

Materials

A patatin-rich liquid protein concentrate was obtained from Solanic/AVEBE (Veendam, The Netherlands). Maltotriose and maltopentaose were purchased from Carbosynth Ltd. (Compton, UK). Glucose (G8270, purity $\geq 99.5\%$) was purchased from Sigma-Aldrich (St. Louis, MO, USA), xylose (108689, purity $\geq 98\%$) from Merck (Darmstadt, Germany) and maltotriose (OM06486, purity $\geq 98\%$) and maltopentaose (OM06872, purity $\geq 95\%$) were purchased from Carbosynth Ltd. (Compton, UK). All other chemicals were of analytical grade and purchased from either Sigma-Aldrich or Merck.

Protein purification

Patatin was purified using an Äkta Explorer with a Superdex 200 PG (52 x 10 cm; GE Healthcare, Uppsala, Sweden) gel filtration column. The patatin-rich liquid protein concentrate (50 mL) was injected and eluted with 10 mM sodium phosphate buffer pH 7.0 at a linear flow rate of 40 mL min⁻¹. The elution was monitored using UV absorbance at 280 nm. Following elution, the patatin fractions were pooled based on apparent molecular mass, dialyzed against demineralized water and lyophilized. The final purified patatin contained 97 % protein, based on Dumas, of which $\geq 85\%$ was patatin and $\leq 15\%$ was freezing-induced aggregated protein confirmed by analytical scale size-exclusion chromatography.

Glycation

For the glycation, patatin was mixed with xylose, glucose, maltotriose or maltopentaose in demineralized water in a concentration of 10 g L⁻¹ and a molar ratio of 1 lysine: 2 reducing end groups. The pH of the mixtures was set to 8.0 with 0.1 M NaOH. Subsequently, the solutions were frozen and lyophilized. Next, the samples were incubated at 60 °C and a relative humidity of 65 %. Based on previous observations¹⁴, the incubation times with xylose, glucose, maltotriose and maltopentaose were set at 2.5, 4, 24 and 48 h, respectively, to obtain similar number of modified groups. As a reference for the effect of dry heating,

patatin was also incubated for 48 h without carbohydrate (which will be referred to as non-modified patatin). After the glycation, the samples were dialyzed, frozen and lyophilized.

Number of modified groups

MALDI-TOF MS

The increase in molecular mass of the glycated protein, as indication for the number of modified groups, was determined using matrix-assisted laser desorption/ionization time-of flight mass spectrometry (MALDI-TOF MS). The samples (1 g L^{-1}) were dissolved in a 0.1 % (v/v) TFA solution. Samples (10 μL each) were mixed with 10 μL of matrix solution (saturated sinapinic acid in 330 μL 0.1 % TFA in ACN and 670 μL 0.1 % TFA in H₂O). Subsequently, 1 μL of each solution was applied on a stainless steel metal plate. The samples were crystallized and analysed on an Ultraflex extreme workstation (Bruker Daltonics, Bremen, Germany) that was equipped with a 337 nm laser and controlled using FlexControl software. Analysis was performed in positive mode with a laser power intensity of 60 %. Ions were accelerated with a 25 kV voltage and detected using linear mode. A mixture of proteins (Bruker Daltonics; Lot n° 10.207234.325001; mass range 20-70 kDa) was used to calibrate the instrument. The data were analysed using FlexAnalysis software.

The average number of modified groups was calculated from the difference in mass of the peak corresponding to native patatin and the mass of peak corresponding to the glycated patatin divided by the molecular mass of the attached carbohydrate moiety. The range in the number of modified groups was determined from the width of the peak corresponding to patatin subtracted from the width of the peak corresponding to glycated patatin divided by the molecular mass of the anhydrous carbohydrate moiety. The molecular masses of the anhydrous carbohydrate moieties are 132 Da, 162 Da, 486 Da and 810 Da for xylose, glucose, maltotriose and maltopentaose, respectively.

OPA assay

The average number of modified amino groups was determined based on the primary amino groups of the proteins using the o-phthalaldehyde (OPA) assay as described elsewhere¹⁵. All samples were analysed in duplicate. Based on the amino acid sequence of patatin from different potato cultivars it is found that patatin contains 24 ± 1 lysine residues.

Protein solubility

Proteins were suspended in 10 mM sodium phosphate buffer pH 7.0 at a concentration of 10 g L^{-1} for 4 hours at 20 °C. The suspensions were centrifuged (10000g, 10 min, 20 °C) to remove insoluble protein. Subsequently, the nitrogen content of the supernatants was determined using a Flash EA 1112 NC Analyzer (Thermo Fisher Scientific Inc., Waltham,

MA, USA), according to the manufacturer's instructions. The protein solubility was calculated by dividing the nitrogen concentration of the supernatant (% N_{sup}) by the nitrogen concentration of the original suspension (% N_{sus}) multiplied by the molecular mass of conjugate (table 1) divided by the molecular mass of the non-modified patatin.

Apparent molecular mass distribution

(Glycated) protein samples were analysed by high-performance size-exclusion chromatography using an Äkta Micro equipped with a Superdex 200 PC 3.2/30 column (GE Healthcare, Uppsala, Sweden). The samples (20 µL) were injected and eluted with 10 mM sodium phosphate buffer pH 7.0 at a flow rate of 0.06 mL min⁻¹. The elution was monitored using UV absorbance at 280 nm. The column was calibrated with globular proteins with a mass range of 13.7-67 kDa (GE Healthcare).

Determination of adsorption kinetics and surface elastic modulus

(Glycated) protein solutions (0.1 g L⁻¹) were prepared in 10 mM sodium phosphate buffers of pH 5.0 and 7.0. The surface tension and surface elastic modulus as a function of time were measured using an automated drop tensiometer (ADT, Teclis IT Concept, Longessaigne, France). The system is temperature controlled at 20 °C. For the surface tension measurements, the drop volume was kept constant at 7 µL for 3600 s. The surface tension is converted into the surface pressure (Π), which is defined as the change in surface tension compared that of the pure interface (i.e. the air-water interface)¹⁶.

$$\Pi(t) = \gamma_0 - \gamma(t) \quad (1)$$

where t is time, γ_0 is the interfacial tension of the pure fluid [72.8 mN m⁻¹].

The surface elastic modulus was measured by inducing sinusoidal changes in the interfacial area with an amplitude of 5 % and a frequency of 0.1 Hz. The modulus was calculated from the measured changes in surface tension and surface area averaged over a sequence of five sinuses. Every 100 s a sequence of five sinuses was performed. All measurements were performed in duplicate.

Emulsification

The (glycated) protein was dissolved in 10 mM sodium phosphate buffer pH 7.0 at a concentration of 5 g L⁻¹ and subsequently mixed with 10 %(v/v) sunflower oil. A pre-emulsion was prepared using an Ultra turrax Type T-25B (IKA, Staufen, Germany) at 9500 rpm for 1 min. Subsequently, the pre-emulsion was passed 30 times through a Labhoscope 2.0 laboratory scale high-pressure homogenizer (Delta Instruments, Drachten, The Netherlands) operated at 15 MPa.

Effect of pH and ionic strength To test the effect of pH and ionic strength on flocculation, emulsions were prepared as described above. After emulsification, the pH and the ionic strength were adjusted with 0.1 M HCl or 2 M NaCl to obtain emulsions with a pH 3.0-7.0 and ionic strength of 0-200 mM NaCl.

Subsequently, the emulsions were stored for 24 hours at 20 °C prior to further analysis. For selected samples, it was confirmed that no significant changes occurred during this storage period.

Determination of zeta potential of emulsion droplets

Zeta potentials of the emulsion droplets were determined with a Zetasizer Nano ZS (Malvern Instruments, Worcestershire, UK) using the laser Doppler velocimetry technique. The emulsions were diluted 500 times to prevent multiple scattering. The measurements were performed at 25 °C and 40 Volt. Five sequential runs were averaged to obtain the results. Zeta potentials were calculated with Henry's equation¹⁷ (equation 2).

$$\zeta = \frac{3\eta \cdot \mu_e}{2\epsilon F(\kappa\alpha)} \quad (2)$$

in which ζ is the zeta potential [V], η is the viscosity [Pa s], μ_e is the electrophoretic mobility [$\text{m}^2 \text{V}^{-1} \text{s}^{-1}$], ϵ is the dielectric constant of the medium [$\text{C}^2 \text{J}^{-1} \text{m}^{-1}$] and $F(\kappa\alpha)$ is Henry's function [-], which equals 1.5 by using the Smoluchowski approximation¹⁷.

Determination of flocculation

Diffusing wave spectroscopy (DWS)

To determine decay time as indication of droplet flocculation, DWS measurements were performed as described previously¹⁸. The correlation function was averaged from five sequential runs of 120 seconds. The correlation function was normalized by dividing the obtained $g_2(t)-1$ values by the maximum measured value. Normalized autocorrelation curves were fitted using equation 3. This was derived from the equation used by Ruis et al.¹⁸, assuming that $\langle \Delta r^2(t) \rangle = 6Dt^p = \alpha t^x$ for $p < 1$ and $x < 1$.

$$g_2(t) - 1 \approx (e^{-\langle \Delta r^2(t) \rangle})^2 \approx e^{-\alpha t^x} \quad (3)$$

The decay time ($\tau_{1/2}$), which is defined as the time at which $g_2(t)-1$ decayed to half of its initial value, was determined using the fitted equation. An increase of the decay time is related to decreased droplet mobility¹⁹.

Microscopy

To identify whether the increased droplet size was due to flocculation or coalescence, the emulsions were analysed by light microscopy using an Axioscope A01 (Carl Zeiss, Sliedrecht, The Netherlands) at a magnification of 40x.

Determination of theoretical critical layer thickness

The critical layer thickness required for steric stabilization against droplet flocculation was determined based on the DLVO theory with an additional steric interaction. For this determination, the range and magnitude of the colloidal DLVO interactions between the droplets have to be calculated. The DLVO theory assumes that the overall interaction potential (U_{tot}) between two protein-stabilized emulsion droplets is the result of a combination of van der Waals (U_{vdw}) and electrostatic (U_e) interactions (equation 4)^{3, 20}.

$$U_{tot}(h) = U_{vdw}(h) + U_e(h) \quad (4)$$

in which h is the separation distance between the droplets [m].

The van der Waals and electrostatic interactions are respectively described by equations 5 and 6^{3, 20}, respectively.

$$U_{vdw} = -\frac{A}{6} \left(\frac{2R^2}{4Rh + h^2} + \frac{2R^2}{4R^2 + 4Rh + h^2} + \ln \left(\frac{4Rh + h^2}{4R^2 + 4Rh + h^2} \right) \right) \quad (5)$$

$$U_e = 2\pi\epsilon_0\epsilon_r R\Psi_0^2 e^{-\kappa h} \quad (6)$$

in which κ for a monovalent electrolyte is described by equation 7²¹.

$$\kappa = \sqrt{\frac{2N_a e^2 I}{\epsilon_0 \epsilon_r k_B T}} \quad (7)$$

in which A is the Hamaker constant [5.35×10^{-21} J]²², R is the droplet radius [m], ϵ_0 is the dielectric constant of a vacuum [8.85×10^{-12} C² J⁻¹ m⁻¹], ϵ_r is the relative dielectric constant of the medium (80), Ψ_0 is the surface potential of the droplets [V], κ is the reciprocal of the Debye screening length [m⁻¹], N_a is the Avogadro constant [6.022×10^{23} mol⁻¹], e is the elementary charge [1.602×10^{-19} C], I is the ionic strength [mol m⁻³], k_B is the Boltzmann constant [1.38×10^{-23} J K⁻¹] and T is the temperature [K].

As a critical barrier, which is the demarcation between systems stable and unstable against flocculation, an interaction potential of 5 kT is used^{23, 24}. Flocculation is therefore assumed to occur when the primary maximum decreases below 5 kT, or when the secondary minimum decreases below -5 kT (U_{cr}). Based on the DLVO interactions, the separation distance at which the critical barrier is exceeded can be calculated. Using equation 8^{20, 25}, which describes the additional steric interaction (U_s), it can be derived that the steric repulsion increases steeply at close separation ($h \leq 2\delta$). Therefore, the theoretical critical layer thickness to prevent flocculation equals to half of the separation distance at which the critical barrier is exceeded.

$$U_s = \left(\frac{2\delta}{h} \right)^\infty \quad (8)$$

in which δ is the layer thickness of the adsorbed layer [m] and h is the separation distance between the droplets [m].

The thickness of the adsorbed layer (δ) is estimated by the sum of the radius of the protein and the length of the carbohydrate moiety. The radius of the protein is estimated from the molecular mass as described in equation 9.

$$r_{protein} = 0.0666 M^{\frac{1}{3}} \quad (9)$$

in which M is the molecular mass [Da].

The length of the carbohydrate moiety was estimated based on the lowest energy state using ChemBioOffice Ultra 12 (Perkin Elmer, Waltham, MA, USA). The interaction potential is calculated using the droplet zeta potential¹⁶, the average droplet size, and Debye screening length.

Results and discussion

Protein glycation

The molecular mass of patatin was determined using MALDI-TOF MS (figure 1 and table 1). The molecular mass (40659 Da) is around 900-1200 Da more than the calculated mass (39.5-39.8 kDa) based on the amino acid sequence²⁶. This difference is explained by the natural glycosylation of patatin with one carbohydrate moiety, which was reported to have a molecular mass of 1169 Da²⁶.

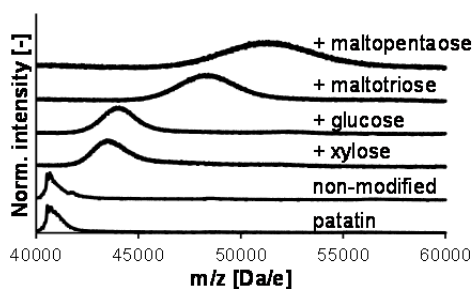


Figure 1. MALDI-TOF MS spectra of patatin glycosylated with the different carbohydrates.

Via the Maillard reaction, mono- and oligosaccharides were covalently coupled to patatin. The MALDI-TOF MS spectra of the modified proteins show that for all samples no non-modified patatin remains (figure 1). The number of modified groups as determined by MALDI-TOF MS decreases with increasing molecular mass of the carbohydrate moiety

(from 21 ± 10 for xylose to 13 ± 8 for maltopentaose) (table 1) even though the larger carbohydrates were incubated longer to correct for their lower reactivity. The indicated range can be explained by the heterogeneity of the modification represented in the width of the peak corresponding to the glycated patatin (figure 1). This shows that not all proteins molecules which are modified with for instance maltopentaose are modified to the same extent, but a range of modification is obtained. In contrast to MALDI-TOF MS results, analysis by the OPA assay shows a similar number of modified groups (16 ± 1 carbohydrate moieties per protein) for all samples. It is postulated that this difference is caused by the fact that the MALDI-TOF MS analysis determines all modified groups independent on the location of the modification, whereas the OPA assay only determines ϵ -amino groups and the terminal amino group²⁷. Modification of arginine, which has been described previously²⁸, could explain the discrepancies. Including arginines as available binding site for the carbohydrate moieties would result in an increase of the available sites from 27 based on ϵ -amino groups and the terminal amino group as determined by OPA to 37 in case arginines are included (10 ± 1 based on the uniprot database). This would also explain the number of modified groups which exceeds the number of ϵ -amino groups and the terminal amino group (table 1). It is observed that the difference between the OPA assay and MALDI-TOF MS (i.e. the number of modified arginines) decreases with increasing molecular mass of the carbohydrate (table 1). This indicates that the reactivity of arginine is more affected by the molecular mass of the carbohydrate moiety than lysine. Because all modified groups are determined by MALDI-TOF MS, these results, therefore, represent the actual number of modified groups and will be used throughout this paper. As an excess of groups are modified, the effect of density is thought to be of minor importance and therefore, effects on emulsion stability are attributed to the size of the carbohydrate moieties added.

The solubility of the glycated proteins at pH 7 is shown in table 1. It was found that the treatment resulted in a small decrease of the solubility from 98 % for patatin to 90 % for non-modified patatin. This might be caused by temperature-induced aggregation. The solubility of the xylose-conjugate (51 %) was significantly lower than that of non-modified patatin (90 %). As the xylose-conjugate formed a brown colour and xylose has been described to possess a higher tendency to form cross-links than other saccharides²⁹, the low solubility is expected to be the result of secondary reactions. These secondary reactions (e.g. dehydration and cyclization) which follow the covalent coupling of the carbohydrate moiety to the protein will eventually result in colour formation and cross-linking of the protein³⁰. The solubility of the other conjugates is similar to that of the non-modified patatin (≈ 90 %) (table 1), indicating the absence of these secondary reactions.

Table 1. Protein solubility and number of modified groups of the (glycated) proteins.

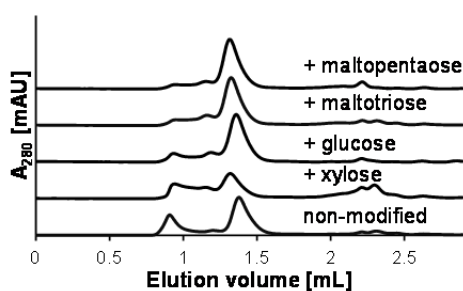
Protein	Dumas	OPA assay		MALDI-TOF MS		
	Protein solubility ^a [%]	Free NH ₂ groups ^b [-]	NH ₂ groups modified ^b [-]	M _w ^c [Da]	Total groups modified [-]	Variation in total groups modified [-]
Patatin	98	27	0	40659		
Non-modified patatin	90	28	0	40659		
Patatin xylose	51	12	15	43420	21	10-29
Patatin glucose	86	10	17	43837	20	9-29
Patatin maltotriose	92	10	17	48066	15	9-21
Patatin maltopentaose	89	12	15	51011	13	7-21

^adetermined at pH 7.0.

^bstandard deviation of the free NH₂ groups determination by the OPA assay is ± 1 .

^cstandard deviation of the M_w determination by MALDI-TOF MS is ± 100 Da.

To check for cross-linked protein aggregates, the glycated protein was analysed using size-exclusion chromatography. The non-modified patatin shows a peak at low elution volume (~ 0.85 mL) which are aggregated proteins resulting from the treatment (figure 2). For the glucose-, maltotriose- and maltopentaose-conjugate, this peak decreases and shifts to larger elution volumes. Therefore, these conjugates do not only show no significant formation of cross-linked protein aggregates, but also prevent the aggregation as a result of the treatment. Furthermore, the elution volume of the peak corresponding to patatin (~ 1.35 mL) deviates for the conjugates compared to the non-modified patatin which is attributed to an increase of the hydrodynamic radius due to glycation with the carbohydrates. As expected from the solubility results, the elution pattern of the xylose-conjugate showed a significant decrease of monomeric protein (i.e. decrease of ± 35 % of the peak area) and the presence of protein aggregates.

**Figure 2.** Apparent molar mass distribution of the (glycated) proteins.

Adsorption kinetics and interfacial rheology

The effect of glycation on the surface pressure and the elastic modulus of the interface was determined at pH 7 and pH 5 (figure 3).

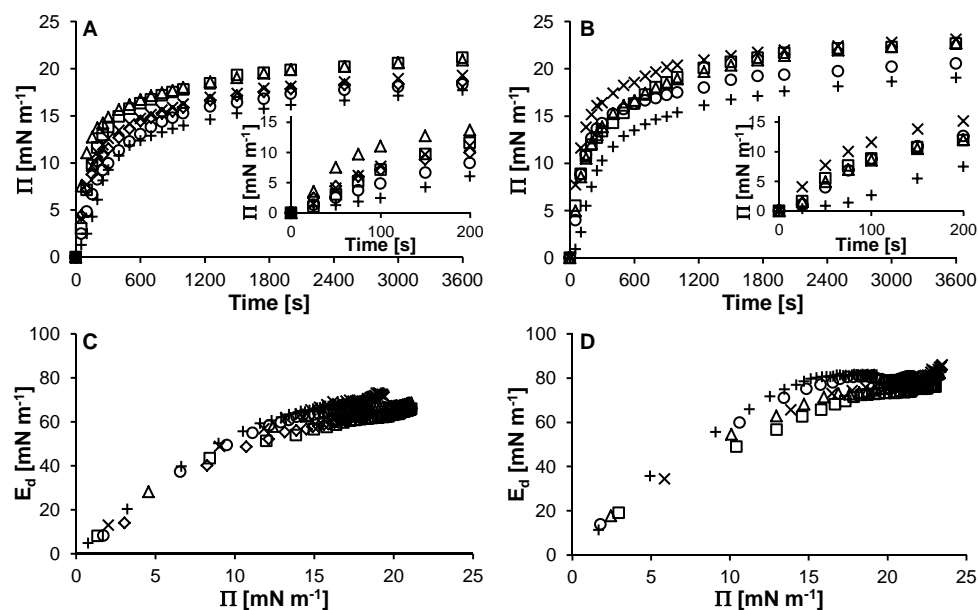


Figure 3. Surface pressure (Π) as function of time for patatin (\square), non-modified patatin (\triangle), patatin xylose (\diamond), patatin glucose (\times), patatin maltotriose (\circ) and patatin maltopentaose ($+$) at pH 7.0 (A) and pH 5.0 (B) and the elastic modulus (E_d) as a function of surface pressure at pH 7.0 (C) and pH 5.0 (D). Inserts show surface pressure at short times.

At pH 7, the initial adsorption rate and the final surface pressure decrease with increasing molecular mass of the carbohydrate moiety (figure 3A). As the attachment of a carbohydrate moiety is expected to increase the hydrophilicity of the protein, the decrease of the adsorption rate and surface pressure is postulated to be caused by an overall decrease of the hydrophobicity of the protein. As a comparison, alkylated-BSA showed an increase of the initial adsorption rate and the surface pressure which was attributed to an increased surface hydrophobicity³¹. For all proteins, the elastic modulus, which gives an indication of the interactions between the adsorbed proteins, is similar (figure 3C). This is in contrast to the expectations as glycation was expected to result in a decrease of the interactions between the adsorbed proteins and as a consequence also in a decrease of the elastic modulus. At pH 5, the initial adsorption rate is less affected by glycation, only the maltopentaose conjugate shows slower adsorption (figure 3B). Moreover, the surface pressure and elastic modulus of all proteins at 3600 seconds was higher at pH 5 than at pH

7 (figures 3B and D). The increase in surface pressure around the iso-electric point ($pI = 4.7$) is thought to be caused by a small change of the surface load due to a reduction of the electrostatic barrier, as was also described for BSA³² and ovalbumin³³.

Although there are minor changes in the surface pressure and elastic modulus at different temperatures, these differences are not expected to influence the flocculation behaviour.

Emulsion characteristics

Zeta potential of the emulsion droplets

Glycation results in the modification of lysine and to a lesser extent arginine groups. Therefore, it is expected to lower the iso-electric point of the proteins and as a consequence of the emulsion droplets. However, the zeta potential of the emulsion droplets is not affected by glycation (figure 4). Previously, it was also described that the zeta potential of proteins in solution deviated from the zeta potential of the protein-stabilized emulsion droplets (chapter 3). This was postulated to be caused by a difference in surface load.

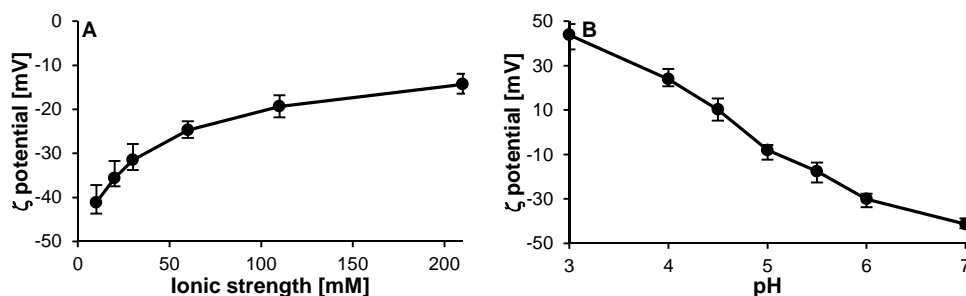


Figure 4. Average zeta potential of the emulsions stabilized by the different (glycated) proteins as a function of ionic strength (A) and pH (B). The markers and error bars respectively indicate the average zeta potential and the variation between the zeta potentials of patatin, non-modified patatin, patatin xylose, patatin glucose, patatin maltotriose and patatin maltopentaose.

Consequently, as the zeta potential of the emulsion droplets is not influenced by glycation, differences in the flocculation behaviour cannot be explained by differences in charge and consequently electrostatic interactions.

Emulsion flocculation

The effect of ionic strength and pH on flocculation

The influence of ionic strength on flocculation behaviour of (glycated) patatin-stabilized emulsions and, as a consequence on the decay time, is shown in figure 5A. For all (glycated) proteins, flocculation is observed at high ionic strength (i.e. ≥ 30 mM). While glycation does not affect the stability against flocculation at higher ionic strength, the stability of pH-induced flocculation improves as a result of glycation (figure 5B). Glycation

with xylose and glucose resulted only in minor changes of the flocculation behaviour compared to the non-modified patatin, whereas modification with maltotriose and maltopentaose results in complete stability against pH-induced flocculation. It is important to note that for maltotriose and maltopentaose a lower number of modified groups was reached (table 1). This shows that, in the case of ≥ 15 modified groups (± 0.23 carbohydrate moiety nm^{-2}), the size of the carbohydrate moieties is more important than the number of modified groups (i.e. density).

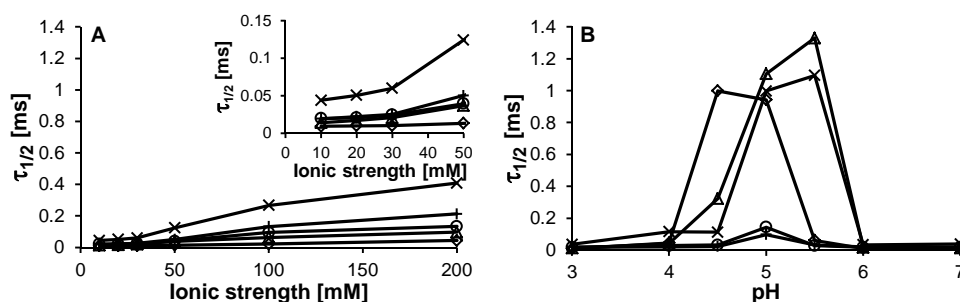


Figure 5. Decay time ($\tau_{1/2}$) of emulsions stabilized by non-modified patatin (Δ), patatin xylose (\diamond), patatin glucose (\times), patatin maltotriose (\circ) and patatin maltopentaose ($+$) as a function of ionic strength (A) and pH (B). The insert shows the decay time at low ionic strength.

In addition, the zeta potential of the droplets (figure 4B) as well as the interfacial properties (figures 3C and D) is similar for all conjugates. Consequently the stability against flocculation cannot be attributed to either electrostatic repulsion, or interfacial properties. The fact that the interfacial properties do not correlate to the macroscopic behaviour has previously been described for foam stability³⁴. As this stabilizing effect is observed by increasing the molecular mass of the carbohydrate moiety, steric repulsion is postulated to be the cause of the observed differences. This is in line with other studies, which describe that the emulsion stability is not affected by modification with mono- and disaccharides^{10, 35, 36}. In the case of the tri- and pentamer, steric repulsion counteracts the van der Waals attraction in case of decreased electrostatic repulsion (i.e. at high ionic strength and around the pI) and thereby prevents flocculation. Apparently, the critical layer thickness (δ_{cr}) for steric stabilization against flocculation is exceeded by conjugation of maltotriose (1.62 nm) to patatin (2.28 nm). Covalent coupling of glucose (0.61 nm) to patatin (2.28 nm), on the other hand, does not exceed δ_{cr} . Therefore, the critical layer thickness is expected to be between 2.89 nm (i.e. glucose-conjugate) and 3.90 nm (i.e. maltotriose-conjugate).

Determination of theoretical critical layer thickness

The experimental data indicates that, besides the DLVO interactions (i.e. electrostatic repulsion and van der Waals attraction), steric repulsion is an important interaction related

to the flocculation behaviour of emulsions stabilized by glycosylated proteins. A critical layer thickness for steric stabilization was determined to be between 2.89 and 3.90 nm. To verify that steric interactions stabilize the emulsions against flocculation and to quantitatively describe the data, the critical layer thickness (δ_{cr}) is theoretically determined. This δ_{cr} is the minimal thickness of the adsorbed layer needed to prevent the droplets to exceed the critical barrier. Equation 4 is used to calculate the distance at which the critical barrier is exceeded. From equation 8, it follows that the steric repulsion of the adsorbed layer steeply increases if the separation distance decreases to twice the adsorbed layer thickness. Therefore, the critical layer thickness to prevent flocculation equals half of the separation distance at which the critical barrier is exceeded.

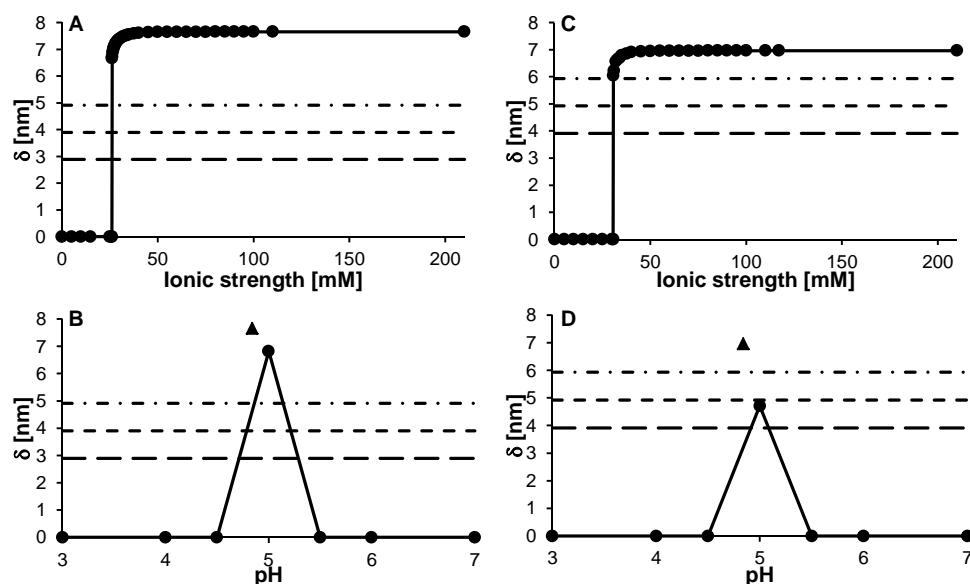


Figure 6. The theoretical critical layer thickness (δ) (\bullet) as function of ionic strength (A and C) and pH (B and D). The horizontal lines represent the layer thickness of adsorbed conjugates of patatin with glucose (long dashes), maltotriose (dashes) and maltopentaose (dash dot). The critical layer thickness at the pI (i.e. $\zeta = 0$ and $U_e = 0$) is shown as a separate point (\blacktriangle) in B and D. Calculations were performed using equations 4 and 8 and the following parameters: $R = 0.77 \mu\text{m}$, $I = 0.01 \text{ M}$ (B and D only), Ψ_0 is the determined ζ potential (figure 4). For A and B, the $A_H = 1.3 \text{ kT}$ and $\delta = \text{protein radius} + \text{length carbohydrate moiety}$. For C and D, the $A_H = 1.175 \text{ kT}$ and $\delta = 1.45 \times \text{protein radius} + \text{length carbohydrate moiety}$.

It is found that the critical layer thickness sharply increases at an ionic strength of 25 mM and at a pH close to the iso-electric point (i.e. $4.5 \leq \text{pH} \leq 5.5$) (figures 6A and B). At low ionic strength (i.e. $I \leq 25 \text{ mM}$) and a pH away from the pI (i.e. $4.5 \geq \text{pH} \geq 5.5$), the

adsorbed layer of the non-modified protein (i.e. 2.28 nm) is already sufficient to prevent flocculation (figures 6A and B). This is in line with the experimental data (figure 5). At high ionic strength or a pH close to the pI the adsorbed layers of the conjugates should not be sufficiently thick to provide steric stabilization. Nonetheless, experimentally the maltotriose- and maltopentaose-conjugates were found to stabilize against pH-induced flocculation. This difference between the experimental results and theoretical predictions may be the result of difficulties to identify the exact values of the Hamaker constant and layer thickness. In the above calculations a Hamaker constant (A_H) of 1.3 kT was used. In literature, however, the Hamaker constant (A_H), which is reported for protein-stabilized emulsions, varies from around 1 kT (i.e. 4×10^{-21} J)^{19, 37, 38} to around 1.3 kT (i.e. 5.3×10^{-21} J)^{22, 39, 40}. To test the influence of the A_H on critical layer thickness, calculations were performed using values between 1 and 1.3 kT. The critical layer thickness over ionic strength decreases linearly with decreasing Hamaker constant. In contrast, the critical layer thickness over pH (except at the pI) shows two regimes. At $A_H \leq 1.17$ kT, the emulsion flocculates in the primary minimum, at $A_H \geq 1.175$ kT in the secondary minimum. As a result, in this region, the critical layer thickness for steric stabilization at pH 5 increases steeply from below 2 nm to around 4.7 nm. Since a critical layer thickness of below 2 nm obtained for $A_H \leq 1.17$ kT would mean that patatin and other proteins (e.g. β -lactoglobulin and ovalbumin) would not flocculate at pH 5, it is considered to be not realistic for these systems. Therefore, the calculations are performed with a A_H of 1.175 kT. This alteration of the Hamaker constant from 1.3 to 1.175 kT results in a slight decrease of the theoretical critical layer thickness (figures 6C and D).

In addition to the Hamaker constant, the exact value for the layer thickness is equally difficult to determine. In literature, the reported layer thickness of adsorbed protein varies between the radius of the protein²⁰, as assumed in the above calculations, and 1.45 x radius (i.e. 2.9 nm for β -lactoglobulin adsorbed to a latex sphere)¹⁰. Using the latter value for the calculation of the layer thickness and 1.175 kT for the Hamaker constant figures 6C and D were constructed. With these values, the emulsions stabilized by the maltotriose- and maltopentaose-conjugates are theoretically expected to be stable against flocculation at pH 5, which was also observed experimentally. However, at high ionic strength (i.e. $I \geq 30$ mM) and at the pI, all emulsions are still expected to flocculate (figures 6C and D). In order to obtain stability against flocculation at all conditions (i.e. $I \leq 1$ M and $\text{pH} = \text{pI}$), the layer thickness of the adsorbed layer should exceed 7 nm (figures 6C and D). This fits with the observation that an emulsion stabilized by a β -lactoglobulin-dextran conjugate (molecular mass dextran = 18.3 kDa) with a layer thickness of 8.3 nm was stable against flocculation at increased ionic strength¹³.

Conclusion

Covalent coupling maltotriose and maltopentaose to patatin resulted in stability against pH-induced flocculation. This effect is postulated to be caused by steric stabilization. The critical thickness of the adsorbed layer for steric stabilization against pH-induced flocculation was found to be between 2.89 nm and 3.90 nm. Theoretical determinations based on the DLVO interactions (i.e. electrostatic and van der Waals interaction) with an additional steric interaction fitted the experimental data. This validates that steric repulsion results in the observed differences between the emulsions stabilized by the different glycosylated proteins.

References

1. Dickinson, E., Flocculation of protein-stabilized oil-in-water emulsions. *Colloids Surf., B* **2010**, 81, (1), 130-140.
2. Zhai, J.; Wooster, T. J.; Hoffmann, S. V.; Lee, T.; Augustin, M. A.; Aguilar, M., Structural rearrangement of β -lactoglobulin at different oil-water interfaces and its effect on emulsion stability. *Langmuir* **2011**, 27, (15), 9227-9236.
3. Kulmyrzaev, A. A.; Schubert, H., Influence of KCl on the physicochemical properties of whey protein stabilized emulsions. *Food Hydrocolloids* **2004**, 18, (1), 13-19.
4. Auroy, P.; Auvray, L.; Léger, L., Silica particles stabilized by long grafted polymer chains: From electrostatic to steric repulsion. *J. Colloid Interface Sci.* **1992**, 150, (1), 187-194.
5. Dunlap, C. A.; Côté, G. L., β -Lactoglobulin-dextran conjugates: effect of polysaccharide size on emulsion stability. *J. Agric. Food Chem.* **2005**, 53, (2), 419-423.
6. Dickinson, E., Hydrocolloids as emulsifiers and emulsion stabilizers. *Food Hydrocolloids* **2009**, 23, (6), 1473-1482.
7. Evans, M.; Ratcliffe, I.; Williams, P. A., Emulsion stabilisation using polysaccharide-protein complexes. *Curr. Opin. Colloid Interface Sci.* **2013**, 18, (4), 272-282.
8. Kato, Y.; Aoki, T.; Kato, N.; Nakamura, R.; Matsuda, T., Modification of ovalbumin with glucose 6-phosphate by amino-carbonyl reaction. Improvement of protein heat stability and emulsifying activity. *J. Agric. Food Chem.* **1995**, 43, (2), 301-305.
9. Diftis, N.; Kiosseoglou, V., Physicochemical properties of dry-heated soy protein isolate-dextran mixtures. *Food Chem.* **2006**, 96, (2), 228-233.
10. Wooster, T. J.; Augustin, M. A., The emulsion flocculation stability of protein-carbohydrate diblock copolymers. *J. Colloid Interface Sci.* **2007**, 313, (2), 665-675.
11. Stenkamp, V. S.; Berg, J. C., The role of long tails in steric stabilization and hydrodynamic layer thickness. *Langmuir* **1997**, 13, (14), 3827-3832.
12. Bijsterbosch, H. D.; Cohen Stuart, M. A.; Fleer, G. J., Effect of block and graft copolymers on the stability of colloidal silica. *J. Colloid Interface Sci.* **1999**, 210, (1), 37-42.
13. Wooster, T. J.; Augustin, M. A., β -Lactoglobulin-dextran Maillard conjugates: their effect on interfacial thickness and emulsion stability. *J. Colloid Interface Sci.* **2006**, 303, (2), 564-572.
14. ter Haar, R.; Schols, H. A.; Gruppen, H., Effect of saccharide structure and size on the degree of substitution and product dispersity of α -lactalbumin glycosylated via the Maillard reaction. *J. Agric. Food Chem.* **2011**, 59, (17), 9378-9385.
15. Butré, C. I.; Wierenga, P. A.; Gruppen, H., Effects of ionic strength on the enzymatic hydrolysis of diluted and concentrated whey protein isolate. *J. Agric. Food Chem.* **2012**, 60, (22), 5644-5651.
16. Walstra, P., *Physical chemistry of foods*. Marcel Dekker, Inc.: New York, NY, USA, 2003.

17. Jachimska, B.; Wasilewska, M.; Adamczyk, Z., Characterization of globular protein solutions by dynamic light scattering, electrophoretic mobility, and viscosity measurements. *Langmuir* **2008**, *24*, (13), 6866-6872.
18. Ruis, H. G. M.; van Grujthuisen, K.; Venema, P.; van der Linden, E., Transitions in structure in oil-in-water emulsions as studied by diffusing wave spectroscopy. *Langmuir* **2007**, *23*, (3), 1007-1013.
19. Blijdenstein, T. B. J.; Hendriks, W. P. G.; van der Linden, E.; van Vliet, T.; van Aken, G. A., Control of strength and stability of emulsion gels by a combination of long- and short-range interactions. *Langmuir* **2003**, *19*, (17), 6657-6663.
20. Kim, H. J.; Decker, E. A.; McClements, D. J., Impact of protein surface denaturation on droplet flocculation in hexadecane oil-in-water emulsions stabilized by β -lactoglobulin. *J. Agric. Food Chem.* **2002**, *50*, (24), 7131-7137.
21. Israelachvili, J. N., *Intermolecular and surface forces*. Third ed.; Academic Press: New York, NY, USA, 2011.
22. Silvestre, M. P. C.; Decker, E. A.; McClements, D. J., Influence of copper on the stability of whey protein stabilized emulsions. *Food Hydrocolloids* **1999**, *13*, (5), 419-424.
23. Hesselink, F. T.; Vrij, A.; Overbeek, J. T. G., Theory of the stabilization of dispersions by adsorbed macromolecules. II. Interaction between two flat particles. *J. Phys. Chem.* **1971**, *75*, (14), 2094-2103.
24. Wiese, G. R.; Healy, T. W., Effect of particle size on colloid stability. *Trans. Faraday Soc.* **1970**, *66*, 490-499.
25. Vincent, B.; Young, C. A.; Tadros, T. F., Equilibrium aspects of heteroflocculation in mixed sterically-stabilised dispersions. *Faraday Discuss. Chem. Soc.* **1978**, *65*, 296-305.
26. Pots, A. M.; Gruppen, H.; Hessing, M.; van Boekel, M. A. J. S.; Voragen, A. G. J., Isolation and characterization of patatin isoforms. *J. Agric. Food Chem.* **1999**, *47*, (11), 4587-4592.
27. Broersen, K.; Elshof, M.; De Groot, J.; Voragen, A. G. J.; Hamer, R. J.; De Jongh, H. H. J., Aggregation of β -lactoglobulin regulated by glycosylation. *J. Agric. Food Chem.* **2007**, *55*, (6), 2431-2437.
28. Brands, C. M. J.; van Boekel, M. A. J. S., Kinetic modeling of reactions in heated monosaccharide-casein systems. *J. Agric. Food Chem.* **2002**, *50*, (23), 6725-6739.
29. ter Haar, R.; Westphal, Y.; Wierenga, P. A.; Schols, H. A.; Gruppen, H., Cross-linking behavior and foaming properties of bovine α -lactalbumin after glycation with various saccharides. *J. Agric. Food Chem.* **2011**, *59*, (23), 12460-12466.
30. Liu, J.; Ru, Q.; Ding, Y., Glycation a promising method for food protein modification: physicochemical properties and structure, a review. *Food Res. Int.* **2012**, *49*, (1), 170-183.
31. Cho, D.; Narsimhan, G.; Franses, E. I., Adsorption dynamics of native and alkylated derivatives of bovine serum albumin at air-water interfaces. *J. Colloid Interface Sci.* **1996**, *178*, (1), 348-357.
32. Cho, D.; Narsimhan, G.; Franses, E. I., Adsorption dynamics of native and pentylated bovine serum albumin at air-water interfaces: surface concentration/surface pressure measurements. *J. Colloid Interface Sci.* **1997**, *191*, (2), 312-325.
33. Wierenga, P. A.; Meinders, M. B. J.; Egmond, M. R.; Voragen, A. G. J.; De Jongh, H. H. J., Quantitative description of the relation between protein net charge and protein adsorption to air-water interfaces. *J. Phys. Chem. B* **2005**, *109*, (35), 16946-16952.
34. Wierenga, P. A.; van Norél, L.; Basheva, E. S., Reconsidering the importance of interfacial properties in foam stability. *Colloids Surf., A* **2009**, *344*, (1-3), 72-78.
35. Medrano, A.; Abirached, C.; Moyna, P.; Panizzolo, L.; Añón, M. C., The effect of glycation on oil-water emulsion properties of β -lactoglobulin. *LWT - Food Sci. Technol.* **2012**, *45*, (2), 253-260.

36. Akhtar, M.; Dickinson, E., Whey protein–maltodextrin conjugates as emulsifying agents: An alternative to gum arabic. *Food Hydrocolloids* **2007**, 21, (4), 607-616.
37. Narsimhan, G., Maximum disjoining pressure in protein stabilized concentrated oil-in-water emulsions. *Colloids Surf.* **1992**, 62, (1-2), 41-55.
38. Radford, S. J.; Dickinson, E., Depletion flocculation of caseinate-stabilised emulsions: What is the optimum size of the non-adsorbed protein nano-particles? *Colloids Surf., A* **2004**, 238, (1–3), 71-81.
39. Dimitrova, T. D.; Leal-Calderon, F.; Gurkov, T. D.; Campbell, B., Disjoining pressure vs thickness isotherms of thin emulsion films stabilized by proteins. *Langmuir* **2001**, 17, (26), 8069-8077.
40. Damodaran, S., Protein stabilization of emulsions and foams. *J. Food Sci.* **2005**, 70, (3), R54-R66.

Chapter 5

Improved emulsion stability by succinylation of patatin is caused by partial unfolding rather than charge effects

Abstract

This study investigates the influence of succinylation on the molecular properties (i.e. charge, structure and hydrophobicity) and the flocculation behaviour of patatin-stabilized oil-in-water emulsions. Patatin was succinylated to five degrees (0 % (R_0) to 57 % ($R_{2.5}$)). Succinylation not only resulted in a change of the protein charge but also in (partial) unfolding of the secondary structure, and consequently in an increased initial adsorption rate of the protein to the oil-water interface. The stability against salt-induced flocculation showed two distinct regimes, instead of a gradual shift in stability as expected by the DLVO theory. While flocculation was observed at ionic strengths > 30 mM for the emulsions stabilized by the variants with the lowest degrees of modification (R_0 - R_1), the other variants ($R_{1.5}$ - $R_{2.5}$) were stable against flocculation ≤ 200 mM. This was related to the increased initial adsorption rate, and the consequent transition from a protein-poor to a protein-rich regime. This was confirmed by the addition of excess protein to the emulsions stabilized by R_0 - R_1 which resulted in stability against salt-induced flocculation. Therefore, succinylation of patatin indirectly results in stability against salt-induced flocculation, by increasing the initial adsorption rate of the protein to the oil-water interface, leading to a shift to the protein-rich regime.

Based on: Delahaije, R.J.B.M.; Wierenga, P.A.; Giuseppin, M.L.F.; Gruppen, H. Improved emulsion stability by succinylation of patatin is caused by partial unfolding rather than charge effects. *J. Colloid Interface Sci.* **2014**, 430, 69-77.

Introduction

Many studies have been devoted to the destabilization mechanisms (e.g. creaming, coalescence, and flocculation) of oil-in-water emulsions stabilized by globular proteins. The flocculation behaviour of these emulsions has often been qualitatively described based on colloidal interactions (e.g. electrostatic interactions)¹. For emulsions stabilized by globular proteins, flocculation typically occurs under conditions where the net interaction between the droplets is attractive (i.e. high ionic strength and pH close to the iso-electric point)^{2,3}. This was, for instance, shown for patatin (molecular mass: 40 kDa; pI: 4.7), a globular plant protein isolated from potato, as well as for globular animal proteins (e.g. β -lactoglobulin and ovalbumin) (chapter 3). To prevent flocculation, repulsive interactions (i.e. electrostatic and steric) should be of sufficient range and strength to counteract the attractive van der Waals interaction¹.

Steric interactions have been described to result in stability against pH-induced flocculation of emulsions stabilized by glycosylated proteins (e.g. patatin glycosylated with maltotriose) (chapter 4)⁴⁻⁶. The present study focuses on the effect of electrostatic interactions on the flocculation behaviour of patatin-stabilized emulsions. The range and strength of the electrostatic interactions depend on the ionic strength of the solution and the surface charge of the protein, respectively. The latter is affected by the pH of the solution, but can also be chemically modified by succinylation. Succinylation increases the net surface charge above the iso-electric point by converting a positively charged lysine group into a negatively charged carboxylic group. It can, therefore, be used as a tool to study the effect of surface charge under constant conditions (i.e. pH and ionic strength).

However, it must be noted that succinylation does not only change the charge, but can also result in changes in protein structure or structural stability. Succinylation of β -lactoglobulin, for example, results in a loss of secondary structure with increasing degree of modification (i.e. increase of random coil from 24 to 69 % with increase of the degree of modification from 0 to 99 %)⁷. The decreased stability is considered to be induced by the increase of surface charge and consequently the increase of electrostatic repulsion within the molecule⁸. On the other hand, no changes in the secondary and tertiary structure were observed by succinylation of lysozyme and ovalbumin^{9,10}. Still, a decrease in the structural stability against heat and guanidine hydrochloride was found after succinylation of lysozyme^{9,11}. These results indicate that the effect of succinylation on the protein structure is influenced by (1) the protein molecule and (2) the degree/extent of modification. For patatin, increasing the surface charge (i.e. by increasing the pH from pH 6 to pH 8) was described to result in (partial) unfolding of the protein¹². Therefore, increasing the surface charge by succinylation may also affect the patatin structure.

The two effects resulting from succinylation (i.e. increase of the surface charge and (partial) unfolding) were shown to affect the interfacial properties of proteins in different ways. Firstly, the increase in surface charge results in an increase of the energy barrier for adsorption at the air-water interface^{7, 10}. This decreases the adsorption rate and adsorbed amount (figure 1A). Unfolding, on the other hand, will lead to exposure of hydrophobic amino acid residues, resulting in a reduction of the barrier for adsorption at the air-water interface. This increases the adsorption rate of the protein to the interface¹³⁻¹⁵ (figure 1B). In both cases, increasing the ionic strength, and thereby decreasing the electrostatic repulsion, will affect the adsorption behaviour. In the first case, an increase of the ionic strength diminishes the electrostatic barrier, resulting in similar adsorption rates and adsorbed amounts for proteins with different surface charge (i.e. non-modified and succinylated) (figure 1C). In the case of (partial) unfolding, the increase of the ionic strength will only lead to a slight increase of the adsorption rate and the adsorbed amount (figure 1D).

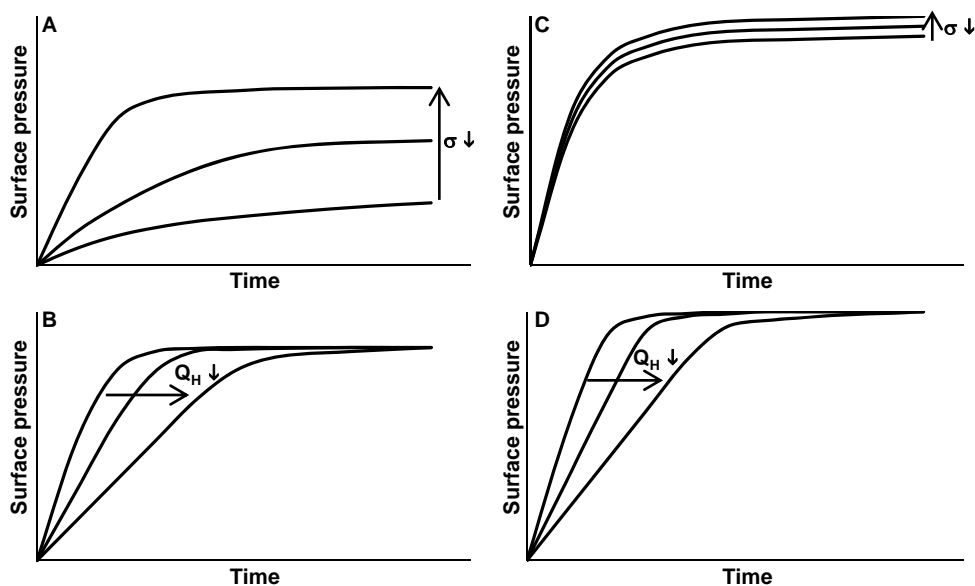


Figure 1. Illustration of expected surface pressure as function of time for proteins with varying surface charge (σ) at low (A) and high ionic strength (C) and for proteins with varying exposed hydrophobicity (Q_H) at low (B) and high ionic strength (D).

As succinylation may alter different properties of the protein (e.g. charge, folding state), and these alterations may affect the adsorption in various ways, it is important to determine the effect of the modification on the protein properties. Therefore, this study systematically investigates the effect of succinylation on the physico-chemical properties of the patatin molecule (i.e. surface charge, folding and hydrophobicity). In addition, the effect on the

flocculation behaviour of emulsions stabilized by five (succinylated) patatin variants with increasing degree of modification is determined.

Materials and methods

Materials

Patatin-rich liquid protein concentrate was obtained from Solanic/AVEBE (Veendam, The Netherlands). All other chemicals were of analytical grade and purchased from either Sigma-Aldrich (St. Louis, MO, USA) or Merck (Darmstadt, Germany).

Protein purification

Patatin was purified from the patatin-rich liquid protein concentrate using size-exclusion chromatography as described previously (chapter 4), and stored as lyophilized powder. The final purified patatin contained 97 % protein (N x 6.40). As confirmed by analytical scale size-exclusion chromatography, $\geq 85\%$ was present as dimeric patatin, and $\leq 15\%$ was freezing-induced aggregated protein.

Succinylation

Patatin (25 g L^{-1}) was dissolved in milliQ water. The pH of the patatin solutions was set to pH 8.0 with 1 M NaOH. Subsequently, succinic anhydride was added in five steps to a final molar ratio of 0, 0.5, 1, 1.5, 2 and 2.5 succinic anhydride: lysine groups (further referred to as R_0 , $R_{0.5}$, R_1 , $R_{1.5}$, R_2 and $R_{2.5}$). Prior to each addition of succinic anhydride, the pH was set to pH 8.0 by the addition of 0.2 M NaOH using a pH stat (Metrohm, Herisau, Switzerland) at room temperature. After addition of all succinic anhydride, the solution was stirred for another 30 minutes, followed by dialysis against demineralized water and lyophilization.

Degree of modification (DM)

The average degree of modification was calculated from the decrease of primary amino groups of the proteins (i.e. ϵ -amino and terminal amino groups) determined using the o-phthaldialdehyde (OPA) assay as described previously¹⁶. All samples were analysed in duplicate. The degree of modification was calculated from equation 1.

$$DM = \frac{NH_{2, \text{patatin}} - NH_{2, \text{free}}}{NH_{2, \text{patatin}}} \times 100\% \quad (1)$$

in which DM is the degree of modification [%] and $NH_{2, \text{patatin}}$ and $NH_{2, \text{free}}$ are the total number of NH_2 groups in non-modified patatin and the number of free NH_2 groups in the succinylated patatin variant, respectively. Based on the amino acid sequence of patatin from

different potato cultivars obtained from the uniprot database, a patatin molecule was expected to contain 24 ± 1 lysine residues.

Zeta potential of protein solution

Zeta potentials of (succinylated) patatin variants were determined with a Zetasizer Nano ZS (Malvern Instruments, Worcestershire, UK) using the laser Doppler velocimetry technique. The proteins were dissolved in 10 mM sodium phosphate buffer pH 7.0 at a concentration of 10 g L^{-1} . The measurements were performed at $25 \text{ }^\circ\text{C}$ and 40 volt. Five sequential runs were averaged to obtain the results. Zeta potentials were calculated with Henry's equation¹⁷ (equation 2).

$$\zeta = \frac{3\eta \cdot \mu_e}{2\epsilon F(\kappa\alpha)} \quad (2)$$

in which ζ is the zeta potential [V], η is the viscosity [$0.8872 \times 10^{-3} \text{ Pa s}$], μ_e is the electrophoretic mobility [$\text{m}^2 \text{ V}^{-1} \text{ s}^{-1}$], ϵ is the dielectric constant of the medium [$7.08 \times 10^{-10} \text{ C}^2 \text{ J}^{-1} \text{ m}^{-1}$] and $F(\kappa\alpha)$ is Henry's function [-], which equals 1.5 for the Smoluchowski approximation¹⁷.

Secondary, tertiary and quaternary structure

Far-UV Circular Dichroism (CD)

The secondary structure of the (succinylated) patatin variants was determined using far-UV CD. Proteins were dissolved at a concentration of 0.1 g L^{-1} in a 10 mM sodium phosphate buffer pH 7.0. The spectra (190-260 nm) were recorded as averages from 10 spectra on a Jasco J-715 spectropolarimeter (Jasco, Tokyo, Japan). The measurements were performed at $20 \text{ }^\circ\text{C}$ in quartz cuvettes with an optical path length of 1 mm. After subtracting the spectra of the protein-free sample, the relative content of secondary structure elements was estimated using a non-linear least squares fitting procedure¹⁸. The standard error of the fit was in the range of 0.4-0.6 % for all variants.

Near-UV CD

Changes in tertiary structure of the (succinylated) patatin variants were determined using near-UV CD. The measurements were performed as described for the secondary structure determination with a protein concentration of 1 g L^{-1} , a spectra recorded from 250-350 nm and an optical path length of 10 mm.

Intrinsic fluorescence

As indication for changes in the tertiary structure, the exposure of tryptophan and tyrosine residues was determined using intrinsic fluorescence. The (succinylated) proteins were dissolved in 10 mM sodium phosphate buffer pH 7.0 in a concentration of 1 g L^{-1} . These solutions were then excited at 280 nm, and the emission spectrum was collected from 290-500 nm using a Varian Cary Eclipse fluorescence spectrophotometer (Agilent

Technologies, Santa Clara, CA, USA). The emission and excitation slits were set to 5 nm and the measurements were performed at 25 °C.

Size-exclusion chromatography

The quaternary structure of the patatin variants (5 g L⁻¹ in 10 mM sodium phosphate buffer pH 7.0) was analysed by high-performance size-exclusion chromatography using an Äkta Micro equipped with a Superdex 200 PC 3.2/30 column (GE Healthcare, Uppsala, Sweden). Prior to analysis, the samples were centrifuged (16100g, 10 min, 20 °C) to remove non-dissolved protein. Subsequently, the samples (20 µL) were injected and eluted with 10 mM sodium phosphate buffer pH 7.0 at a flow rate of 0.08 ml min⁻¹. The elution was monitored using UV absorbance at 280 nm. The column was calibrated with globular proteins with a mass range of 13.7-67 kDa (GE Healthcare).

Exposed hydrophobicity

The exposed hydrophobicity of the patatin variants was determined by a fluorescence assay using N,N-dimethyl-6-propionyl-2-naphthylamine (PRODAN) as fluorescent probe. The (succinylated) patatin variants were dissolved in 10 mM sodium phosphate buffer pH 7.0 in concentrations between 6.25 x 10⁻⁶ - 2.50 x 10⁻⁴ M. PRODAN was dissolved in methanol at a concentration of 1.76 x 10⁻⁴ M. Subsequently, 1 mL of protein solution and 2.5 mL of PRODAN solution were mixed and incubated for 15 minutes in the dark. An excitation wavelength of 365 nm was used, and the emission spectra were collected from 400-620 nm using a Varian Cary Eclipse fluorescence spectrophotometer (Agilent Technologies). The emission and excitation slits were set to 5 nm and the measurements were performed at 25 °C. The increase in fluorescence intensity upon binding of the probe to the accessible hydrophobic regions of the protein is used as a measure of protein exposed hydrophobicity. The relative exposed hydrophobicity was calculated by linear regression from the initial slope of the fluorescence intensity (based on the area) versus protein concentration.

Adsorption kinetics and surface elastic modulus

Solutions of (succinylated) patatin variants (0.1 g L⁻¹) were prepared in a 10 mM sodium phosphate buffer pH 7.0 in the absence or presence of 190 mM NaCl. The surface tension and surface elastic modulus as a function of time were measured using an automated drop tensiometer (ADT, Teclis IT Concept, Longessaigne, France). The system was temperature controlled at 20 °C. For the surface tension measurements, the drop volume was kept constant at 7 µL for 3600 s. The change in surface tension compared to that of the pure interface (i.e. the air-water interface) was expressed as the surface pressure (equation 3)¹⁹.

$$\Pi(t) = \gamma_0 - \gamma(t) \quad (3)$$

where γ_0 is the measured interfacial tension of the pure buffer [72.8 mN m⁻¹].

The surface elastic modulus was measured by inducing sinusoidal changes in the interfacial area with an amplitude of 5 % and a frequency of 0.1 Hz. The modulus was calculated from the measured changes in surface tension and surface area averaged over a sequence of five sinuses. Every 100 s a sequence of five sinuses was performed. All measurements were performed in duplicate.

Adsorbed amount

As an indication of the amount of protein adsorbed at the oil-water interface, the amount of protein adsorbed at the air-water interface was determined using a Multiskop ellipsometer (Optrel, Sinzing, Germany). Adsorption of protein to the air-water interface results in an increase of the ellipsometric angles (Δ and ψ) of the reflected monochromatic laser light ($\lambda = 632.8$ nm, angle of incidence = 50°). From the ellipsometric angles, the refractive index (n_{adsorbed}) and thickness (d_{adsorbed}) of the adsorbed layers are fitted using a model based on two bulk phases (i.e. air and water) and one adsorbed layer. The fitting parameters for the model were: $n_{\text{air}} = 1.000$, $n_{\text{buffer}} \approx n_{\text{water}} = 1.333$, $dn/dc = 0.185$ mL g⁻¹ and the angle of incidence was 50° .

The adsorbed amount (Γ) is obtained from the fitted refractive index (n_{adsorbed}) and thickness (d_{adsorbed}) of the adsorbed layer using equation 4²⁰.

$$\Gamma(t) = \frac{(n_{\text{adsorbed}}(t) - n_{\text{buffer}})}{\frac{dn}{dc}} \cdot d_{\text{adsorbed}}(t) \quad (4)$$

where Γ is the adsorbed amount [mg m⁻²], n_{adsorbed} and n_{buffer} are the refractive index of the adsorbed layer and the buffer, respectively, dn/dc is the refractive index increment [i.e. 0.185 mL g⁻¹, typical for globular proteins^{20, 21}] and d_{adsorbed} is the thickness of the adsorbed layer. For the measurements, the (succinylated) patatin variants (3 g L⁻¹) were dissolved in 10 mM sodium phosphate buffer pH 7.0 in the presence or absence of 190 mM NaCl. Prior to each measurement, the buffer with or without 190 mM NaCl was measured for 600 seconds. Next, the concentrated protein solution was added to reach a final concentration of 0.1 g L⁻¹.

Emulsification

The (succinylated) patatin variants were dissolved in 10 mM sodium phosphate buffer pH 7.0 at a concentration of 5 g L⁻¹ and subsequently mixed with 10 %(v/v) sunflower oil. A pre-emulsion was prepared using an Ultra turrax Type T-25B (IKA, Staufen, Germany) at 9500 rpm for 1 min. Subsequently, the pre-emulsion was passed 30 times through a Labhoscope 2.0 laboratory scale high-pressure homogenizer (Delta Instruments, Drachten, The Netherlands) operated at 15 MPa.

Effect of ionic strength To determine the effect of the Debye screening length and zeta potential on the flocculation behaviour of the emulsions, emulsions were prepared as described above. After emulsification, the ionic strength was adjusted with 2 M NaCl to obtain emulsions with an ionic strength of 10-200 mM.

Effect of protein concentration To determine the effect of excess (non-adsorbed) protein on the flocculation behaviour of the emulsions, emulsions were prepared as described above. After emulsification, a concentrated protein solution (200 g L⁻¹) was added to the emulsion to reach final concentrations of 5, 7.5, 10, 12.5, 15 or 20 g L⁻¹. The ionic strength of these emulsions was then adjusted to 10, 100 or 200 mM with 2 M NaCl.

Subsequently, the emulsions were stored for 24 hours at 20 °C prior to further analysis. For selected samples, it was confirmed that no significant changes occurred during this storage period.

Zeta potential of emulsion droplets

Zeta potentials of the emulsion droplets were determined with a Zetasizer Nano ZS (Malvern Instruments) using the laser Doppler velocimetry technique. The emulsions were diluted 500 times to prevent multiple scattering. The measurements were performed at 25 °C and 40 Volt. The results of five sequential runs were averaged. Zeta potentials were calculated with Henry's equation¹⁷ (equation 2).

Theoretical estimation of the flocculation behaviour

The flocculation behaviour is estimated based on the DLVO theory. This theory describes the interactions between two proteins (U_{tot}) by combining van der Waals attraction (U_{vdW}) and electrostatic repulsion (U_e) (equation 5)²².

$$U_{tot}(h) = U_{vdW}(h) + U_e(h) \quad (5)$$

in which h is the separation distance between the proteins [m].

The van der Waals and electrostatic interactions are described by equations 6 and 7²², respectively.

$$U_{vdW} = -\frac{A}{6} \left(\frac{2R^2}{4Rh + h^2} + \frac{2R^2}{4R^2 + 4Rh + h^2} + \ln \frac{4Rh + h^2}{4R^2 + 4Rh + h^2} \right) \quad (6)$$

$$U_e(h) = 2\pi\epsilon_0\epsilon_r R\Psi_0^2 e^{-\kappa h} \quad (7)$$

in which κ for a monovalent electrolyte is described by equation 8²².

$$\kappa = \sqrt{\frac{2N_a e^2 I}{\epsilon_0 \epsilon_r k_B T}} \quad (8)$$

in which A is the Hamaker constant [4.83×10^{-21} J] (chapter 4), R is the radius of the emulsion droplet [m], ϵ_0 is the dielectric constant of a vacuum [8.85×10^{-12} C² J⁻¹ m⁻¹], ϵ_r is the relative dielectric constant of the medium (80), Ψ_0 is the surface potential [V], κ is the reciprocal of the Debye screening length [m⁻¹], N_a is the Avogadro constant [6.022×10^{23} mol⁻¹], e is the elementary charge [1.602×10^{-19} C], I is the ionic strength [mol m⁻³], k_B is the Boltzmann constant [1.38×10^{-23} J K⁻¹] and T is the temperature [K].

As a critical barrier, which is the demarcation between systems stable and unstable towards flocculation, an interaction potential of 5 kT is used^{23, 24}. Flocculation occurs within the timespan of the experiment when the primary maximum decreases below 5 kT or the secondary minimum decreases below -5 kT (U_{cr}). Subsequently, the theoretical calculations will be compared with theory to determine to which extent the DLVO theory coincides with the experimental data. The interaction potential is calculated using the droplet zeta potential¹⁹, the average droplet size and Debye screening length.

Determination of flocculation

Laser diffraction

Droplet size distribution was measured using laser light diffraction (Mastersizer 2000, Malvern Instruments) equipped with a Hydro SM sample dispersion unit. The volume-surface average diameter ($d_{3,2}$) (equation 9) was reported as an average of at least five runs.

$$d_{3,2} = \frac{\sum N_i d_i^3}{\sum N_i d_i^2} \quad (9)$$

in which N_i and d_i represent the number and diameter of droplets of size class i , respectively.

Diffusing wave spectroscopy (DWS)

As indication of droplet flocculation, DWS measurements were performed as described previously²⁵. The autocorrelation function was averaged from five sequential runs of 120 seconds. Subsequently, the autocorrelation functions were normalized by dividing the obtained $g_2(t)-1$ values by the maximum measured value. Normalized autocorrelation functions were then fitted using equation 10. This was derived from the equation used by Ruis et al.²⁵, assuming that $\langle \Delta r^2(t) \rangle = 6Dt^p$ for $p < 1 = \alpha t^x$ for $x < 1$.

$$g_2(t) - 1 \approx (e^{-\langle \Delta r^2(t) \rangle})^2 \approx e^{-\alpha t^x} \quad (10)$$

The decay time ($\tau_{1/2}$), which is defined as the time at which $g_2(t)-1$ decayed to half of its initial value, was determined using the fitted equation. An increase of the decay time is related to decreased droplet mobility²⁶.

Microscopy

To identify whether the increase in droplet size observed in DWS was due to flocculation or coalescence, the emulsions were analysed by light microscopy using an Axioscope A01 (Carl Zeiss, Sliedrecht, The Netherlands) at a magnification of 40x.

Results and discussion

Characterization of emulsion stability against flocculation

The extent of flocculation of the emulsions stabilized by the (succinylated) patatin variants was determined from the decay time ($\tau_{1/2}$) (figure 2). For the emulsions stabilized by the variants with the lowest degrees of modification (i.e. R₀-R₁), the decay time increases with increasing ionic strength exceeding 30 mM, indicating flocculation. That the observed changes were indeed due to flocculation and not due to coalescence was confirmed by microscopy. Typical examples of normal (pH 7), and flocculated emulsions (pH 5) are shown in chapter 3 (figure 4), where it was also shown that the flocculated emulsion at pH 5 could be dissociated by the addition of SDS. In contrast to the emulsions stabilized by the lowest degrees of modification, the decay time of emulsions stabilized by the other variants is not affected by an ionic strength until at least 200 mM, demonstrating the absence of flocculation. This shows that succinylation of patatin results in increased stability against salt-induced flocculation.

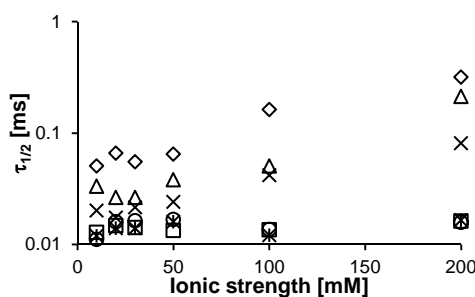


Figure 2. Decay time ($\tau_{1/2}$) of emulsion stabilized by R₀ (◇), R_{0.5} (△), R₁ (×), R_{1.5} (*), R₂ (○) and R_{2.5} (□) at pH 7.0 as a function of ionic strength.

Molecular properties

To determine the cause of the increased flocculation stability of emulsion stabilized by succinylated patatin, the molecular properties of the (succinylated) patatin variants were studied. The number of modified groups was determined from the decrease of primary amino groups (i.e. ϵ -amino groups of lysine and the terminal amino group). The non-modified patatin has 28 ± 1 primary amino groups, which is higher than the 24 ± 1 groups expected based on the amino acid sequence. This discrepancy is expected to be

caused by differences in the amino acid sequence between cultivars. Moreover, the value is in agreement with values obtained from a different batch (data not shown). Modification with succinic anhydride results in a decrease of primary amino groups from 28 to 12 with increasing molar ratio of succinic anhydride: lysine groups from 0 to 2.5 (table 1). This corresponds with an increase of the degree of modification of from 0 to 57 %. Concomitantly, the zeta potential of the (succinylated) patatin variants increases from -18 mV to -27 mV with increasing molar ratio (figure 3).

Table 1. Chemical and interfacial properties of the (succinylated) patatin variants.

	free NH ₂ groups ^a	DM [%]	10 mM			200 mM		
			ζ potential protein [mV]	ζ potential emulsion [mV]	Γ _{sat} ^b [mg m ⁻²]	ζ potential protein [mV]	ζ potential emulsion [mV]	Γ _{sat} ^b [mg m ⁻²]
R ₀	28	0	-18	-47	2.1	-9	-17	2.7
R _{0.5}	28	0	-23	-46	1.7	-14	-20	2.5
R ₁	19	32	-26	-52	2	-15	-22	2.5
R _{1.5}	17	39	-28	-49	1.9	-17	-24	2.4
R ₂	13	54	-27	-42	1.9	-17	-21	2.3
R _{2.5}	12	57	-27	-40	1.8	-17	-22	2.5

^athe standard deviation of the free NH₂ group determination by the OPA assay is ± 1.

^bstandard deviation of the adsorbed amount determination at the air-water interface is ± 0.15 mg m⁻².

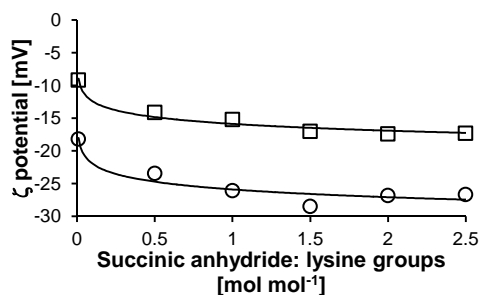


Figure 3. Zeta potential of the succinylated patatin variants (10 g L⁻¹) in 10 mM sodium phosphate buffer pH 7.0 in the absence (○) and presence of 190 mM NaCl (□).

As the increase of charge, indicated by an increase of the zeta potential, can destabilize or alter the structure of the protein, the effect of succinylation on the structure of patatin was determined by circular dichroism, intrinsic fluorescence and size-exclusion chromatography. The secondary structure of non-modified patatin (R₀) consisted of 25 % α-helices, 68 % β-structures (β-strands and β-turns) and 7 % random coil (figure 4A). This differs from other studies, which reported 30 % α-helices, 45-50 % β-structures and 15-20 % random coil^{12, 27}. This variation is expected to be caused by differences between the

cultivars and in the isolation method. With increasing degree of succinylation the random coil content gradually increases from 7 % to 37 % with a concomitant loss of β -structure, mainly β -strands, from 68 % to 32 % (figure 4A). A similar loss of secondary structure has also been described for β -lactoglobulin⁷. The tertiary and quaternary (i.e. dimer at pH 7²⁸) structure, on the other hand, were not significantly affected by the modification (figure 4B). Therefore, the tertiary and quaternary structure of patatin are more stable against changes in the protein charge than the secondary structure. In literature, the secondary structure of patatin was also described to be affected by an increasing pH (i.e. pH 6 to pH 8), and the consequent increase of surface charge¹².

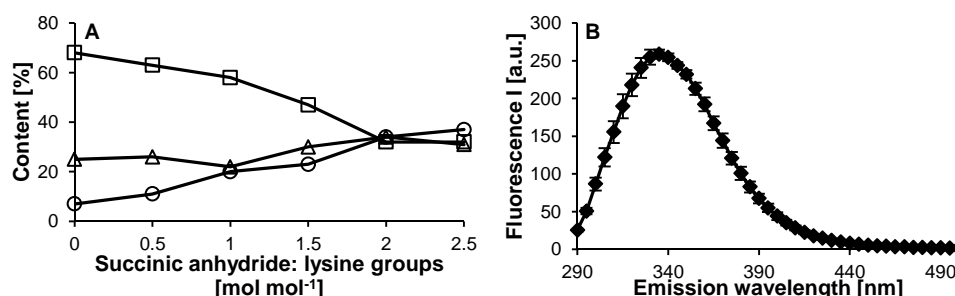


Figure 4. Content of α -helices (Δ), β -structures (β -sheets and β -turns; \square) and random coil (\circ) in (succinylated) patatin variants (0.1 g L^{-1}) in 10 mM sodium phosphate buffer pH 7.0 fitted from the far-UV CD spectra of R_0 (\diamond), $R_{0.5}$ (Δ), R_1 (\times), $R_{1.5}$ ($*$), R_2 (\circ) and $R_{2.5}$ (\square) (A) and the average fluorescence intensity spectrum of all (succinylated) patatin variants from intrinsic fluorescence (B; error bars indicate standard deviation).

As changes in the protein structure are often described to result in an increase of the exposed hydrophobicity⁸, the exposed hydrophobicity of the (succinylated) patatin variants was determined. To prevent charge effects on the determination of the protein exposed hydrophobicity, a neutral probe (i.e. PRODAN) was chosen. In contrast to the expectations, the exposed hydrophobicity was similar for all patatin variants (figure 5). However, it must be noted that absolute quantification of exposed hydrophobicity is difficult. This was illustrated by the fact that different values for hydrophobicity were found for the same protein using different probes and conditions (e.g. pH)²⁹.

So, not only the charge, but also the secondary structure of patatin is affected by succinylation.

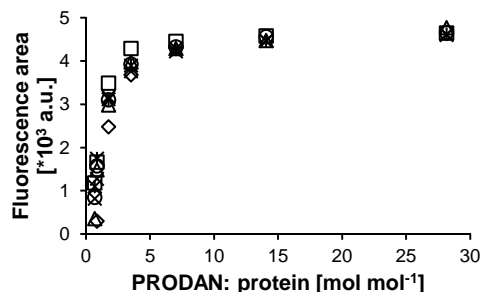


Figure 5. Protein exposed hydrophobicity of R_0 (\diamond), $R_{0.5}$ (\triangle), R_1 (\times), $R_{1.5}$ ($*$), R_2 (\circ) and $R_{2.5}$ (\square).
Interfacial properties

At low ionic strength, the elastic modulus (E_d)-surface pressure (Π) curves of all patatin variants were similar (figure 6C). This shows that the interactions between the adsorbed proteins are similar. Moreover, it indicates that the adsorption kinetics can be derived from the Π -t curve (figure 6A). While the initial adsorption rate is similar for all variants, the final surface pressure at 3600 seconds decreases with increasing surface charge (i.e. 20.3 mN m^{-1} for R_0 to 16.9 mN m^{-1} for $R_{2.5}$). In addition, the amount of adsorbed protein (Γ) was also similar for all variants (i.e. $1.92 \pm 0.13 \text{ mg m}^{-2}$) (table 1).

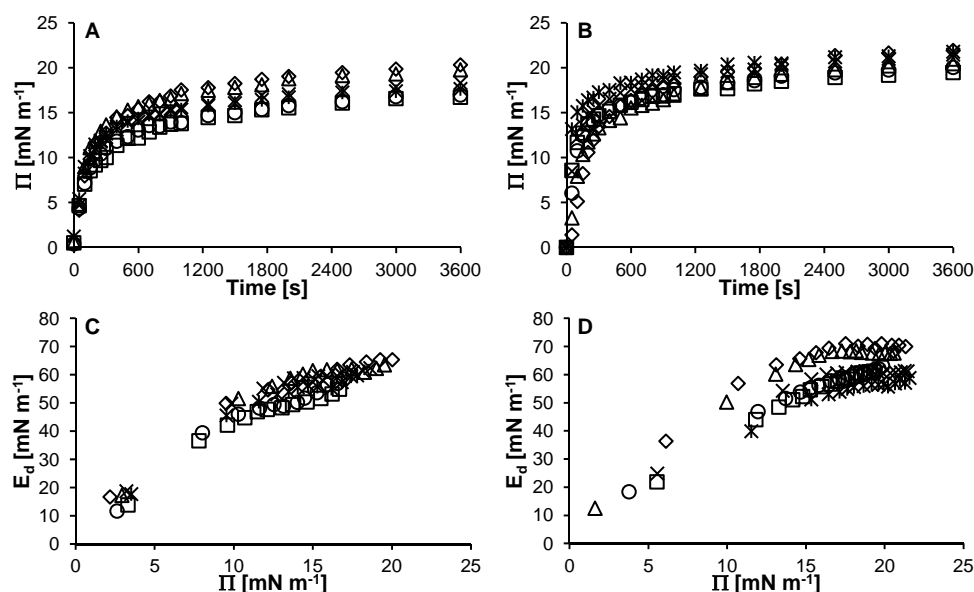


Figure 6. Surface pressure (Π) as a function of time and elastic modulus (E_d) as a function of surface pressure for R_0 (\diamond), $R_{0.5}$ (\triangle), R_1 (\times), $R_{1.5}$ ($*$), R_2 (\circ) and $R_{2.5}$ (\square) in 10 mM sodium phosphate buffer pH 7.0 in the absence (A and C) and presence of 190 mM NaCl (B and D).

A decrease of surface pressure with increasing surface charge has also been described for succinylated BSA⁷ and ovalbumin¹⁰. This was explained by an increase of the electrostatic barrier for adsorption and as a result a lower adsorbed amount^{7, 10, 30}. Although succinylation of patatin resulted in a decrease of the surface pressure, the adsorbed amount was not affected (table 1). Moreover, in contrast to the observations for the succinylated patatin variants, for succinylated ovalbumin, the adsorbed amount, the initial adsorption rate and the elastic modulus were described to decrease with increasing surface charge. This was attributed to an increase of the electrostatic barrier for adsorption and a decrease of the interactions between the adsorbed proteins¹⁰. Therefore, the results indicate that in addition to the increased charge another change in the protein structure/properties occurred that resulted in faster, or at least equal, adsorption rate, despite the increased charge.

In the case that succinylation would only influence the surface charge, the differences in adsorption kinetics observed at low ionic strength (i.e. 10 mM) were expected to decrease at increased ionic strength (i.e. 200 mM), as a result of charge screening (figures 1A and C). At high ionic strength, all properties (i.e. Π , E_d , Γ) increased compared to at low ionic strength (table 1 and figure 6). Moreover, it is observed that, like at low ionic strength, the adsorbed amount is similar for all variants (i.e. $2.49 \pm 0.14 \text{ mg m}^{-2}$) and the final surface pressure decreases with increasing surface charge (i.e. 21.9 mN m^{-1} for R_0 to 19.5 mN m^{-1} for $R_{2.5}$) (figure 6B). The difference between the interfacial properties of the patatin variants decreases with increasing ionic strength. In contrast to the observations at low ionic strength, the initial adsorption rate increased with increasing surface charge (figure 6B) and the elastic modulus decreased for the variants with a higher surface charge (i.e. R_1 - $R_{2.5}$) at high ionic strength (figure 6D). An increase of the adsorbed amount, surface pressure and initial adsorption rate with increasing ionic strength was also observed for ovalbumin¹⁰ and BSA⁷. This was explained by a decrease of the electrostatic repulsion and the Debye screening length. If the interfacial properties, however, would only be affected by electrostatic interactions, the initial adsorption rate of all variants at high ionic strength was expected to be similar (figure 1C). As the modification in the case of the patatin variants destabilizes the protein structure (as indicated by (partial) unfolding of the secondary structure), it would be logical to postulate that not only the charge, but also the exposure of hydrophobic amino acid residues affect the interfacial properties. An increase of the exposed hydrophobicity has been described to reduce the barrier for adsorption and as a consequence to increase the initial adsorption rate¹⁴ (figure 1B). The observations at low ionic strength (i.e. similar initial adsorption rates, Γ and E_d) can also be explained with the additional effect of exposed hydrophobicity. However, this increase is in contrast with the results of the PRODAN assay (figure 5). This may be explained by the fact that the hydrophobicity measurement is not sensitive to the changes (e.g. structural changes) that affect the interfacial properties.

In summary, the interfacial properties are explained by a combined effect of (1) the increase of the electrostatic repulsion and (2) the changes in the protein structure with increasing degree of modification.

Emulsion properties

The decay time of the emulsions at low ionic strength was determined as an indication for the initial droplet size (figure 7). The decay time decreases with increasing degree of modification for the emulsions stabilized by the variants with the lowest degrees of modification (i.e. R₀-R₁). For the emulsions stabilized by the variants with the highest degrees of modification (i.e. R_{1.5}-R_{2.5}), the decay time is similar.

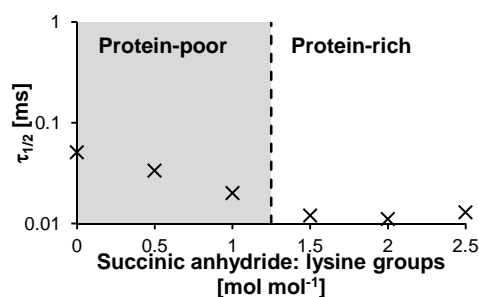


Figure 7. Decay time ($\tau_{1/2}$) of emulsion stabilized by the (succinylated) patatin variants (5 g L⁻¹, 10 mM sodium phosphate buffer pH 7.0).

This behaviour may be explained by an increase of the steric repulsion between the emulsion droplets or an increase of the initial adsorption rate. Steric repulsion depends on the radius of the protein and hence the thickness of the adsorbed layer. The radius of the protein was, however, not affected by modification, as confirmed by size-exclusion chromatography. This shows that the steric repulsion between the droplets has not changed. The initial adsorption rate, on the other hand, increased with increasing modification (figure 6B). Therefore, this behaviour is attributed to an increase of the initial adsorption rate, rather than steric effects.

The two regimes, shown in figure 7, correspond with the observations for one protein (e.g. β -lactoglobulin) with increasing protein concentrations (chapter 3). At low protein concentration (i.e. protein-poor regime), the droplet size or decay time decreases with increasing protein concentration. In this regime, the stabilization of smaller droplets is limited by the protein concentration in the continuous phase^{31, 32}. At higher protein concentrations (i.e. protein-rich regime), on the other hand, the droplet size stabilizes at an equilibrium droplet size. In this regime, sufficient protein is present to stabilize the smallest droplet size obtained under these conditions (i.e. protein is in excess), hence the name protein-rich regime. The protein-poor regime corresponds with emulsions stabilized by the

variants with the lowest degrees of modification (figure 7). The protein-rich regime corresponds with the emulsions stabilized by the variants with the highest degrees of modification. As the protein concentration is similar for all emulsions, these differences indicate that either the adsorption rate increases or that the adsorbed amount decreases (at a similar adsorption rate) with increasing degree of modification. At the air-water interface, the initial adsorption rate and Γ were similar for all patatin variants (table 1 and figure 6). This was explained by the contribution of electrostatics (i.e. counteracting adsorption) and hydrophobicity (i.e. stimulating adsorption). In literature, hydrophobicity is described to be more important for the adsorption at the oil-water interface compared to adsorption at the air-water interface³³. In addition, the adsorbed amount at the air-water and the oil-water interface has been described to be independent of the exposed hydrophobicity (chapter 3)¹⁴. Therefore, an increase of the initial adsorption rate with increasing degree of modification is postulated to be the reason for the observed differences between the variants.

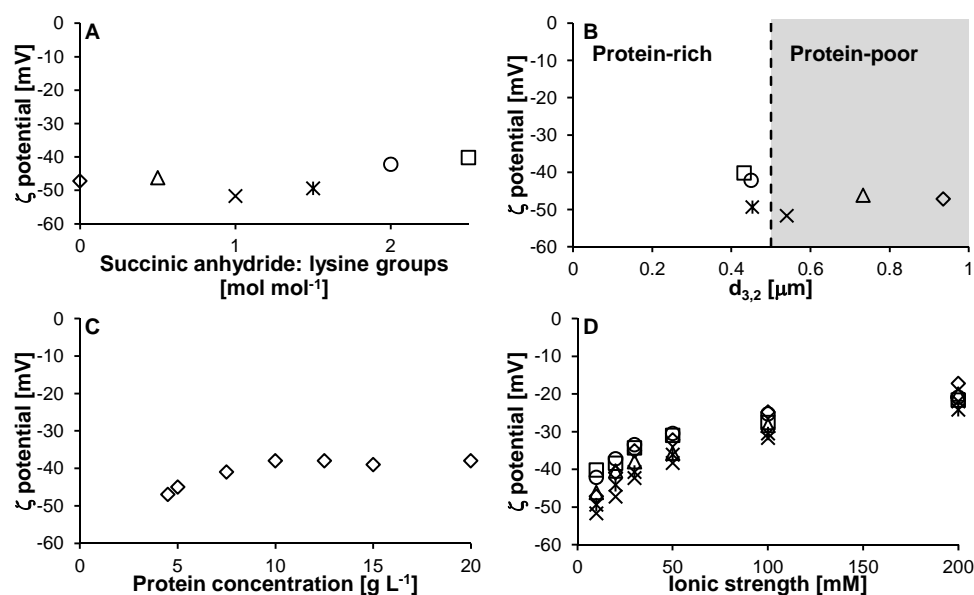


Figure 8. Zeta potential of the emulsions stabilized by R₀ (◇), R_{0.5} (△), R₁ (×), R_{1.5} (*), R₂ (○) and R_{2.5} (□) in 10 mM sodium phosphate buffer pH 7.0 (A), as a function of droplet size (B), as a function of protein concentration (C) and as a function of ionic strength (D).

The zeta potential of the emulsion droplets stabilized by R₀-R₁ shows a small increase with increasing surface charge of the protein (i.e. -47 mV for R₀ to -52 mV for R₁) (figure 8A). This is in line with the expectations as the surface charge of the protein increased, whereas the adsorbed amount was similar (table 1), resulting in an increase of the charges per unit area (i.e. surface charge, and as a consequence also the zeta potential). For the variants with

a high degree of modification (i.e. $R_{1.5}$ - $R_{2.5}$), on the other hand, the zeta potential of the emulsion droplets decreases with increasing surface charge (-49 mV for $R_{1.5}$ to -40 mV for $R_{2.5}$). This decrease was not expected based on the adsorbed amount (i.e. similar for all variants) and the zeta potential (i.e. more negative with increasing degree of modification) of the proteins (table 1). Nevertheless, it was shown to correspond with the protein-rich regime (figure 8B). Therefore, it is expected to be caused by the proteins in the continuous phase (i.e. excess protein). As the proteins in the continuous phase have a lower zeta potential (i.e. -18 mV to -27 mV) than the emulsion droplets (i.e. \geq -52 mV) (table 1), an increase of excess protein is expected to result in a decrease of the zeta potential. To verify this, experiments were performed where proteins were added to the continuous phase of emulsions (figure 8C). With increasing (serum) protein concentration, the zeta potential decreases (i.e. -47 mV for 5 g L^{-1} to -38 mV for 20 g L^{-1}). This confirms that the zeta potential determination of the emulsion droplets is based on the combined effect of the zeta potential of the emulsion droplets, which depends on the adsorbed amount and the charge of the adsorbed protein, and on the zeta potential of the excess protein.

Furthermore, the zeta potential of the emulsion droplets was determined as a function of ionic strength (figure 8D). For all variants, the zeta potential decreases with increasing ionic strength due to charge screening. As a consequence the electrostatic interactions between the emulsion droplets also decrease (equation 7). To confirm that the emulsion properties, like the interfacial properties, are not only affected by electrostatic interactions, the decay time was plotted as function of zeta potential (figure 9). This behaviour, shown in figure 9, clearly shows two regimes, corresponding to the protein-poor and protein-rich regime (i.e. emulsion stabilized by R_0 - R_1 and $R_{1.5}$ - $R_{2.5}$, respectively) (figure 7). Therefore, it was concluded that the presence of excess protein rather than electrostatics prevents salt-induced flocculation, as previously has been described for other globular proteins (chapter 3).

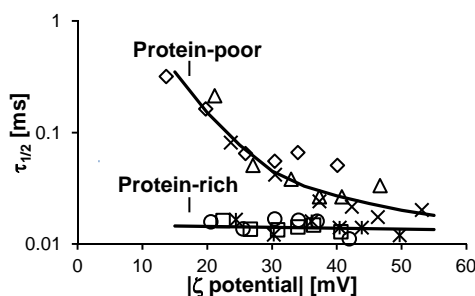


Figure 9. Decay time ($\tau_{1/2}$) of emulsion stabilized by R_0 (\diamond), $R_{0.5}$ (\triangle), R_1 (\times), $R_{1.5}$ ($*$), R_2 (\circ) and $R_{2.5}$ (\square) at pH 7.0 as a function of the absolute zeta potential of the emulsion droplet.

The origin for this stabilizing effect of excess protein has not been elucidated yet. It has been ascribed to steric repulsion as a result of multilayer adsorption³⁴. Another explanation is that the excess protein prevents the formation of incompletely covered interface (chapter 3)^{34,35}. It was found that the equilibrium adsorbed amount increases with increasing ionic strength (table 1). So, in the absence of excess protein, an increase of the ionic strength will result in an incompletely covered interface. In the case of multilayer adsorption, an increase of serum concentration (i.e. excess protein) is expected to result in an increase of Γ and consequently an increase of the zeta potential. Since the zeta potential decreases, rather than increases, with increasing protein (serum) protein concentration (figure 8C), a multilayer formation is not likely. Moreover, the adsorbed amount at the air-water interface is also not affected (table 1), indicating a similar adsorbed amount for the different patatin variants. Hence, the excess protein is postulated to prevent the formation of incompletely covered interface with increasing ionic strength.

Theoretical prediction of the flocculation behaviour

To verify that not only electrostatics are of importance, the flocculation behaviour is predicted using the DLVO theory (i.e. combination of electrostatic repulsion and van der Waals attraction). In this study, flocculation is assumed to occur if the primary maximum is lower than 5 kT or the secondary minimum is deeper than -5 kT (U_{cr}). Based on the size ($d_{3,2}$) and the zeta potential of the emulsion droplets, the minimum zeta potential required to prevent flocculation (Ψ_{cr}) was calculated as a function of ionic strength (figure 10).

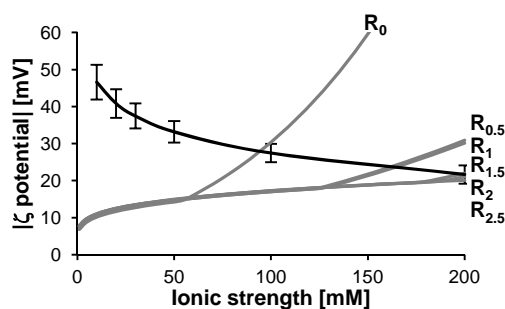


Figure 10. Average zeta potential of the emulsion droplets as function of ionic strength. The error bars indicate the standard deviation and the grey lines represent the critical interaction potential of 5 kT (U_{cr}) given the radius and zeta potential of the droplets stabilized by the (succinylated) patatin variants and the ionic strength of the solutions.

As a result of the decreasing droplet size with increasing degree of modification, the Ψ_{cr} also decreases. If the Ψ_{cr} is compared with the experimental values of the zeta potential, it can be observed that the ionic strength at which flocculation is expected increases with increasing degree of modification (i.e. > 50 mM for R_0 , > 100 mM for $R_{0.5}$ - $R_{1.5}$ and > 200

mM for R₂ and R_{2.5}). Therefore, for all variants, the emulsions are expected to be stable against flocculation ≤ 50 mM. In addition, the variants with the highest degree of modification (i.e. R₂ and R_{2.5}) are even expected to be stable at 200 mM. The experimental data (figure 2), however, does not fit with the theoretical prediction (figure 10). This underlines that the observations indeed cannot only be explained based on electrostatics.

Verification of the effect of excess protein

To confirm the effect of excess protein on the flocculation behaviour, additional protein is added after emulsification. The emulsions formed at low protein concentration (i.e. 5 g L⁻¹; figure 11A) became more stable against salt-induced flocculation when the protein concentration was increased to 20 g L⁻¹ (figure 11B).

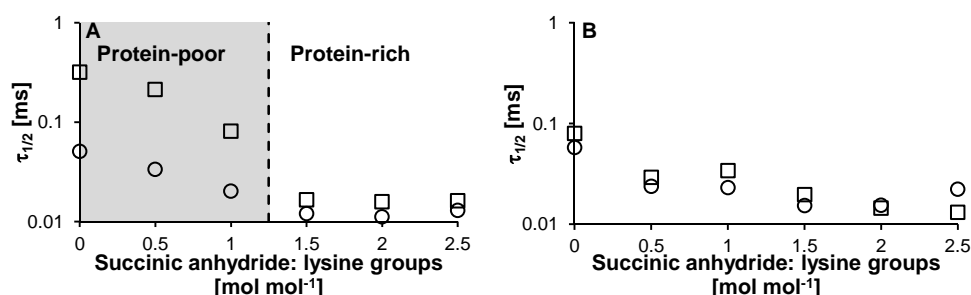


Figure 11. Decay time ($\tau_{1/2}$) of emulsion stabilized by the (succinylated) patatin variants at a protein concentration of 5 g L⁻¹ (A) and 20 g L⁻¹ (B) in 10 mM sodium phosphate buffer pH 7.0 in the absence (○) and presence of 190 mM NaCl (□).

So, the stability against salt-induced flocculation is caused by the presence of excess protein rather than the difference in surface charge. The presence of excess protein (i.e. protein-poor regime) was shown to correspond with the emulsions stabilized by the variants with the highest degree of modification (i.e. R_{1.5}-R_{2.5}). This is caused by a higher initial adsorption rate to the oil-water interface with increasing degree of modification as a result of (partial) unfolding of the secondary structure.

Conclusion

This study shows that not only the charge, but also the initial adsorption rate of the (succinylated) patatin variants towards adsorption to the oil-water interface increases with increasing degree of modification. This results in two regimes, the protein-poor regime (i.e. R₀-R₁ at 5 g L⁻¹) and the protein-rich regime (i.e. R_{1.5}-R_{2.5} at 5 g L⁻¹ and R₀-R₁ at 20 g L⁻¹). In the protein-poor regime (i.e. R₀-R₁ at 5 g L⁻¹), flocculation occurs with increasing ionic strength. In the protein-rich regime (i.e. R_{1.5}-R_{2.5} at 5 g L⁻¹ and R₀-R₁ at 20 g L⁻¹), however, the emulsions are stable against flocculation until an ionic strength of at least 200 mM. This

shows that salt-induced flocculation can be prevented by the presence of excess protein. This stabilizing effect was ascribed to prevention of the formation of incompletely covered interface.

References

1. Dickinson, E., Flocculation of protein-stabilized oil-in-water emulsions. *Colloids Surf., B* **2010**, 81, (1), 130-140.
2. Damodaran, S., Protein stabilization of emulsions and foams. *J. Food Sci.* **2005**, 70, (3), R54-R66.
3. Zhai, J.; Wooster, T. J.; Hoffmann, S. V.; Lee, T.; Augustin, M. A.; Aguilar, M., Structural rearrangement of β -lactoglobulin at different oil-water interfaces and its effect on emulsion stability. *Langmuir* **2011**, 27, (15), 9227-9236.
4. Dunlap, C. A.; Côté, G. L., β -Lactoglobulin-dextran conjugates: effect of polysaccharide size on emulsion stability. *J. Agric. Food Chem.* **2005**, 53, (2), 419-423.
5. Dickinson, E., Hydrocolloids as emulsifiers and emulsion stabilizers. *Food Hydrocolloids* **2009**, 23, (6), 1473-1482.
6. Evans, M.; Ratcliffe, I.; Williams, P. A., Emulsion stabilisation using polysaccharide-protein complexes. *Curr. Opin. Colloid Interface Sci.* **2013**, 18, (4), 272-282.
7. Song, K. B.; Damodaran, S., Influence of electrostatic forces on the adsorption of succinylated β -lactoglobulin at the air-water interface. *Langmuir* **1991**, 7, (11), 2737-2742.
8. Creighton, T. E., *Proteins: structure and molecular properties*. 2 ed.; W.H. Freeman: New York, NY, USA, 2002.
9. van der Veen, M.; Norde, W.; Cohen Stuart, M., Effects of succinylation on the structure and thermostability of lysozyme. *J. Agric. Food Chem.* **2005**, 53, (14), 5702-5707.
10. Wierenga, P. A.; Meinders, M. B. J.; Egmond, M. R.; Voragen, A. G. J.; De Jongh, H. H. J., Quantitative description of the relation between protein net charge and protein adsorption to air-water interfaces. *J. Phys. Chem. B* **2005**, 109, (35), 16946-16952.
11. Ong, H. N.; Arumugam, B.; Tayyab, S., Succinylation-induced conformational destabilization of lysozyme as studied by guanidine hydrochloride denaturation. *J. Biochem.* **2009**, 146, (6), 895-904.
12. Pots, A. M.; de Jongh, H. H. J.; Gruppen, H.; Helling, M.; Voragen, A. G. J., The pH dependence of the structural stability of patatin. *J. Agric. Food Chem.* **1998**, 46, (7), 2546-2553.
13. Damodaran, S.; Song, K. B., Kinetics of adsorption of proteins at interfaces: role of protein conformation in diffusional adsorption. *Biochim. Biophys. Acta, Protein Struct. Mol. Enzymol.* **1988**, 954, 253-264.
14. Wierenga, P. A.; Meinders, M. B. J.; Egmond, M. R.; Voragen, A. G. J.; de Jongh, H. H. J., Protein exposed hydrophobicity reduces the kinetic barrier for adsorption of ovalbumin to the air-water interface. *Langmuir* **2003**, 19, (21), 8964-8970.
15. Cho, D.; Narsimhan, G.; Franses, E. I., Adsorption dynamics of native and alkylated derivatives of bovine serum albumin at air-water interfaces. *J. Colloid Interface Sci.* **1996**, 178, (1), 348-357.
16. Butré, C. I.; Wierenga, P. A.; Gruppen, H., Effects of ionic strength on the enzymatic hydrolysis of diluted and concentrated whey protein isolate. *J. Agric. Food Chem.* **2012**, 60, (22), 5644-5651.
17. Jachimska, B.; Wasilewska, M.; Adamczyk, Z., Characterization of globular protein solutions by dynamic light scattering, electrophoretic mobility, and viscosity measurements. *Langmuir* **2008**, 24, (13), 6866-6872.

18. De Jongh, H. H. J.; Goormaghtigh, E.; Killian, J. A., Analysis of circular dichroism spectra of oriented protein-lipid complexes: toward a general application. *Biochemistry* **1994**, *33*, (48), 14521-14528.
19. Walstra, P., *Physical chemistry of foods*. Marcel Dekker, Inc.: New York, NY, USA, 2003.
20. De Feijter, J. A.; Benjamins, J.; Veer, F. A., Ellipsometry as a tool to study the adsorption behavior of synthetic and biopolymers at the air-water interface. *Biopolymers* **1978**, *17*, (7), 1759-1772.
21. Ball, V.; Ramsden, J. J., Buffer dependence of refractive index increments of protein solutions. *Biopolymers* **1998**, *46*, (7), 489-492.
22. Israelachvili, J. N., *Intermolecular and surface forces*. Third ed.; Academic Press: New York, NY, USA, 2011.
23. Hesselink, F. T.; Vrij, A.; Overbeek, J. T. G., Theory of the stabilization of dispersions by adsorbed macromolecules. II. Interaction between two flat particles. *J. Phys. Chem.* **1971**, *75*, (14), 2094-2103.
24. Wiese, G. R.; Healy, T. W., Effect of particle size on colloid stability. *Trans. Faraday Soc.* **1970**, *66*, 490-499.
25. Ruis, H. G. M.; van Gruijthuisen, K.; Venema, P.; van der Linden, E., Transitions in structure in oil-in-water emulsions as studied by diffusing wave spectroscopy. *Langmuir* **2007**, *23*, (3), 1007-1013.
26. Blijdenstein, T. B. J.; Hendriks, W. P. G.; van der Linden, E.; van Vliet, T.; van Aken, G. A., Control of strength and stability of emulsion gels by a combination of long- and short-range interactions. *Langmuir* **2003**, *19*, (17), 6657-6663.
27. van Koningsveld, G. A.; Gruppen, H.; de Jongh, H. H. J.; Wijngaards, G.; van Boekel, M. A. J. S.; Walstra, P.; Voragen, A. G. J., Effects of ethanol on structure and solubility of potato proteins and the effects of its presence during the preparation of a protein isolate. *J. Agric. Food Chem.* **2002**, *50*, (10), 2947-2956.
28. Pots, A. M.; Gruppen, H.; de Jongh, H. H. J.; van Boekel, M. A. J. S.; Walstra, P.; Voragen, A. G. J., Kinetic modeling of the thermal aggregation of patatin. *J. Agric. Food Chem.* **1999**, *47*, (11), 4593-4599.
29. Alizadeh-Pasdar, N.; Li-Chan, E. C. Y., Comparison of protein surface hydrophobicity measured at various pH values using three different fluorescent probes. *J. Agric. Food Chem.* **2000**, *48*, (2), 328-334.
30. Cho, D.; Narsimhan, G.; Franses, E. I., Adsorption dynamics of native and pentylated bovine serum albumin at air-water interfaces: surface concentration/surface pressure measurements. *J. Colloid Interface Sci.* **1997**, *191*, (2), 312-325.
31. Tcholakova, S.; Denkov, N. D.; Sidzhakova, D.; Ivanov, I. B.; Campbell, B., Interrelation between drop size and protein adsorption at various emulsification conditions. *Langmuir* **2003**, *19*, (14), 5640-5649.
32. McClements, D. J., Protein-stabilized emulsions. *Curr. Opin. Colloid Interface Sci.* **2004**, *9*, (5), 305-313.
33. Beverung, C. J.; Radke, C. J.; Blanch, H. W., Protein adsorption at the oil/water interface: characterization of adsorption kinetics by dynamic interfacial tension measurements. *Biophys. Chem.* **1999**, *81*, (1), 59-80.
34. Tcholakova, S.; Denkov, N. D.; Ivanov, I. B.; Campbell, B., Coalescence in β -lactoglobulin-stabilized emulsions: effects of protein adsorption and drop size. *Langmuir* **2002**, *18*, (23), 8960-8971.
35. Kim, H. J.; Decker, E. A.; McClements, D. J., Influence of free protein on flocculation stability of β -lactoglobulin stabilized oil-in-water emulsions at neutral pH and ambient temperature. *Langmuir* **2004**, *20*, (24), 10394-10398.

Chapter 6

Quantitative description of the parameters affecting the adsorption behaviour of globular proteins

Abstract

The adsorption behaviour of proteins depends significantly on their molecular properties and system conditions. To study this relation, the effect of relative exposed hydrophobicity, protein concentration and ionic strength on the adsorption rate and adsorbed amount is studied using β -lactoglobulin, ovalbumin and lysozyme. The curves of surface elastic modulus versus surface pressure of all three proteins, under different conditions (i.e. concentration and ionic strength) superimposed. This showed that the interactions between the adsorbed proteins are similar and that the adsorbed proteins retain their native state. In addition, the adsorption rate (k_{adsorb}) was shown to scale with the relative hydrophobicity and ionic strength. Moreover, the adsorbed amount was shown to be dependent on the protein charge and the ionic strength. Based on these results, a model is proposed to predict the maximum adsorbed amount (Γ_{max}). The model approximates the adsorbed amount as a close-packed monolayer using a hard-sphere approximation with an effective protein radius which depends on the electrostatic repulsion. The theoretical adsorbed amount was in agreement with experimental Γ_{max} ($\pm 10\%$).

Introduction

Protein adsorption is important for the stabilization of interfaces, and thereby the formation of foams and emulsions¹. If the adsorbed amount is close to the maximum (Γ_{\max}), emulsion droplets are considered to be stable against coalescence and flocculation. Of course, the timescale within which Γ_{\max} is reached is equally important. This is described by the adsorption rate (k_{adsorb}). Despite the importance of protein adsorption, it is not well understood how the adsorption rate is affected by system conditions and the molecular properties of the protein. Therefore, this study focusses on elucidating the effect of protein relative exposed hydrophobicity for different proteins, protein concentration and ionic strength on the adsorption behaviour.

The adsorption rate has been described to be influenced by exposed hydrophobicity and the electrostatic repulsion (i.e. surface charge or pH and ionic strength)^{1,2}. For a single protein, an increase of the exposed hydrophobicity has been described to decrease the barrier for adsorption to the air-water interface, resulting in a higher adsorption rate^{2,3}. Similarly, a decrease of the surface charge or an increase of the ionic strength decreases the electrostatic barrier and thereby increases the adsorption rate^{4,6}. This shows that the adsorption rate is a function of exposed hydrophobicity and the electrostatic repulsion.

The maximum amount of protein that can be adsorbed at the interface depends on the size of the protein. The maximum fraction of the surface area which is covered by spherical particles (such as globular proteins) at the jamming limit has been described to be 0.547⁷ (i.e. saturation coverage), assuming no diffusion of the proteins at the interface. This was derived from the random sequential adsorption model, where the adsorbing particles are hard particles that have no charge. Whereas, for proteins, the maximum adsorbed amount for proteins is not affected by the exposed hydrophobicity³, it is affected by electrostatic repulsion (chapter 5)⁴, as was also observed for the adsorption rate. This shows that the maximum adsorbed amount of protein should be a function of the protein radius and the electrostatic repulsion. Despite the available experimental data, there is no model to predict the maximum adsorbed amount of any protein under given conditions (e.g. pH and ionic strength).

To obtain more information on the parameters determining the adsorption behaviour, this study systematically investigates the effect of ionic strength, protein concentration and relative exposed hydrophobicity on Γ_{\max} and k_{adsorb} . To this end, three different globular proteins (β -lactoglobulin, ovalbumin and lysozyme) are used. Based on these results, a model will be proposed to predict the maximum adsorbed amount.

Materials and methods

Materials

Lysozyme (Lys; L6876, Lot n° 051K7028; purity > 95 % based on size-exclusion chromatography), β -lactoglobulin (β -lg; L0130, Lot n° SLBC2933V; protein content of 99 % (N x 6.38)⁸, of which 94 % β -lactoglobulin based on SDS-PAGE), ovalbumin (Ova; A5503 Lot n° 031M7008V; protein content of 98 % (N x 6.22)⁸, of which 92 % ovalbumin based on agarose gel electrophoresis) and 8-anilino-1-naphthalenesulfonic acid (ANSA; A5144) were purchased from Sigma-Aldrich (St. Louis, MO, USA). All other chemicals were of analytical grade and purchased from either Sigma-Aldrich or Merck (Darmstadt, Germany).

Lysozyme (5 g L⁻¹) was dissolved in 10 mM sodium phosphate buffer pH 5.7. The protein solution was divided into 60 mL samples, which were heated at 83 °C for 0, 15, 30, 60 and 90 minutes (further referred to as Lys₀, Lys₁₅, Lys₃₀, Lys₆₀ and Lys₉₀). After the heat treatment, the protein solutions were cooled on ice-water for 5 minutes and stored at -20 °C.

Secondary and tertiary structure

The secondary and tertiary structure of the (heated) lysozyme variants was determined using far-UV and near-UV CD, respectively according to the method described previously⁹. The lysozyme solutions were diluted to a concentration of 0.1 g L⁻¹ with 10 mM sodium phosphate buffer pH 7.0.

Apparent molecular mass distribution

The (heated) lysozyme solutions were analysed by high-performance size-exclusion chromatography using an Äkta Micro equipped with a Superdex 75 PC 3.2/30 column (GE Healthcare, Uppsala, Sweden). Prior to analysis, the solutions (5 g L⁻¹) were centrifuged. Then, the solutions (20 μ L) were injected and eluted with 10 mM sodium phosphate buffer pH 7.0 containing 90 mM NaCl at a flow rate of 0.06 mL min⁻¹. The elution was monitored using UV absorbance at 280 nm. The column was calibrated with globular proteins with a mass range of 13.7-67 kDa (GE Healthcare).

Quantification of exposed hydrophobicity

The increase in fluorescence intensity upon binding of 8-anilino-1-naphthalenesulfonic acid (ANSA) to the accessible hydrophobic regions of the protein is used as a measure of the protein surface hydrophobicity¹⁰. The (heated) lysozyme solutions were diluted with 10 mM sodium phosphate buffer pH 7.0 to a concentration of 0.1 g L⁻¹. The measurements were performed on a Varian Cary Eclipse fluorescence spectrophotometer (Agilent

Technologies, Santa Clara, CA, USA) as described elsewhere³. The emission spectrum was measured from 400 to 650 nm and the measurements were performed at 25 °C. The fluorescence spectrum with the highest area was corrected with the area of the buffer. Subsequently, the relative exposed hydrophobicity (Q_H) was expressed as the area of the sample relative to the area of the sample with the maximum area (i.e. β -lactoglobulin).

Zeta potential

Zeta potentials of the proteins in solution were determined with a Zetasizer Nano ZSP (Malvern Instruments, Worcestershire, UK) using the laser Doppler velocimetry technique. The proteins (10 g L⁻¹) were dissolved in 10 mM sodium phosphate buffer pH 7.0. The measurements were performed at 25 °C and 40 Volt. The results of five sequential runs were averaged. Zeta potentials were calculated with Henry's equation¹¹ (equation 1).

$$\zeta = \frac{3\eta\mu_e}{2\varepsilon F(\kappa\alpha)} \quad (1)$$

in which ζ is the zeta potential [V], η is the viscosity [0.8872 x 10⁻³ Pa s], μ_e is the electrophoretic mobility [m² V⁻¹ s⁻¹], ε is the dielectric constant of the medium [7.08 x 10⁻¹⁰ C² J⁻¹ m⁻¹] and $F(\kappa\alpha)$ is Henry's function [-], which equals 1.5 using the Smoluchowski approximation¹¹.

Dynamic light scattering

The hydrodynamic radius of the (heated) lysozyme variants was determined with a Zetasizer Nano ZS (Malvern Instruments). The pH of the (heated) lysozyme solutions in 10 mM sodium phosphate buffer pH 5.7 (5 g L⁻¹) was adjusted to pH 7.0 with 0.1 M NaOH. The results of at least five sequential runs were averaged. The measurements were performed at 25 °C.

Adsorbed amount

Experimental adsorbed amount

The amount of protein adsorbed at the air-water interface was experimentally determined using a Multiskop ellipsometer (Optrel, Sinzing, Germany). Adsorption of protein to the air-water interface results in an increase of the ellipsometric angles (Δ and ψ) of the reflected monochromatic laser light ($\lambda = 632.8$ nm, angle of incidence = 50°). From the ellipsometric angles, the refractive index (n_{adsorbed}) and thickness (d_{adsorbed}) of the adsorbed layers are fitted using a model based on two bulk phases (i.e. air and water) and one adsorbed layer. The fitting parameters for the model were: $n_{\text{air}} = 1.000$, $n_{\text{buffer}} \approx n_{\text{water}} = 1.333$, $dn/dc = 0.185$ mL g⁻¹ (typical for globular proteins^{12, 13}) and the angle of incidence was 50°.

The adsorbed amount (Γ) is calculated from the fitted refractive index (n_{adsorbed}) and thickness (d_{adsorbed}) of the adsorbed layer using equation 2¹².

$$\Gamma(t) = \frac{(n_{\text{adsorbed}}(t) - n_{\text{buffer}})}{\frac{dn}{dc}} d_{\text{adsorbed}}(t) \quad (2)$$

where t is the time [s], Γ is the adsorbed amount [mg m^{-2}], n_{adsorbed} and n_{buffer} are the refractive index of the adsorbed layer and the buffer [-], respectively, dn/dc is the refractive index increment [L g^{-1}] and d_{adsorbed} is the thickness of the adsorbed layer [m].

For all measurements, the buffer was measured for 600 seconds. Next, the concentrated protein solutions were added. After 24 hours, the ellipsometric angles were determined for 3600 seconds. The maximum adsorbed amount (Γ_{max}) was averaged over 3600 seconds (i.e. ~ 200 measurements). Four different sets of experiments were performed:

Effect of protein concentration β -Lactoglobulin was dissolved in 10 mM sodium phosphate buffer pH 7.0 at concentrations of 3, 7.5, 15, 30 and 150 g L^{-1} . After measuring the buffer, protein solution was added to reach final concentrations of 0.1, 0.25, 0.5, 1 and 5 g L^{-1} in a constant volume.

Effect of ionic strength β -Lactoglobulin (3 g L^{-1}) was dissolved in 10 mM sodium phosphate buffer pH 7.0 containing 0, 20, 40, 90 or 190 mM NaCl. After measuring the buffer, protein solution was added to reach a final concentration of 0.1 g L^{-1} .

Effect of exposed hydrophobicity β -Lactoglobulin, ovalbumin and lysozyme (3 g L^{-1}) were dissolved in 10 mM sodium phosphate buffer pH 7.0. After measuring the buffer, protein solution was added to reach a final concentration of 0.1 g L^{-1} .

Effect of protein radius and exposed hydrophobicity The (heated) lysozyme variants (3 g L^{-1}) were dissolved in 10 mM sodium phosphate buffer pH 7.0. After measuring the buffer, protein solution was added to reach a final concentration of 0.1 g L^{-1} .

Theoretical adsorbed amount

Based on the experimental data, a predictive model was developed to predict the theoretical adsorbed amount of a close-packed monolayer ($\Gamma_{\text{mono, theory}}$). For hard disks of radius R at a two-dimensional interface, a saturation coverage at the jamming limit (θ_{∞}) of 0.547 was derived from the random sequential adsorption (RSA) model⁷. If proteins are considered to behave as hard spheres, the adsorbed amount can be derived from equation 3.

$$\Gamma_{\text{mono, theory}} = \frac{10^3 M_w}{\pi R_{\text{eff}}^2 N_a} \theta_{\infty} \quad (3)$$

in which $\Gamma_{\text{mono, theory}}$ is the theoretical maximum adsorbed amount of a monolayer [mg m^{-2}], M_w is the molecular mass of the protein [g mol^{-1}], R_{eff} is the effective radius of a globular protein [m], N_a is the Avogadro constant [$6.022 \times 10^{23} \text{ mol}^{-1}$] and θ_{∞} is the saturation coverage [0.547]⁷.

Since proteins typically have a charge, the effective radius has to be approximated by including a term for the long-range electrostatic repulsion. This effective radius is then the minimal distance at which two proteins can approach, in other words R_{eff} is the sum of the protein radius (R_p) and a characteristic distance due to electrostatic repulsion ($\frac{1}{2} h_{\text{min}}$)¹⁴ (equation 4).

$$R_{\text{eff}} = R_p + \frac{1}{2} h_{\text{min}} \quad (4)$$

in which h_{min} is the minimal separation distance at close packing [m]. For a globular protein, R_p is estimated using equation 5¹⁵.

$$R_p = \left(\frac{3vM_w}{4\pi N_a} \right)^{\frac{1}{3}} \quad (5)$$

in which v is the partial specific volume of a protein [$0.73 \times 10^{-6} \text{ m}^3 \text{ g}^{-1}$]¹⁵.

At h_{min} , the kinetic interaction (U_{kin}) is in equilibrium with the repulsive interaction (U_e) - the attractive interaction (U_a). Hence, at this equilibrium, U_e should be in equilibrium with the sum of U_{kin} and U_a (further referred to as U_{driving}). The electrostatic repulsion (U_e) [J] at h_{min} is described by equation 6¹⁶.

$$U_e = 2\pi\epsilon_0\epsilon_r R_p \Psi_0^2 e^{-\kappa h_{\text{min}}} \quad (6)$$

where κ , the inverse Debye screening length [m^{-1}], for a monovalent electrolyte is described by equation 7¹⁶.

$$\kappa = \sqrt{\frac{2N_a e^2 I}{\epsilon_0 \epsilon_r k_B T}} \quad (7)$$

in which ϵ_0 is the dielectric constant of a vacuum [$8.85 \times 10^{-12} \text{ C}^2 \text{ J}^{-1} \text{ m}^{-1}$], ϵ_r is the relative dielectric constant of the medium (80), Ψ_0 is the surface potential [V], e is the elementary charge [$1.602 \times 10^{-19} \text{ C}$], I is the ionic strength [mol m^{-3}], k_B is the Boltzmann constant [$1.38 \times 10^{-23} \text{ J K}^{-1}$] and T is the temperature [K].

Two regimes are distinguished. In the case that the U_{driving} is in equilibrium with U_e at a certain separation distance, h is expressed by equation 8. If U_e does not exceed U_{driving} at any value for $h > 0$, h is 0 (equation 9).

$$h_{\text{min}} = -\ln\left(\frac{U_{\text{driving}}}{2\pi\epsilon_0\epsilon_r R_p \Psi_0^2}\right) \kappa^{-1} \text{ for } U_{\text{driving}} < U_e \quad (8)$$

$$h_{\text{min}} = 0 \text{ for } U_{\text{driving}} \geq U_e \quad (9)$$

The effective radius is obtained by combining equations 4 and 8, resulting in equation 10. Then, the theoretical effective radius is determined by fitting the experimental data assuming a constant U_{driving} for one protein under different conditions. The obtained U_{driving}

can then be applied to extrapolate the data to other conditions (i.e. ionic strength and surface charge).

$$R_{eff} = R_p - \frac{1}{2} \ln \left(\frac{U_{driving}}{2\pi\epsilon_0\epsilon_r R_p \Psi_0^2} \right) \kappa^{-1} \quad (10)$$

Assuming a constant $U_{driving}$ (independent of Ψ_0 and κ^{-1}), equation 10 for a constant Ψ_0 (i.e. constant pH) can be simplified to equation 11.

$$R_{eff} = R_p - \frac{1}{2} \ln \left(\frac{x}{R_p} \right) \kappa^{-1} \quad (11)$$

in which x is a constant [m] depending on the $U_{driving}$, ϵ and Ψ_0 .

Adsorption kinetics and surface elastic modulus

The surface tension and surface elastic modulus as a function of time were measured using an automated drop tensiometer (ADT, Teclis IT Concept, Longessaigne, France). The system was temperature controlled at 20 °C. For the surface tension measurements, the drop volume was kept constant at 7 μ L for 3600 s. The change in surface tension compared to that of the pure interface (i.e. the air-water interface) was expressed as the surface pressure (equation 12)¹⁷.

$$\Pi(t) = \gamma_0 - \gamma(t) \quad (12)$$

where γ_0 is the measured interfacial tension of the buffer [72.8 mN m⁻¹].

The surface elastic modulus (E_d) was measured by inducing sinusoidal changes in the interfacial area with an amplitude of 5 % and a frequency of 0.1 Hz. The modulus was calculated from the measured changes in surface tension and surface area averaged over a sequence of five sinuses. Every 100 s a sequence of five sinuses was performed. All measurements were performed in duplicate. Four different sets of experiments were performed:

Effect of protein concentration β -Lactoglobulin was dissolved in concentrations of 0.01, 0.025, 0.05, 0.1, 0.5 and 1 g L⁻¹ in 10 mM sodium phosphate buffer pH 7.0.

Effect of ionic strength β -Lactoglobulin was dissolved in a concentration of 0.05 g L⁻¹ in 10 mM sodium phosphate buffer pH 7.0 containing 0, 20, 40, 90 or 190 mM NaCl.

Effect of exposed hydrophobicity β -Lactoglobulin, ovalbumin and lysozyme were dissolved in a concentration of 0.1 g L⁻¹ in 10 mM sodium phosphate buffer pH 7.0.

Effect of protein radius and exposed hydrophobicity The (heated) lysozyme solutions were diluted to a concentration of 0.1 g L⁻¹ with 10 mM sodium phosphate buffer pH 7.0.

Results and discussion

Protein characterization

Lysozyme was heated to obtain variants with different relative exposed hydrophobicity and a similar structure. The secondary and tertiary structure of the heated lysozyme variants as determined by circular dichroism were not significantly different from that of the native lysozyme (data not shown). The relative exposed hydrophobicity (Q_H) of the heated, refolded lysozyme, on the other hand, increased steeply after 60 minutes of heating from 0.06 for Lys_0 to 0.24 and 0.85 for Lys_{60} and Lys_{90} , respectively (figure 1A). In addition, size-exclusion chromatography showed a decrease of the total absorbance by 20-25 % at pH 7.0, whereas no soluble aggregates were observed (data not shown). The radius of the heated, refolded lysozyme, however, increased with increasing heating time (figure 1B). This shows that although no significant structural changes were observed as a result of refolding, the minor changes upon heating resulted in an increased relative exposed hydrophobicity and a loss of solubility due to the formation of aggregates.

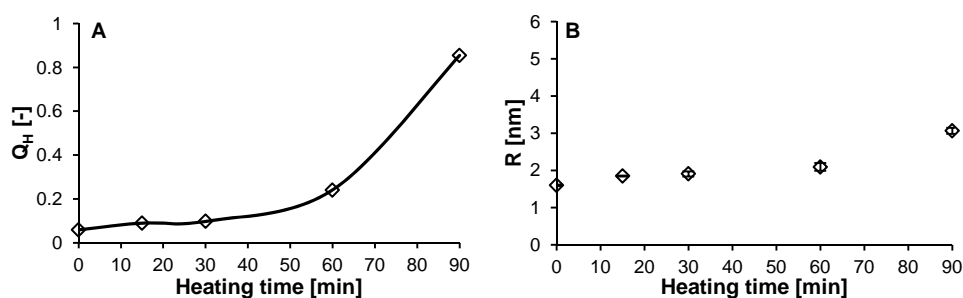


Figure 1. Effect of heating time on the relative exposed hydrophobicity (Q_H) (A) and radius (B) of the (heated) lysozyme variants measured at 20 °C (10 mM sodium phosphate buffer pH 7.0). The markers in B are average values with the error bars indicating the standard deviation.

In addition to the (heated) lysozyme variants, ovalbumin and β -lactoglobulin are used. Native β -lactoglobulin and ovalbumin are more hydrophobic than native lysozyme (i.e. $Q_H = 0.06, 0.19$ and 1.00 for lysozyme, ovalbumin and β -lactoglobulin, respectively) (table 1). At the same time, the theoretical radius and theoretical net surface charge of the native proteins are quite similar (1.9 ± 0.4 nm and 24.0 ± 2.0 mC m⁻²). These theoretical radii are in agreement with experimental data from literature¹⁸⁻²⁰ showing that the theoretical radius is a good approximation of the protein radius. Surprisingly, the zeta potentials of the proteins in solution vary significantly (i.e. $-21.2, -16.5$ and 2.0 mV for β -lactoglobulin, ovalbumin and lysozyme, respectively) (table 1).

Summarizing, the selective proteins display a range of values for radius, relative exposed hydrophobicity and zeta potential which allows the analysis of the effect of these parameters on the adsorbed amount and the adsorption kinetics.

Table 1. Protein properties obtained from literature, theory and experiment.

Protein	Literature ^a				Theory		Experiment		
	ExPasy code	M _w [kDa]	pI	#COOH/#NH ₂ ^b	D _s ^c [x 10 ⁻¹⁰ m ² s ⁻¹]	σ _w ^d [mC m ⁻²]	Q _H [-]	Γ _{max} [mg m ⁻²]	ζ potential [mV]
β-Lg	P02754	18.3	4.83	26/18	1.40/1.11	-21.9	1.00	1.69 ± 0.10	-21.2
Ova	P01012	42.8	5.19	47/35	1.05	-24.2	0.19	1.80 ± 0.11	-16.5
Lys	P00698	14.3	9.32	9/17	1.52	25.8	0.06	1.95 ± 0.14	2.0

^avalues obtained from the Swiss-Prot database (<http://www.expasy.org>).

^b#COOH and #NH₂ are the maximum number of negatively charged (aspartic and glutamic acid) and positively charged (arginine and lysine) groups in the primary sequence, respectively.

^ctheoretical diffusion coefficient calculated from the radius using the Stokes-Einstein equation ($D_s = k_B T / 6\pi\eta R$). The radius was calculated from the M_w (equation 5).

^dtheoretical net charge density at pH 7.0.

Adsorbed amount (Γ_{max})

Effect of ionic strength (I)

At 0.1 g L⁻¹, the maximum adsorbed amount (Γ_{max}) of β-lactoglobulin increases with increasing ionic strength (i.e. 1.69 mg m⁻² at 10 mM to 2.27 mg m⁻² at 200 mM) (figure 2A). This increase of Γ_{max} with ionic strength is in line with previous observations for ovalbumin⁴ and patatin (chapter 5). Under these conditions (i.e. constant surface charge (Ψ₀), protein radius (R_p) and driving interaction (U_{driving})), the effect of ionic strength is attributed to a decrease of the electrostatic repulsion due to charge screening. As a consequence, the Debye screening length decreases, resulting in a smaller effective radius of the protein (R_{eff}) (equation 11). Hence, more protein molecules can adsorb to the interface, resulting in an increase of Γ_{max} (equation 3). Based on equations 11 and 3 (constant U_{driving} and Ψ₀), the theoretical adsorbed amount of a close-packed monolayer is calculated (table 2). The predicted theoretical adsorbed amounts (Γ_{mono, theory}) are in agreement with the experimental Γ_{max} (deviation ± 10 %), which is comparable to the variation in the experimental data. For β-lactoglobulin at pH 7, the U_{driving} at h = h_{min} equals to 0.86 kT and x = 1.77 x 10⁻⁹ m. To verify that the theoretical prediction also holds for proteins with a different surface charge (Ψ₀) (constant U_{driving} and κ⁻¹), previously reported experimental adsorbed amounts for (succinylated) ovalbumin⁴ were compared with the model (table 2). A good fit of the data was obtained, showing that equation 3 can also be

applied to predict the maximum adsorbed amount for varying surface charge. U_{driving} under these conditions equals to 0.55 kT. The difference between the U_{driving} at equilibrium for ovalbumin (0.55 kT) and β -lactoglobulin (0.86 kT) is postulated to be caused by a difference in the attractive hydrophobic interaction, originating from the difference in hydrophobicity (table 1).

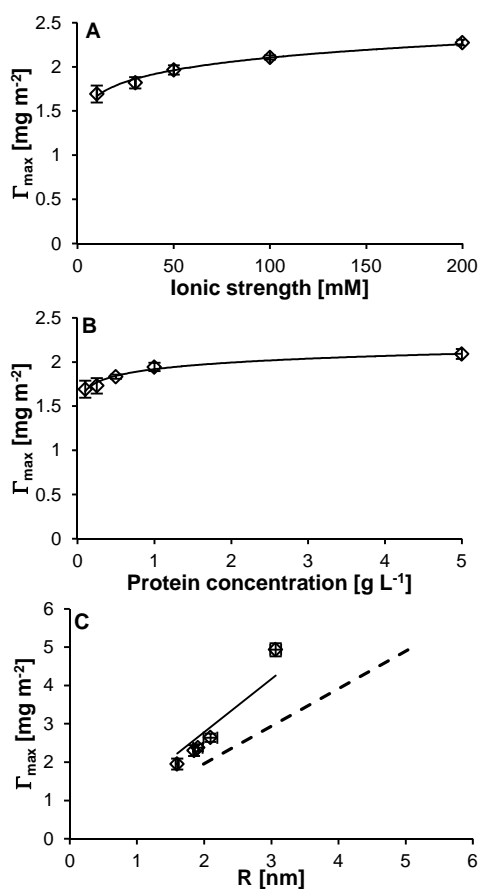


Figure 2. Maximum adsorbed amount (Γ_{max}) as a function of ionic strength at $C = 0.1 \text{ g L}^{-1}$ and $\text{pH} = 7.0$ (A) and protein concentration at $I = 10 \text{ mM}$ and $\text{pH} = 7.0$ (B) for β -lactoglobulin, and as function protein radius (C) for the (heated) lysozyme variants at $I = 10 \text{ mM}$, $\text{pH} = 7.0$ and $C = 0.1 \text{ g L}^{-1}$. Solid lines are guides to the eye. The dashed line in figure C corresponds to the theoretical adsorbed amount of a monolayer calculated using equation 3. All markers are average values with the error bars indicating the standard deviation.

Effect of protein concentration (C)

At low concentrations (i.e. $< 1 \text{ g L}^{-1}$), the maximum adsorbed amount increases with protein concentration (i.e. 1.7 mg m^{-2} at 0.1 g L^{-1} to 1.9 mg m^{-2} for 1 g L^{-1}), and then reaches a plateau at higher concentrations ($\sim 2.1 \pm 0.1 \text{ mg m}^{-2}$ for 5 g L^{-1}) (figure 2B). This is in line with previous data of ovalbumin²¹ and BSA¹². This observation can be explained by the fact that the adsorbed amount in time depends on the protein concentration as described by equation 13²².

$$\frac{d\Gamma}{dt} = C_b \sqrt{\frac{D_s}{\pi t}} \quad (13)$$

where Γ is the adsorbed amount [mg m^{-2}], C_b is the bulk protein concentration [mg m^{-3}], D_s is the diffusion coefficient [$\text{m}^2 \text{ s}^{-1}$] and t is the time [s].

Consequently, at low protein concentrations more time is required to reach a certain adsorbed amount (i.e. factor 10 in concentration relates to a factor 100 in time).

From equation 3, it can be concluded that the difference in adsorbed amount as a result of the protein concentration (i.e. constant R_{eff}) relates to a difference in the saturation coverage (θ). Extrapolation of the data from figure 2B to 300 g L^{-1} results in a Γ_{max} of $\pm 2.5 \text{ mg m}^{-2}$. This corresponds, based on an effective radius of 2.55 nm (i.e. $R_p = 2.21$ and $\frac{1}{2}h_{\text{min}} = 0.34$), with a saturation coverage at the jamming limit (θ_{∞}) of 0.82 . This is in line with the maximum monolayer surface coverage assuming diffusion of proteins at the interface²³. It is therefore concluded that the saturation coverage, which is reached within experimental timescales, depend on the protein concentration. For β -lactoglobulin at higher protein concentrations, the saturation coverage of 0.547 is an underestimation.

Effect of exposed hydrophobicity (Q_H)

The maximum adsorbed amount determined for different globular proteins varies from 1.69 for β -lactoglobulin to 1.95 mg m^{-2} for lysozyme (table 1). The experimentally determined adsorbed amounts of β -lactoglobulin and ovalbumin are in agreement with the theoretically estimated adsorbed amounts for an adsorbed monolayer calculated using equation 3 with a saturation coverage of 0.547 (table 2) (e.g. $\Gamma_{\text{max}} = 1.8 \pm 0.11 \text{ mg m}^{-2}$ and $\Gamma_{\text{mono, theory}} = 1.73 \text{ mg m}^{-2}$ for ovalbumin ($R_{\text{eff}} = 2.33 + 0.34 \text{ nm}$)). Moreover, a close-packed monolayer has also been described for ovalbumin²⁴ and BSA^{12, 25}. Surprisingly, a higher adsorbed amount was determined for lysozyme than for β -lactoglobulin. This is in contrast to the expectations since the M_w of lysozyme is lower. It, however, shows a correlation with the surface charge, as the surface charge (i.e. zeta potential) of lysozyme is lower than the surface charge of ovalbumin and β -lactoglobulin (table 1). As a consequence, the effective radius of the protein is expected to decrease, as was also observed for the succinylated ovalbumin (table 2). The maximum adsorbed amount of lysozyme is, however, higher than theoretically expected (i.e. $\Gamma_{\text{max}} = 1.95 \pm 0.14 \text{ mg m}^{-2}$ and $\Gamma_{\text{mono, theory}} = 1.58 \text{ mg m}^{-2}$ for R_{eff}

= R_p). This discrepancy is explained by a higher saturation coverage ($\theta \approx 0.65$) for lysozyme.

Table 2. Experimental and theoretical adsorbed amount for β -lactoglobulin, (succinylated) ovalbumin, lysozyme and ovalbumin.

	Experiment						Theory			Δ	
	I [mM]	Ψ_0 [mV]	Γ_{\max} [mg m ⁻²]	R_{eff}^b [nm]	R_p^c [nm]	$\frac{1}{2}h^d$ [nm]	$\frac{1}{2}h^e$ [nm]	R_{eff}^f [nm]	$\Gamma_{\text{mono,theory}}^g$ [mg m ⁻²]	$ \Delta\Gamma_{\max} $ [mg m ⁻²]	$ \Delta\Gamma_{\max} $ [%]
β -Lg	10	-21.2	1.69	2.50	2.21	0.29	0.34	2.55	1.62	0.07	4.1
	30	-21.2	1.82	2.41	2.21	0.20	0.20	2.41	1.82	0.00	0.2
	50	-21.2	1.96	2.32	2.21	0.11	0.15	2.36	1.89	0.07	3.5
	100	-21.2	2.10	2.24	2.21	0.03	0.11	2.32	1.97	0.13	6.8
	200	-21.2	2.27	2.16	2.21	0.00	0.08	2.29	2.02	0.25	12.3
Ova ^a	10	-17	1.6	2.78	2.33	0.45	0.59	2.92	1.45	0.15	10.1
	10	-19	1.3	3.09	2.33	0.76	0.93	3.26	1.17	0.13	11.4
	10	-20	1.1	3.35	2.33	1.02	1.08	3.41	1.06	0.04	3.5
	10	-22	1.0	3.52	2.33	1.19	1.37	3.70	0.90	0.10	10.8
	10	-24	0.9	3.71	2.33	1.38	1.64	3.97	0.79	0.11	14.5
	10	-26	0.8	3.93	2.33	1.60	1.88	4.21	0.70	0.10	14.6
Ova	10	-16.5	1.80	2.62	2.33	0.29	0.34	2.67	1.73	0.07	3.8
Lys	10	2.0	1.95	1.46	1.62	0.00	0.00	1.62	1.58	0.37	23.3

^aexperimental data obtained from literature⁴.

^b R_{eff} determined from equation 3 with a θ_{∞} of 0.547.

^c R_p determined from equation 5.

^d $\frac{1}{2}h$ determined from equation 4.

^e $\frac{1}{2}h$ determined from equation 8 assuming a constant U_{driving} .

^f R_{eff} determined from equation 4.

^g $\Gamma_{\text{mono,theory}}$ determined from equation 3 with a θ_{∞} of 0.547.

Effect of protein radius (R_p)

For the (heated) lysozyme variants, the adsorbed amount increases markedly for the variants heated for more than 60 minutes (i.e. 1.9 mg m⁻² for Lys₀ to 2.6 and 4.9 mg m⁻² for Lys₆₀ and Lys₉₀, respectively). This increase corresponds with the increase of the relative exposed hydrophobicity (figure 1A) and protein radius (figure 1B). As the adsorbed amount

was independent of the exposed hydrophobicity³, the increase is explained by the aggregation. Hence, the thickness of the adsorbed layer increases, resulting in an increase of the maximum adsorbed amount at an equal saturation coverage (θ) (equations 3 and 4). The linear relationship ($R^2 = 0.96$) between the protein radius and the maximum adsorbed amount seems to confirm this (figure 2C). It must, however, be noted that the maximum adsorbed amount of the (heated) lysozyme variants is higher than that the theoretical adsorbed amount corresponding to a close-packed monolayer. This may be explained by a non-spherical shape of the aggregate.

Summarizing, the concentration affects the saturation coverage at a certain time. This is also reflected in the experimental data. It, however, does not affect the theoretical maximum adsorbed amount at saturation. In addition, an increase of ionic strength and radius resulted in an increase of Γ_{\max} . This is related to a decrease of the Debye screening length and an increase of the layer thickness, respectively. As the adsorbed amounts were in agreement with the theoretical values for a close-packed monolayer, Γ_{\max} of a globular protein can be predicted to within $\pm 10\%$ by $\Gamma_{\text{mono, theory}}$ (equation 3) with an x , which at pH 7 is 1.77×10^{-9} m for ovalbumin and β -lactoglobulin and 0 m for lysozyme (equation 11).

Adsorption kinetics (k_{adsorb})

As an indication for the interactions between the adsorbed proteins, the elastic modulus (E_d) is plotted against the surface pressure (Π) (figures 3A-D). The E_d - Π curves of all proteins, at all concentrations, ionic strengths, and relative exposed hydrophobicities superimpose to a single curve. This shows that the interactions between the adsorbed proteins are similar. Moreover, it indicates that the behaviour of the proteins at the interface is not affected by the conditions or the molecular properties of these proteins. Furthermore, the fact that the curves do not decrease at higher surface pressure and reach an elastic modulus of $> 80 \text{ mN m}^{-1}$, indicates that the proteins do not unfold at the interface²⁶. As the curves superimpose, the equation of state (Π - Γ curve) is also similar. As a consequence, a faster increase of surface pressure (i.e. higher $d\Pi/dt$) can be interpreted as a higher adsorption rate ($d\Gamma/dt$, or k_{adsorb}).

The adsorption kinetics (i.e. initial adsorption rate in the first 20 seconds ($d\Pi/dt$) and the final surface pressure after 3600 seconds (Π_{final})) were determined at the air-water interface (figure 3E-H).

Effect of protein concentration (C)

From figure 3E it was deduced that the initial adsorption rate and final surface pressure increase linear with protein concentration at low concentrations (i.e. < 0.5 and 0.1 g L^{-1} for $d\Pi/dt$ and Π_{final} , respectively) (no further data shown). At higher concentrations, they become concentration independent (i.e. $d\Pi/dt = 0.026$ and $0.649 \text{ mN m}^{-1} \text{ s}^{-1}$ and $\Pi_{\text{final}} = 11.8$ and 18.9 mN m^{-1} for 0.01 g L^{-1} , 10 mM and 1 g L^{-1} , 10 mM , respectively) (figure 3E).

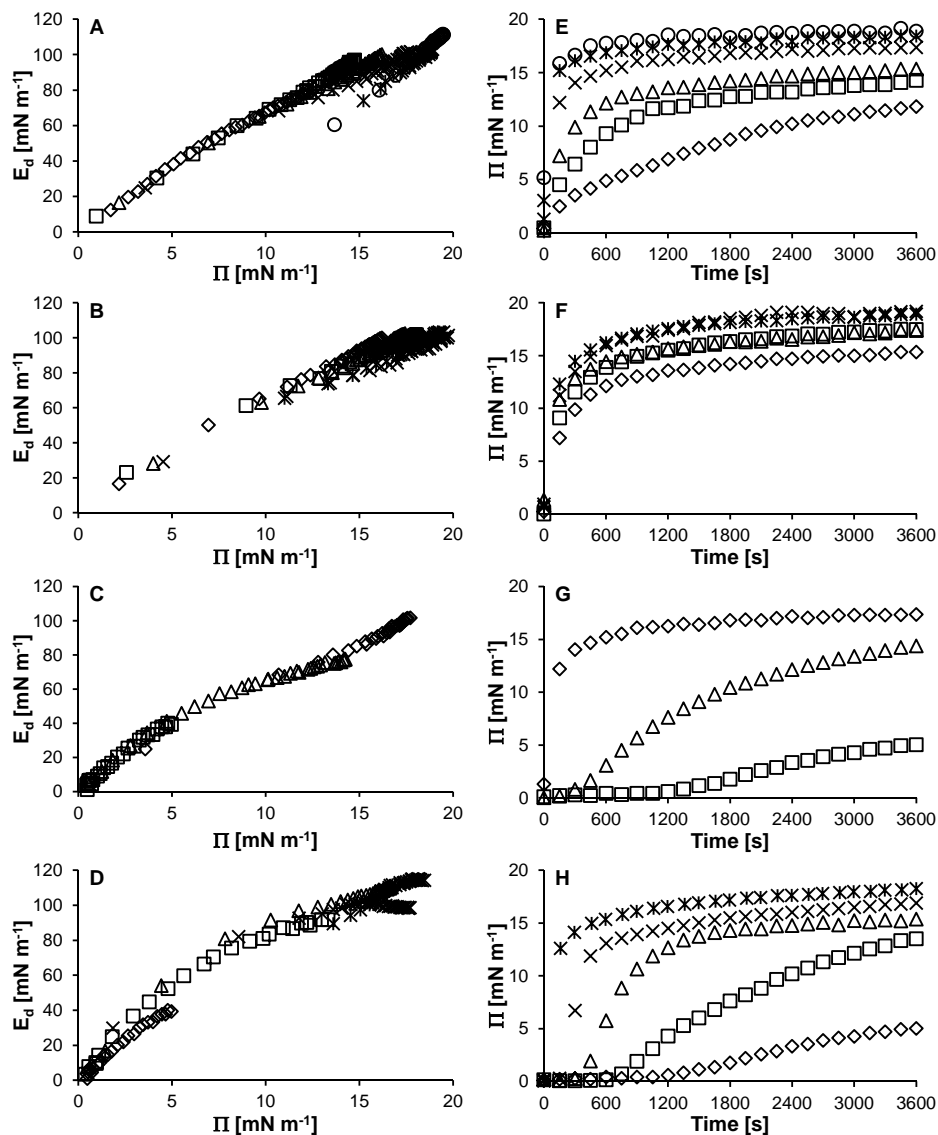


Figure 3. Surface pressure (Π) as a function of time and elastic modulus (E_d) as function of surface pressure for β -lactoglobulin at different protein concentrations at $I = 10$ mM and $\text{pH} = 7.0$ (A and E); 0.01 (\diamond), 0.025 (\square), 0.05 (\triangle), 0.1 (\times), 0.5 ($*$) and 1 g L^{-1} (\circ) and different ionic strengths at $\text{pH} = 7.0$ and $C = 0.05$ g L^{-1} (B and F); 10 (\diamond), 30 (\square), 50 (\triangle), 100 (\times) and 200 mM ($*$), for different proteins at $I = 10$ mM, $\text{pH} = 7.0$ and $C = 0.1$ g L^{-1} (C and G); β -lactoglobulin (\diamond), lysozyme (\square) and ovalbumin (\triangle) and for (heated) lysozyme variants at different relative exposed hydrophobicity at $I = 10$ mM, $\text{pH} = 7.0$ and $C = 0.1$ g L^{-1} (D and H); 0.03 (\diamond), 0.05 (\square), 0.05 (\triangle), 0.12 (\times), 0.44 ($*$) and 1.00 (\circ).

The observed increase of the adsorption rate with increasing protein concentration has previously been described for lysozyme, β -casein^{27, 28}, BSA^{28, 29}, β -lactoglobulin and ovalbumin^{18, 30}. Moreover, the final surface pressure at 1 g L⁻¹ is in agreement with the value reported for this concentration (i.e. 18 ± 1 mN m⁻¹)¹⁹. As the equation of state is similar, the observed increase (i.e. ± 25 -fold increase of $d\Pi/dt$ from 0.01 g L⁻¹ to 1 g L⁻¹) is explained by an increase of adsorbed amount of protein with increasing protein concentration. Similarly, the increase of the final surface pressure with concentration (i.e. 1.6-fold) also relates an increase of the adsorbed amount (equation 13).

Effect of ionic strength (I)

As expected, the $d\Pi/dt$ and Π_{final} for β -lactoglobulin at 0.05 g L⁻¹ increase with increasing ionic strength (i.e. $d\Pi/dt = 0.145$ and 0.267 mN m⁻¹ s⁻¹ and $\Pi_{\text{final}} = 15.3$ and 18.9 mN m⁻¹ for 10 mM and 200 mM, respectively) (figure 3F). In literature, the initial adsorption rate and the final surface pressure were also described to increase with ionic strength for β -lactoglobulin⁵, ovalbumin⁴, BSA⁶ and patatin (chapter 5). This behaviour has been ascribed to a decrease of the electrostatic repulsion due to charge screening. Hence, the electrostatic barrier for adsorption decreases, promoting protein adsorption. For β -lactoglobulin, this results in an increase of the initial adsorption rate by 1.8-fold and the final surface pressure by 1.2-fold from 10 to 200 mM⁴.

Effect of exposed hydrophobicity (Q_H)

The adsorption behaviour of the different globular proteins shows clear differences (i.e. $d\Pi/dt = 0.005$ and 0.245 mN m⁻¹ s⁻¹ and $\Pi_{\text{final}} = 5$ and 17.4 mN m⁻¹ for lysozyme and β -lactoglobulin, respectively) (figure 3G). The initial adsorption rate and final surface pressure of β -lactoglobulin have previously been described to be higher than for lysozyme¹⁹ and ovalbumin³⁰. This was attributed to a reduction of the energy barrier for adsorption that results from an increase of exposed hydrophobicity^{2, 3}. This has also been described for ovalbumin³ and BSA³¹ variants with different exposed hydrophobicities. Hence, it was concluded that the adsorption kinetics increase with increasing relative exposed hydrophobicity.

Effect of protein radius and exposed hydrophobicity (R_p and Q_H)

The initial adsorption rate and the final surface pressure increase with protein radius and relative exposed hydrophobicity (i.e. $d\Pi/dt = 0.004$ and 0.07 mN m⁻¹ s⁻¹ and $\Pi_{\text{final}} = 5.0$ and 18.3 mN m⁻¹ for Lys₀ and Lys₉₀, respectively) (figure 3H). Based on the protein radius, the adsorption rate was expected to decrease. As a consequence, the observed increase of $d\Pi/dt$ is attributed to an increase of the relative exposed hydrophobicity.

Summarizing, while the interactions between the adsorbed proteins are not affected by the conditions (i.e. C , I , Q_H and R), an increase of concentration, ionic strength and especially relative exposed hydrophobicity resulted in an increase of $d\Pi/dt$ and Π_{final} (i.e. k_{adsorb}). Hence, k_{adsorb} can be expressed as a function of these parameters (equation 14).

$$k_{adsorb} \propto Q_H I \quad (14)$$

As, for the systems under the conditions investigated, the relative exposed hydrophobicity is the main parameter influencing the adsorption rate, k_{adsorb} can be approximated by Q_H . It must, however, be noted that there is also an interaction between these parameters. For example, fast adsorbing proteins (i.e. high hydrophobicity) are less affected by changes in ionic strength than slow adsorbing proteins. Currently, this interaction is not sufficiently understood to allow a quantitative description as was obtained for the adsorbed amount. This has for instance been shown in the case of succinylated β -lactoglobulin at different ionic strengths⁵.

Conclusion

Based on the results, it is concluded that the adsorption behaviour of protein can be understood from the protein charge, relative exposed hydrophobicity and radius. The E_d - Π curves of the different proteins and the different conditions (i.e. C and I) superimpose, showing that the interactions between the adsorbed proteins are similar and the adsorbed proteins retain their native state. The adsorption rate (k_{adsorb}) of different proteins at one pH can be described by $k_{adsorb} \propto Q_H I$. The maximum adsorbed amount (Γ_{max}) of proteins at the interface can be theoretically predicted assuming a completely covered monolayer ($\Gamma_{mono, theory}$): $\Gamma_{mono, theory} = 10^3 M_w \theta_{\infty} / \pi R_{eff}^2 N_a$ with a saturation coverage (θ_{∞}) of 0.547 according to $R_{eff} = R_p - \frac{1}{2} \ln(U_{driving} / 2\pi\epsilon_0\epsilon_r R_p \Psi_0^2) \kappa^{-1}$ and the random sequential adsorption (RSA) model.

References

1. Wierenga, P. A.; Gruppen, H., New views on foams from protein solutions. *Curr. Opin. Colloid Interface Sci.* **2010**, 15, (5), 365-373.
2. Damodaran, S.; Song, K. B., Kinetics of adsorption of proteins at interfaces: role of protein conformation in diffusional adsorption. *Biochim. Biophys. Acta, Protein Struct. Mol. Enzymol.* **1988**, 954, 253-264.
3. Wierenga, P. A.; Meinders, M. B. J.; Egmond, M. R.; Voragen, A. G. J.; de Jongh, H. H. J., Protein exposed hydrophobicity reduces the kinetic barrier for adsorption of ovalbumin to the air-water interface. *Langmuir* **2003**, 19, (21), 8964-8970.
4. Wierenga, P. A.; Meinders, M. B. J.; Egmond, M. R.; Voragen, A. G. J.; De Jongh, H. H. J., Quantitative description of the relation between protein net charge and protein adsorption to air-water interfaces. *J. Phys. Chem. B* **2005**, 109, (35), 16946-16952.
5. Song, K. B.; Damodaran, S., Influence of electrostatic forces on the adsorption of succinylated β -lactoglobulin at the air-water interface. *Langmuir* **1991**, 7, (11), 2737-2742.
6. MacRitchie, F.; Alexander, A. E., Kinetics of adsorption of proteins at interfaces. Part III. The role of electrical barriers in adsorption. *J. Colloid Sci.* **1963**, 18, (5), 464-469.
7. Talbot, J.; Tarjus, G.; Van Tassel, P. R.; Viot, P., From car parking to protein adsorption: an overview of sequential adsorption processes. *Colloids Surf., A* **2000**, 165, (1-3), 287-324.

8. Creusot, N.; Wierenga, P. A.; Laus, M. C.; Giuseppin, M. L. F.; Gruppen, H., Rheological properties of patatin gels compared with β -lactoglobulin, ovalbumin, and glycinin. *J. Sci. Food Agric.* **2011**, *91*, (2), 253-261.
9. Broersen, K.; Elshof, M.; De Groot, J.; Voragen, A. G. J.; Hamer, R. J.; De Jongh, H. H. J., Aggregation of β -lactoglobulin regulated by glycosylation. *J. Agric. Food Chem.* **2007**, *55*, (6), 2431-2437.
10. Alizadeh-Pasdar, N.; Li-Chan, E. C. Y., Comparison of protein surface hydrophobicity measured at various pH values using three different fluorescent probes. *J. Agric. Food Chem.* **2000**, *48*, (2), 328-334.
11. Jachimska, B.; Wasilewska, M.; Adamczyk, Z., Characterization of globular protein solutions by dynamic light scattering, electrophoretic mobility, and viscosity measurements. *Langmuir* **2008**, *24*, (13), 6866-6872.
12. De Feijter, J. A.; Benjamins, J.; Veer, F. A., Ellipsometry as a tool to study the adsorption behavior of synthetic and biopolymers at the air-water interface. *Biopolymers* **1978**, *17*, (7), 1759-1772.
13. Ball, V.; Ramsden, J. J., Buffer dependence of refractive index increments of protein solutions. *Biopolymers* **1998**, *46*, (7), 489-492.
14. Maranzano, B. J.; Wagner, N. J., The effects of interparticle interactions and particle size on reversible shear thickening: hard-sphere colloidal dispersions. *J. Rheo.* **2001**, *45*, (5), 1205-1222.
15. Erickson, H. P., Size and shape of protein molecules at the nanometer level determined by sedimentation, gel filtration, and electron microscopy. *Biol. Proced. Online* **2009**, *11*, (1), 32-51.
16. Israelachvili, J. N., *Intermolecular and surface forces*. Third ed.; Academic Press: New York, NY, USA, 2011.
17. Walstra, P., *Physical chemistry of foods*. Marcel Dekker, Inc.: New York, NY, USA, 2003.
18. Blank, M.; Lee, B. B.; Britten, J. S., Adsorption kinetics of ovalbumin monolayers. *J. Colloid Interface Sci.* **1975**, *50*, (2), 215-222.
19. Lad, M. D.; Birembaut, F.; Matthew, J. M.; Frazier, R. A.; Green, R. J., The adsorbed conformation of globular proteins at the air/water interface. *Phys. Chem. Chem. Phys.* **2006**, *8*, (18), 2179-2186.
20. Verheul, M.; Pedersen, J. S.; Roefs, S. P. F. M.; de Kruif, K. G., Association behavior of native β -lactoglobulin. *Biopolymers* **1999**, *49*, (1), 11-20.
21. Pezennec, S.; Gauthier, F.; Alonso, C.; Graner, F.; Croguennec, T.; Brulé, G.; Renault, A., The protein net electric charge determines the surface rheological properties of ovalbumin adsorbed at the air-water interface. *Food Hydrocolloids* **2000**, *14*, (5), 463-472.
22. Ward, A. F. H.; Tordai, L., Time-dependence of boundary tensions of solutions I. The role of diffusion in time-effects. *J. Chem. Phys.* **1946**, *14*, (7), 453-461.
23. Dickinson, E., Adsorbed protein layers at fluid interfaces: interactions, structure and surface rheology. *Colloids Surf., B* **1999**, *15*, (2), 161-176.
24. De Feijter, J. A.; Benjamins, J., Adsorption kinetics of proteins at the air-water interface. In *Food emulsions and foams*, Dickinson, E., Ed. Woodhead publishing: Cambridge, England 1987; pp 72-85.
25. McClellan, S. J.; Franses, E. I., Effect of concentration and denaturation on adsorption and surface tension of bovine serum albumin. *Colloids Surf., B* **2003**, *28*, (1), 63-75.
26. Noskov, B. A., Protein conformational transitions at the liquid-gas interface as studied by dilational surface rheology. *Adv. Colloid Interface Sci.* **2014**, *206*, 222-238.
27. Graham, D. E.; Phillips, M. C., Proteins at liquid interfaces: I. kinetics of adsorption and surface denaturation. *J. Colloid Interface Sci.* **1979**, *70*, (3), 403-414.
28. Tripp, B. C.; Magda, J. J.; Andrade, J. D., Adsorption of globular proteins at the air/water interface as measured via dynamic surface tension: concentration dependence, mass-transfer considerations, and adsorption kinetics. *J. Colloid Interface Sci.* **1995**, *173*, (1), 16-27.

29. MacRitchie, F.; Alexander, A. E., Kinetics of adsorption of proteins at interfaces. Part I. The role of bulk diffusion in adsorption. *J. Colloid Sci.* **1963**, 18, (5), 453-457.
30. Wierenga, P. A.; Egmond, M. R.; Voragen, A. G. J.; de Jongh, H. H. J., The adsorption and unfolding kinetics determines the folding state of proteins at the air-water interface and thereby the equation of state. *J. Colloid Interface Sci.* **2006**, 299, (2), 850-857.
31. Cho, D.; Narsimhan, G.; Franses, E. I., Adsorption dynamics of native and alkylated derivatives of bovine serum albumin at air-water interfaces. *J. Colloid Interface Sci.* **1996**, 178, (1), 348-357.

Chapter 7

Quantitative description of the parameters resulting in stability of protein-stabilized emulsions

Abstract

Recently, the stability of protein-stabilized emulsions was proposed to be dominated by excess proteins in the continuous phase, rather than by inter-droplet interactions. In other words, for a given condition (e.g. pH) and protein, there is a minimal or critical protein concentration (C_{cr}) above which the emulsion is stable. Consequently, a prediction of C_{cr} , based on the protein molecular properties and system conditions, enables the prediction of emulsion stability. To achieve this, the effect of protein concentration, ionic strength and exposed hydrophobicity on the C_{cr} are determined in this study. The main parameters affecting the C_{cr} were the adsorbed amount, and the adsorption rate. The adsorbed amount was predicted from the protein radius, surface charge and ionic strength according to a recently developed model (chapter 6). The adsorption rate, which depends on the protein charge and exposed hydrophobicity, was in this case approximated by the relative exposed hydrophobicity (Q_H). The obtained model showed good correspondence with the experimental data, but was furthermore shown to be applicable to describe data obtained from literature. Hence, the surface coverage model can be applied to predict emulsion stability.

Introduction

The (de-)stabilization of protein-stabilized emulsions is often attributed to colloidal interactions between emulsion droplets (i.e. electrostatic and van der Waals interactions)¹⁻³. In this colloidal model, only the properties of the adsorbed layer are considered, since they are the basis of the colloidal interactions between emulsion droplets. In contrast to this model, recent experiments have shown that under similar conditions (i.e. ionic strength), the stability of an emulsion against flocculation depends on the presence of excess proteins in the continuous phase (chapters 3 and 5). This stabilizing effect is postulated to be caused by adsorption of proteins when the maximum adsorbed amount (Γ_{\max}) at the interface increases due to a decrease of the electrostatic repulsion. Therefore, it will be referred to as the surface coverage model. According to this model, there is a critical protein concentration (C_{cr}), above which an emulsion at given conditions will be stable due to the presence of excess proteins. This study aims to identify how C_{cr} depends on the molecular properties of the protein and the system conditions (e.g. ionic strength), and to provide a model to predict the value of C_{cr} .

A critical concentration has also been described in the formation of emulsions, where two distinct concentration regimes are observed^{4, 5}. At low protein concentrations, the droplet size decreases with increasing concentration (referred to as protein-poor regime). In this regime, stabilization of smaller droplets is limited by the protein concentration in the continuous phase. The maximum adsorbed amount (Γ_{\max}) in this regime corresponds closely to that of a monolayer⁵⁻⁷. The droplet size ($d_{3,2}$) in the protein-poor regime (regime I) is then the minimal droplet size where all the surface area can be covered (sufficiently) with protein. This minimal droplet size is therefore affected by the volume fraction oil (Φ_{oil}) and maximum adsorbed amount (Γ_{\max}), in addition to the protein concentration (C). Consequently, if the droplet size, calculated from equation 1⁴, is plotted against the protein concentration, different curves are obtained depending on Φ_{oil} and Γ_{\max} (figure 1A).

At high concentrations (protein-rich regime; regime II) the droplet size becomes concentration independent ($d_{3,2} = d_{3,2, \text{min}}$) (equation 2). In this regime, there is sufficient protein to stabilize smaller droplets, but the minimum droplet size is determined by the power input, interfacial tension and mass density of the continuous phase⁸.

$$d_{3,2(I)} \approx \frac{6\Phi_{\text{oil}}\Gamma_{\max}}{(1-\Phi_{\text{oil}})C} \quad (1)$$

$$d_{3,2(II)} = d_{3,2, \text{min}} \quad (2)$$

where Φ_{oil} is the volume fraction oil [-], Γ_{\max} is the maximum adsorbed amount [mg m^{-2}] and C is the protein concentration [g L^{-1}].

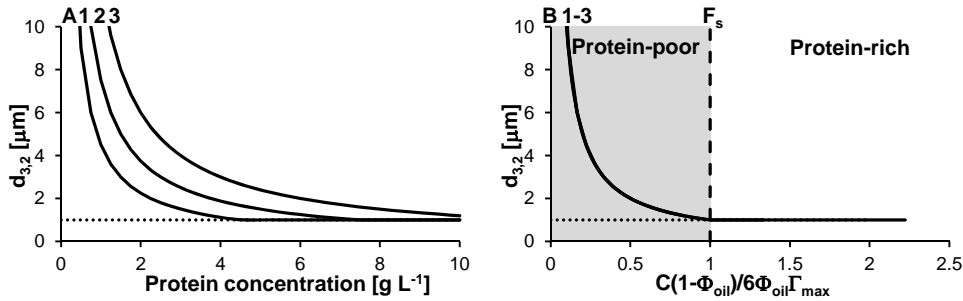


Figure 1. Average droplet size ($d_{3,2}$) as function of protein concentration (A) and as function of $C(1-\Phi_{oil})/6\Phi_{oil}\Gamma_{max}$ (B) calculated from equation 1 with a $d_{3,2, \min}$ of $1 \mu\text{m}$ (equation 2) for emulsions with $\Phi_{oil} = 0.2$ and $\Gamma_{max} = 3 \text{ mg m}^{-2}$ (1), $\Phi_{oil} = 0.2$ and $\Gamma_{max} = 5 \text{ mg m}^{-2}$ (2) and $\Phi_{oil} = 0.4$ and $\Gamma_{max} = 3 \text{ mg m}^{-2}$ (3). The dotted lines in A and B represent $d_{3,2, \min}$ and the grey area in B represents the protein-poor regime.

By correcting for the C , Φ_{oil} and Γ_{max} , all curves superimpose onto a single curve (figure 1B). In this curve one point (F_s) is identified, where all curves transition from the protein-poor to the protein-rich regime. Since this point, or stability factor (F_s), includes terms for the volume fraction oil and Γ_{max} , the value of C_{cr} can in principle be determined. However, in addition to these parameters (i.e. C , Φ_{oil} and Γ_{max}), the exposed hydrophobicity (Q_H) has recently been suggested to affect the transition between the protein-poor and protein-rich regime, and thereby C_{cr} (chapter 5). This is due to the fact that an increase in exposed hydrophobicity decreases the barrier for adsorption to the air-water interface, resulting in a higher adsorption rate⁹(chapter 6). The maximum adsorbed amount at the air-water and the oil-water interface has, on the other hand, been described to be independent of the exposed hydrophobicity of the protein (chapters 3 and 6)⁹. Hence, a higher adsorption rate translates into faster monolayer coverage. This helps to prevent coalescence during homogenization, and is expected to result in the formation of smaller droplets under similar conditions. Hence, the critical concentration to reach the protein-rich regime decreases with increasing exposed hydrophobicity. As this effect of exposed hydrophobicity is related to an increase of the adsorption rate (k_{adsorb}), it is proposed that equation 1 for the protein-poor regime can be rewritten as equation 3.

$$d_{3,2(I)} \approx \frac{6\Phi_{oil}\Gamma_{max}}{(1-\Phi_{oil})Ck_{adsorb}} \quad (3)$$

To verify whether the behaviour of a protein-stabilized emulsion can indeed be described by equation 3, the effect and contribution of C , Γ_{max} and k_{adsorb} on emulsion stabilization was studied for different proteins at various ionic strengths.

Materials and methods

Materials

Lysozyme (Lys; L6876, Lot n° 051K7028; purity > 90 % based on size-exclusion chromatography), β -lactoglobulin (β -lg; L0130, Lot n° SLBC2933V; protein content of 99 % (N x 6.38), of which 94 % β -lactoglobulin based on SDS-PAGE) and ovalbumin (Ova; A5503 Lot n° 031M7008V; protein content of 98 % (N x 6.22), of which 92 % ovalbumin based on agarose gel electrophoresis) were purchased from Sigma-Aldrich (St. Louis, MO, USA). All other chemicals were of analytical grade and purchased from either Sigma-Aldrich or Merck (Darmstadt, Germany).

Emulsification

The protein solutions were mixed with 10 % (v/v) sunflower oil. A pre-emulsion was prepared using an Ultra turrax Type T-25B (IKA, Staufen, Germany) at 9500 rpm for 1 min. Subsequently, the pre-emulsion was passed 30 times through a Labhoscope 2.0 laboratory scale high-pressure homogenizer (Delta Instruments, Drachten, The Netherlands) operated at 15 MPa. The solutions were cooled on ice-water during homogenization. Four different sets of experiments were performed:

Effect of protein concentration β -Lactoglobulin was dissolved in 10 mM sodium phosphate buffer pH 7.0 at concentrations of 1, 2, 2.5, 3, 4, 5, 7.5 and 10 g L⁻¹.

Effect of ionic strength β -Lactoglobulin was dissolved in 10 mM sodium phosphate buffer pH 7.0 in the absence or presence of 20 and 190 mM NaCl at concentrations of 1, 2, 2.5, 3, 4, 5, 7.5 and 10 g L⁻¹. Moreover, the ionic strength of the β -lactoglobulin emulsions prepared in the absence of NaCl was adjusted to 30 and 200 mM with 2 M NaCl after emulsification.

Effect of exposed hydrophobicity β -Lactoglobulin, ovalbumin and lysozyme were dissolved in 10 mM sodium phosphate buffer pH 7.0 at concentrations of 1, 2, 2.5, 3, 4, 5, 7.5 and 10 g L⁻¹, 1, 2.5, 5, 7.5, 10, 15 and 20 g L⁻¹ and 2.5, 5, 10, 15, 20, 25 g L⁻¹, respectively.

Subsequently, the emulsions were stored for 24 hours at 20 °C prior to further analysis. For selected samples, it was confirmed that no significant changes occurred during this storage period.

Zeta potential of emulsion droplets

Zeta potentials of the emulsion droplets were determined with a Zetasizer Nano ZS (Malvern Instruments, Worcestershire, UK) using the laser Doppler velocimetry technique. The emulsions were diluted 500 times to prevent multiple scattering. The measurements

were performed at 25 °C and 40 Volt. The results of five sequential runs were averaged. Zeta potentials were calculated with Henry's equation¹⁰ (equation 4).

$$\zeta = \frac{3\eta\mu_e}{2\varepsilon F(\kappa a)} \quad (4)$$

in which ζ is the zeta potential [V], η is the viscosity [0.8872×10^{-3} Pa s], μ_e is the electrophoretic mobility [$\text{m}^2 \text{V}^{-1} \text{s}^{-1}$], ε is the dielectric constant of the medium [$7.08 \times 10^{-10} \text{C}^2 \text{J}^{-1} \text{m}^{-1}$] and $F(\kappa a)$ is Henry's function [-], which equals 1.5 using the Smoluchowski approximation¹⁰.

Determination of droplet size

Laser diffraction

The average droplet size of the emulsions was measured using laser light diffraction (Mastersizer 2000, Malvern Instruments) equipped with a Hydro SM sample dispersion unit. The volume-surface average diameter ($d_{3,2}$) (equation 5) was reported as an average of at least five runs.

$$d_{3,2} = \sum N_i d_i^3 / \sum N_i d_i^2 \quad (5)$$

in which N_i and d_i represent the number and diameter of droplets of size class i , respectively.

Diffusing wave spectroscopy (DWS)

As indication of the droplet size *in situ*, without dilution, DWS measurements were performed as described previously¹¹. The autocorrelation function was averaged from five sequential runs of 120 seconds. Subsequently, the autocorrelation functions were normalized by dividing the obtained $g_2(t)-1$ values by the maximum measured value. Normalized autocorrelation functions were then fitted using equation 6. This was derived from Ruis et al.¹¹, assuming that $\langle \Delta r^2(t) \rangle = 6Dt^p$ for $p < 1 = \alpha t^x$ for $x < 1$.

$$g_2(t) - 1 \approx (e^{-\langle \Delta r^2(t) \rangle})^2 \approx e^{-\alpha t^x} \quad (6)$$

The decay time ($\tau_{1/2}$), which is defined as the time at which $g_2(t)-1$ decayed to half of its initial value, was determined using the fitted equation. An increase of the decay time is related to decreased droplet mobility¹².

Theoretical prediction of the adsorbed amount of a close-packed monolayer

The adsorbed amount for a close-packed monolayer ($\Gamma_{\text{mono, theory}}$) was predicted using equation 7 (chapter 6). This prediction describes globular proteins as hard disks adsorbing at a two-dimensional interface according to the Random Sequential Adsorption (RSA) model. As a consequence, the saturation coverage at jamming limit (θ_∞) is approximated to be 0.547¹³.

$$\Gamma_{mono, theory} = \frac{10^3 M_w}{\pi R_{eff}^2 N_a} \theta_\infty \quad (7)$$

in which $\Gamma_{mono, theory}$ is the theoretical adsorbed amount of a monolayer [mg m^{-2}], M_w is the molecular mass of the protein [g mol^{-1}], R_{eff} is the effective radius of the protein [m], N_a is the Avogadro constant [$6.022 \times 10^{23} \text{ mol}^{-1}$] and θ_∞ is the saturation coverage, which has a value of 0.547 for non-diffusing particles¹³.

The effective radius of the charged particle (i.e. globular protein) can be estimated by the hard-sphere approximation as the sum of the protein radius (R_p) and a characteristic distance due to electrostatic repulsion¹⁴ (equation 8) (chapter 6). Assuming a constant surface charge, the effective radius (R_{eff}) can be described by equation 9 (chapter 6).

$$R_{eff} = R_p - \frac{1}{2} \ln \left(\frac{U_{driving}}{2\pi\epsilon_0\epsilon_r R_p \Psi_0^2} \right) \kappa^{-1} \quad (8)$$

$$R_{eff} = R_p - \frac{1}{2} \ln \left(\frac{x}{R_p} \right) \kappa^{-1} \quad (9)$$

where R_p is the protein radius [m], $U_{driving}$ is the adsorption driving interaction [J], ϵ_0 is the dielectric constant of a vacuum [$8.85 \times 10^{-12} \text{ C}^2 \text{ J}^{-1} \text{ m}^{-1}$], ϵ_r is the relative dielectric constant of the medium [80], Ψ_0 is the surface potential [V], κ^{-1} is the Debye screening length [m] and x is a constant [m]. The constant was found to be $1.77 \times 10^{-9} \text{ m}$ for β -lactoglobulin and ovalbumin and 0 m for lysozyme at pH 7.0 (chapter 6). The radius of a globular protein and the Debye screening length can be calculated using equations 10¹⁵ and 11¹⁶, respectively.

$$R_p = \left(\frac{3vM_w}{4\pi N_a} \right)^{\frac{1}{3}} \quad (10)$$

$$\kappa^{-1} = \sqrt{\frac{2N_a e^2 I}{\epsilon_0 \epsilon_r k_B T}} \quad (11)$$

in which v is the partial specific volume [$0.73 \times 10^{-6} \text{ m}^3 \text{ g}^{-1}$]¹⁵, e is the elementary charge [$1.602 \times 10^{-19} \text{ C}$], I is the ionic strength [mol m^{-3}], k_B is the Boltzmann constant [$1.38 \times 10^{-23} \text{ J K}^{-1}$] and T is the temperature [K].

Results and discussion

Colloidal model

Based on the simplified colloidal model (i.e. DLVO interactions), it is expected that flocculation of emulsion droplets with a similar radius would occur when the zeta potential of the emulsion droplets decreases below a certain critical value (i.e. decrease of the electrostatic repulsion). To verify this, flocculation of emulsions stabilized by

β -lactoglobulin at two concentrations was studied as a function of the ionic strength. The results show that at a low protein concentration (in this case 2 g L^{-1}), an increase of the ionic strength (i.e. decrease of zeta potential) destabilizes the emulsion, resulting in flocculation indicated by a longer decay time, determined by DWS (figure 2). At a higher protein concentration (in this case 5 g L^{-1}), on the other hand, a similar decrease of the zeta potential does not result in salt-induced flocculation. This shows that the protein concentration (i.e. surface coverage model) is of more importance for the stability of the emulsions than the electrostatic repulsion between droplets. This is in line with previous studies showing the importance of excess protein in the continuous phase for the stability against salt-induced flocculation (chapters 3 and 5). A similar behaviour was observed for emulsions prepared in the presence of NaCl and for emulsions of which the ionic strength was adjusted after emulsification. This shows the analogy between the emulsion formation and stability, and confirms that excess protein is important for both processes (as described by equation 3). In the case of emulsion formation, the destabilizing mechanism is expected to be coalescence, whereas flocculation destabilizes the pre-formed emulsions (in line with the observations in chapters 3 and 5, and the observations in literature¹⁷).

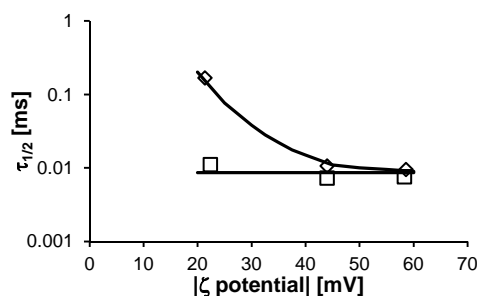


Figure 2. Decay time ($\tau_{1/2}$) as a function of the absolute zeta potential of the emulsion droplets stabilized by β -lactoglobulin at 2 (\diamond) and 5 g L^{-1} (\square) ($\text{pH} = 7.0$ and $\Phi_{\text{oil}} = 0.1$). The solid lines are guides to the eye.

Surface coverage model

The surface coverage model proposes that the stability of a protein-stabilized emulsion is based on excess protein. In this model, instability is thought to be caused by the fact that the maximum adsorbed amount under certain conditions (such as increased ionic strength) increases, thereby resulting in a transition from the protein-rich to the protein-poor regime. If sufficient protein is present in the continuous phase, and if it can adsorb quickly enough, the excess protein will adsorb and stabilize the emulsion.

Effect of adsorption rate (k_{adsorb})

To determine the effect of the adsorption rate (at a constant ionic strength (10 mM)), the decay time and average droplet size of emulsions stabilized by three different proteins

(lysozyme, ovalbumin and β -lactoglobulin) was determined. This shows that C_{cr} shifts from $\geq 25 \text{ g L}^{-1}$ for lysozyme to $\sim 10 \text{ g L}^{-1}$ for ovalbumin and 2 g L^{-1} for β -lactoglobulin (figure 3A). This difference is also reflected in the average droplet size ($d_{3,2}$) at 5 g L^{-1} which varies from $7.33 \mu\text{m}$ for lysozyme to 0.50 and $0.26 \mu\text{m}$ for ovalbumin and β -lactoglobulin, respectively (figure 3B).

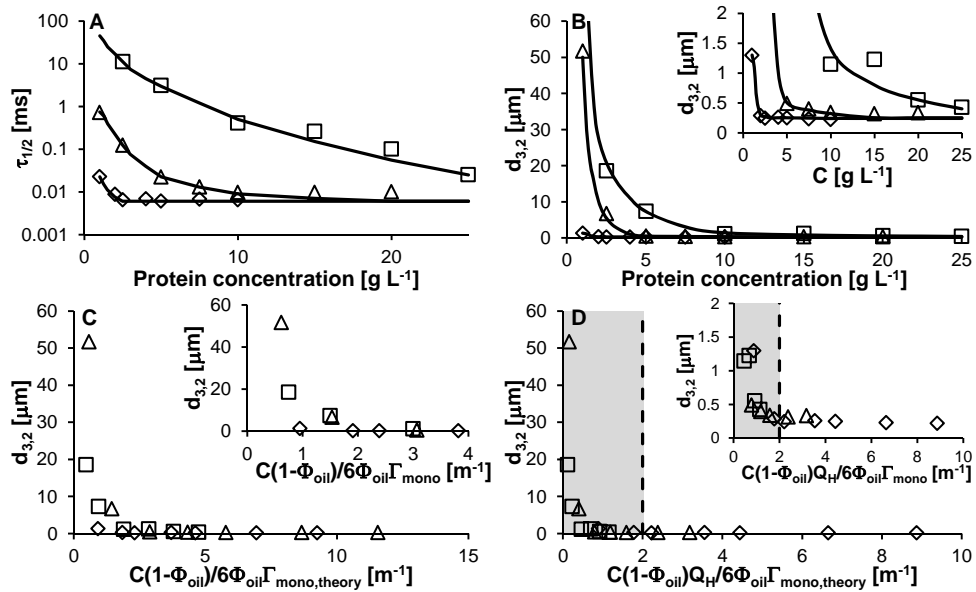


Figure 3. Decay time ($\tau_{1/2}$) (A) and average droplet size ($d_{3,2}$) (B) as function of protein concentration and average droplet size as function of $C(1-\Phi_{oil})/6\Phi_{oil}\Gamma_{max}$ (C) and as function of $C(1-\Phi_{oil})Q_H/6\Phi_{oil}\Gamma_{max}$ (D) for emulsions stabilized by β -lactoglobulin (\diamond), ovalbumin (\triangle) and lysozyme (\square) ($\text{pH} = 7.0$, $I = 10 \text{ mM}$ and $\Phi_{oil} = 0.1$). The grey area represents the protein-poor regime. The inserts show the small droplet size regime. Lines are guides to the eye.

Based on equation 1, the difference between the proteins can be explained by a shift of the maximum adsorbed amount (Γ_{max}). To test this, curves were plotted as described by equation 1, using Γ_{max} calculated assuming a full monolayer coverage ($\Gamma_{mono,theory}$) predicted by a model described previously (chapter 6) (table 1). After this correction, the curves of the different proteins do still not superimpose (figure 3C). This shows that the observed differences between the proteins cannot be explained only by the difference in adsorbed amount. The next step was to include the initial adsorption rate (k_{adsorb}) as described in equation 3. At a given concentration and ionic strength, the adsorption rate was described to increase with increasing relative exposed hydrophobicity (chapter 6)¹⁸. Therefore, the relative exposed hydrophobicity of the protein was used as an indication for k_{adsorb} (table 1). When corrected for Q_H , all curves superimpose (figure 3D). All emulsions above the

stability factor (F_s) of 2 are in the protein-rich regime. This confirms that the critical protein concentration is also affected by the initial adsorption rate (i.e. affinity of the protein towards adsorption to the interface).

Table 1. Protein properties obtained from literature.

Protein	M_w^a [kDa]	Q_H^b [-]	$\Gamma_{\text{mono,theory}}^b$ [mg m ⁻²]	ζ potential ^b [mV]
β -Lactoglobulin	18.3	1.00	1.62 ^c	-21.2
Ovalbumin	42.8	0.19	1.73	-16.5
Lysozyme	14.3	0.06	1.58	2.0

^avalues obtained from the Swiss-Prot database (<http://www.expasy.org>).

^bliterature values (chapter 6).

^c $\Gamma_{\text{mono,theory}}$ for a β -lactoglobulin dimer.

Effect of ionic strength

To determine the effect of ionic strength, the droplet size of emulsions stabilized by β -lactoglobulin at different ionic strengths (i.e. 10 and 200 mM) were determined. As expected, an increase of the ionic strength resulted in an increase of the average droplet size and decay time measured by static light scattering (SLS) and DWS, respectively (figures 4A and B). The increase of the droplet size is also reflected in a shift of the transition between the protein-poor and protein-rich regime from $\sim 2 \text{ g L}^{-1}$ at 10 mM to $\sim 2.5 \text{ g L}^{-1}$ at 200 mM. The effect of ionic strength is explained by an increase of the maximum adsorbed amount (Γ_{max}) with ionic strength as a result of a decrease of the effective radius (R_{eff}) (equation 9). This is confirmed by the fact that the curves superimpose when the data is corrected by $\Gamma_{\text{mono,theory}}$ according to equation 7 (figure 4C). As observed for the different proteins, F_s equals 2.

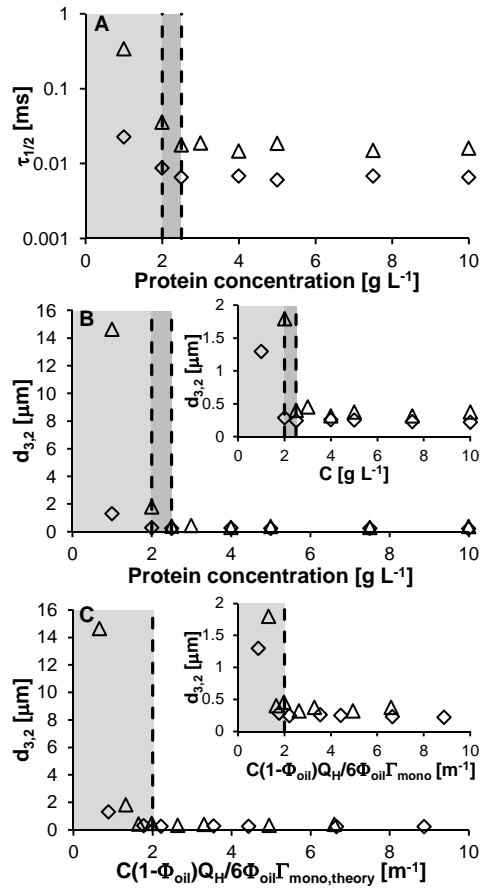


Figure 4. Concentration dependence of the decay time ($\tau_{1/2}$) (A), average droplet size ($d_{3,2}$) (B) and average droplet size as function of $C(1-\Phi_{oil})Q_H/6\Phi_{oil}\Gamma_{mono,theory}$ (C) for β -lactoglobulin-stabilized emulsions at an ionic strength of 10 mM (\diamond) and 200 mM (\triangle) (pH = 7.0 and $\Phi_{oil} = 0.1$). The grey areas in A and B represent the protein-poor regime at ionic strength of 10 (light grey) and 200 mM (dark grey). The grey area in C represents the protein-poor regime. The inserts show the small droplet size regime.

Verification of the surface coverage model

As described above, for different proteins and at different ionic strength, the graph of $d_{3,2}$ as a function of $C(1-\Phi_{oil})Q_H/6\Phi_{oil}\Gamma_{mono,theory}$ shows a point where the emulsions reach the stable regime ($d_{3,2} = d_{3,2,min}$) (i.e. $C_{cr} = 2$). This point is named the stability factor (F_s) and has a value of 2 for all experiments. This shows that equation 3 can be applied to predict the droplet size for the obtained experimental data, when the stability factor of 2 is included (equation 12).

$$d_{3,2} = \frac{F_s 6\Phi_{oil} \Gamma_{mono,theory}}{(1 - \Phi_{oil}) Q_H C} \quad (12)$$

To verify the proposed model for other proteins, concentrates and isolates at different conditions (e.g. ionic strength, Φ_{oil}), experimental data ($d_{3,2}$ as function of concentration) was collected from literature (chapter 3)¹⁹⁻²¹. Subsequently, the curves of the droplet size under these conditions were predicted using equations 2 and 12 assuming that Γ_{max} equals $\Gamma_{mono,theory}$ (equation 7) (chapter 6). In addition, a Q_H of 0.73 for patatin (chapter 3) and 1.00 for whey protein isolate and concentrate (i.e. equal to β -lactoglobulin) were used (figure 5).

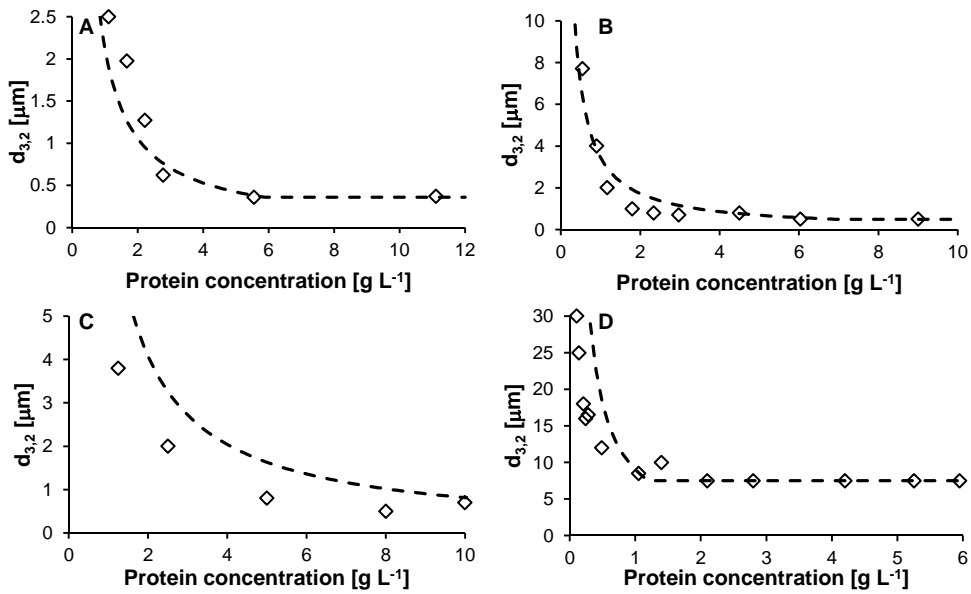


Figure 5. Average droplet size ($d_{3,2}$) for emulsions stabilized by β -lactoglobulin (pH = 7.0, I = 10 mM and $\Phi_{oil} = 0.1$) (chapter 3) (A), patatin (pH = 7.0, I = 50 mM and $\Phi_{oil} = 0.1$)¹⁹ (B), whey protein isolate (pH = 7.0, I = 10 mM and $\Phi_{oil} = 0.3$)²⁰ (C) and whey protein concentrate (pH = 7.0, I = 150 mM and $\Phi_{oil} = 0.28$)²¹ (D). The dashed lines represent the fit of the data using equations 2 and 3, with $k_{adsorb} = Q_H$.

The theoretical predictions of $d_{3,2}$ were in good agreement with the experimental results, confirming that validity of the proposed model.

Using this knowledge, the critical protein concentration (C_{cr}) that separates the protein-poor from the protein-rich regime can be calculated for any protein under any condition using equation 13, where so far k_{adsorb} will be approximated by Q_H .

$$C_{cr} = \frac{F_s 6\Phi_{oil} \Gamma_{mono,theory}}{(1 - \Phi_{oil}) Q_H d_{3,2,min}} \quad (13)$$

Conclusion

The stability of protein-stabilized emulsions depends on the amount of excess protein present in the continuous phase, rather than colloidal interactions between emulsion droplets. The border between the protein-poor to the protein-rich regime is described by the critical protein concentration (C_{cr}). Above C_{cr} , the excess protein stabilizes the emulsion. A surface coverage model was proposed and validated that allows the calculation of C_{cr} for different proteins at different system conditions (i.e. ionic strength and Φ_{oil}).

References

1. Dickinson, E., Flocculation of protein-stabilized oil-in-water emulsions. *Colloids Surf., B* **2010**, 81, (1), 130-140.
2. van Aken, G. A.; Blijdenstein, T. B. J.; Hotrum, N. E., Colloidal destabilisation mechanisms in protein-stabilised emulsions. *Curr. Opin. Colloid Interface Sci.* **2003**, 8, (4-5), 371-379.
3. Damodaran, S., Protein stabilization of emulsions and foams. *J. Food Sci.* **2005**, 70, (3), R54-R66.
4. Tcholakova, S.; Denkov, N. D.; Sidzhakova, D.; Ivanov, I. B.; Campbell, B., Interrelation between drop size and protein adsorption at various emulsification conditions. *Langmuir* **2003**, 19, (14), 5640-5649.
5. McClements, D. J., Protein-stabilized emulsions. *Curr. Opin. Colloid Interface Sci.* **2004**, 9, (5), 305-313.
6. Tcholakova, S.; Denkov, N. D.; Ivanov, I. B.; Campbell, B., Coalescence in β -lactoglobulin-stabilized emulsions: effects of protein adsorption and drop size. *Langmuir* **2002**, 18, (23), 8960-8971.
7. Gurkov, T. D.; Russev, S. C.; Danov, K. D.; Ivanov, I. B.; Campbell, B., Monolayers of globular proteins on the air/water interface: applicability of the Volmer equation of state. *Langmuir* **2003**, 19, (18), 7362-7369.
8. Walstra, P., *Physical chemistry of foods*. Marcel Dekker, Inc.: New York, NY, USA, 2003.
9. Wierenga, P. A.; Meinders, M. B. J.; Egmond, M. R.; Voragen, A. G. J.; de Jongh, H. H. J., Protein exposed hydrophobicity reduces the kinetic barrier for adsorption of ovalbumin to the air-water interface. *Langmuir* **2003**, 19, (21), 8964-8970.
10. Jachimaska, B.; Wasilewska, M.; Adamczyk, Z., Characterization of globular protein solutions by dynamic light scattering, electrophoretic mobility, and viscosity measurements. *Langmuir* **2008**, 24, (13), 6866-6872.
11. Ruis, H. G. M.; van Gruijthuisen, K.; Venema, P.; van der Linden, E., Transitions in structure in oil-in-water emulsions as studied by diffusing wave spectroscopy. *Langmuir* **2007**, 23, (3), 1007-1013.
12. Blijdenstein, T. B. J.; Hendriks, W. P. G.; van der Linden, E.; van Vliet, T.; van Aken, G. A., Control of strength and stability of emulsion gels by a combination of long- and short-range interactions. *Langmuir* **2003**, 19, (17), 6657-6663.
13. Talbot, J.; Tarjus, G.; Van Tassel, P. R.; Viot, P., From car parking to protein adsorption: an overview of sequential adsorption processes. *Colloids Surf., A* **2000**, 165, (1-3), 287-324.
14. Maranzano, B. J.; Wagner, N. J., The effects of interparticle interactions and particle size on reversible shear thickening: hard-sphere colloidal dispersions. *J. Rheo.* **2001**, 45, (5), 1205-1222.
15. Erickson, H. P., Size and shape of protein molecules at the nanometer level determined by sedimentation, gel filtration, and electron microscopy. *Biol. Proced. Online* **2009**, 11, (1), 32-51.

16. Israelachvili, J. N., *Intermolecular and surface forces*. Third ed.; Academic Press: New York, NY, USA, 2011.
17. Kim, H. J.; Decker, E. A.; McClements, D. J., Impact of protein surface denaturation on droplet flocculation in hexadecane oil-in-water emulsions stabilized by β -lactoglobulin. *J. Agric. Food Chem.* **2002**, 50, (24), 7131-7137.
18. Wierenga, P. A.; Egmond, M. R.; Voragen, A. G. J.; de Jongh, H. H. J., The adsorption and unfolding kinetics determines the folding state of proteins at the air-water interface and thereby the equation of state. *J. Colloid Interface Sci.* **2006**, 299, (2), 850-857.
19. van Koningsveld, G. A.; Walstra, P.; Voragen, A. G. J.; Kuijpers, I. J.; van Boekel, M. A. J. S.; Gruppen, H., Effects of protein composition and enzymatic activity on formation and properties of potato protein stabilized emulsions. *J. Agric. Food Chem.* **2006**, 54, (17), 6419-6427.
20. Schwenzfeier, A.; Helbig, A.; Wierenga, P. A.; Gruppen, H., Emulsion properties of algae soluble protein isolate from *Tetraselmis sp.* *Food Hydrocolloids* **2013**, 30, (1), 258-263.
21. Tcholakova, S.; Denkov, N. D.; Ivanov, I. B.; Campbell, B., Coalescence stability of emulsions containing globular milk proteins. *Adv. Colloid Interface Sci.* **2006**, 123-126, 259-293.

Chapter 8

General discussion

The work in this thesis was focussed at obtaining generic understanding of the role of protein molecular properties and system conditions on the occurrence of heat-induced aggregation and flocculation of protein-stabilized emulsions. While both systems have been studied widely in literature, there is little detailed information on how the stability/behaviour in both systems is related to the protein molecular properties and system conditions. This is in part due to the fact that most studies only described the behaviour of a single protein (mainly β -lactoglobulin). Hence, this thesis aims to identify the relation between the protein aggregation and flocculation and the molecular properties of the protein by comparing the aggregation and flocculation behaviour of different proteins. The first question which then arises is whether there is a relation between the properties of the proteins and their behaviour in solution or at the interface. A secondary aim is to identify similarities and differences between these two systems. One important question is whether both systems can indeed be described by protein-protein interactions, and whether similar properties affect both systems.

Understanding the relation between the aggregation and flocculation behaviour and the molecular properties of proteins will allow controlled modifications of the properties to obtain the desired behaviour/functionality. This generic view on the behaviour of proteins can then also be applied for the understanding of more complex systems (such as foods).

Role of protein-protein interactions on protein aggregation

The aggregation process of globular proteins is a two-step process. First, the proteins have to (partially) unfold. Then, the (partially) unfolded proteins can aggregate¹⁻³. Since the denaturation temperature (T_d) of the proteins varies, the question which arises is at which temperature the aggregation behaviour should be compared. One option is to study the behaviour of all proteins at a given temperature. This corresponds with an industrial process, such as pasteurization. This, however, results in variation in the degree of unfolding for the proteins. To control the degree of unfolding in this thesis, the aggregation is, therefore, studied at a temperature relative to the denaturation temperature (T_d). Differences in the aggregation kinetics can then be attributed to the aggregation of the (partially) unfolded protein (i.e. second step of the aggregation process).

The main conclusion, from the comparison of the aggregation behaviour of three different proteins (β -lactoglobulin, patatin and ovalbumin) (chapter 2), is that the aggregation rate and formation of aggregates for these proteins varies significantly. This is in contrast to descriptions in literature^{2,4,5}. Moreover, these differences cannot be understood by looking solely at basic molecular properties such as net surface charge and (exposed) hydrophobicity, thereby also rejecting the hypothesis that protein-protein interactions determine protein aggregation (chapter 1).

One of major observations is that the aggregation rate of β -lactoglobulin is an order of magnitude (i.e. 10 times) slower than that of ovalbumin and patatin. This is postulated to be caused by the fact that (partially) unfolded β -lactoglobulin is less prone to aggregation compared to the other two proteins. This can be rationalized by the fact that β -lactoglobulin has more disulphide bonds than the other two proteins. Hence, β -lactoglobulin only partially unfolds upon heating, whereas ovalbumin and patatin unfold more completely. The fact that β -lactoglobulin only unfolds partially is supported by the observation in literature that only the outer cysteine residue takes part in the aggregation process⁶. In case of complete unfolding all disulphide bonds are expected to interchange. Furthermore, the partially unfolding of bovine β -lactoglobulin used in our studies is also in line with the observations for porcine β -lactoglobulin, which also has two disulphide bonds, but no free cysteine residue. This protein is not prone for aggregation after unfolding⁷, which is attributed to partial unfolding. Consequently, less hydrophobic amino acid residues are exposed, eventually leading to less/slower aggregation. The completely unfolded proteins (i.e. ovalbumin and patatin) expose the internal hydrophobic residues which gives rise to hydrophobic interactions between the molecules. Apparently, the aggregation rate depends on the structural stability and the availability of interactions sites (i.e. free cysteines and exposed hydrophobic amino acid residues).

Besides the aggregation rate, the size of the formed aggregates also varied between the proteins. Ovalbumin was observed to form smaller aggregates than β -lactoglobulin and patatin under similar conditions (i.e. ionic strength and pH) and at an equal fraction aggregated protein (chapter 2). This is in contrast with the generic view that aggregate formation depends on an electrostatic barrier, as this would be similar for all proteins⁵. The observed differences are suggested to be due to the fact that ovalbumin forms more nuclei due to its faster aggregation rate. This is supported by the fact that the fraction aggregated protein at which the larger aggregates are formed is not affected by the conditions.

Although in literature charge and hydrophobicity are considered to be the main parameters influencing the aggregation rate, this study shows that this view has to be refined. The main issue which has to be taken into account is the fact that due to differences in structural stability different intermolecular interactions are important. The aggregation of β -lactoglobulin is dominated by its structural stability as a result of the disulphide bonds. Hence, the internal hydrophobic amino acids do not become (completely) exposed, which results in a lower contribution of hydrophobic interactions between the molecules. Ovalbumin and patatin which unfold more completely are thought to aggregate mainly by the formation of non-covalent interactions. By considering these differences in the aggregate formation between the proteins, the protein which forms the desired aggregates can be selected for a certain application (i.e. system condition).

Role of protein-protein interactions on emulsion flocculation

Similar as aggregation, the influence of conditions on emulsion formation and stability were qualitatively known at the start of the thesis. However, a coherent model with which the effects of protein molecular properties and system conditions could be explained was not available. Based on the results in this thesis, a model was defined that describes the formation and stability of protein-stabilised emulsions exactly in these terms. The main conclusion from this is that emulsion stabilization is dominated by excess protein rather than electrostatic interactions between the adsorbed protein layers (chapters 3, 5 and 7). This is caused by the fact that destabilization is caused by a not completely covered interface. The excess protein can adsorb, when changes in the system conditions (i.e. ionic strength and pH) result in an incompletely covered interface. As surface coverage is the main factor in the stabilization, it is referred to as the surface coverage model. The transition from a stable to an unstable emulsion can be predicted based on a critical protein concentration, which demarcates the transition from the protein-poor to the protein-rich regime (equation 1) (chapter 7).

$$C_{cr} = \frac{F_s 6\Phi_{oil}\Gamma_{mono,theory}}{(1-\Phi_{oil})k_{adsorb}d_{3,2,min}} \quad (1)$$

where C_{cr} is the critical protein concentration [g L^{-1}], F_s is the stability factor (i.e. 2) [s g^{-1}], Φ_{oil} is the volume fraction oil [-], $\Gamma_{mono,theory}$ is the theoretical adsorbed amount of a close-packed monolayer [mg m^{-2}], C is the protein concentration [g L^{-1}], k_{adsorb} is the adsorption rate [g s^{-1}] and $d_{3,2,min}$ is the minimal droplet size which depends on the system conditions [m].

It is important to note that the proteins in the continuous phase are considered to be in their native state. This is based on observations (chapter 3) that the observed stabilising effect of excess protein can be achieved by having higher protein concentrations during the homogenisation step, as well as by adding excess protein after emulsification. It has also previously been shown that homogenization of a protein solution (i.e. BSA in the absence of oil) does not induce structural changes in the proteins⁸. Moreover, additional measures have been taken to avoid excessive heating of the samples during homogenization.

The surface coverage model was verified for patatin, ovalbumin, lysozyme and β -lactoglobulin (including WPI and WPC) under different conditions (Φ_{oil} and $\Gamma_{mono,theory}$) assuming that k_{adsorb} can be approximated by the relative exposed hydrophobicity (Q_H) as also shown in figure 1A.

From the surface coverage model, it follows that the critical protein concentration is affected by system and mechanical properties such as Φ_{oil} and $d_{3,2,min}$ and the adsorbed

amount ($\Gamma_{\text{mono, theory}}$) and adsorption rate (k_{adsorb}), which are affected by the molecular properties of the protein.

Adsorbed amount ($\Gamma_{\text{mono, theory}}$)

A number of models have been proposed to describe the adsorption kinetics ($d\Gamma/dt$)⁹⁻¹¹. Despite the fact that the adsorbed amount at saturation is important for stabilization of emulsions, it cannot be easily derived from these models. Hence, a model was proposed (chapter 6) to predict the effect of system conditions and protein molecular properties on the adsorbed amount of a protein at saturation assuming a close-packed monolayer (equation 2).

$$\Gamma_{\text{mono, theory}} = \frac{10^3 M_w}{\pi R_{\text{eff}}^2 N_a} \theta_{\infty} \quad (2)$$

in which $\Gamma_{\text{mono, theory}}$ is the theoretical maximum adsorbed amount of a monolayer [mg m^{-2}], M_w is the molecular mass of the protein [g mol^{-1}], R_{eff} is the effective radius of a globular protein [m], N_a is the Avogadro constant [$6.022 \times 10^{23} \text{ mol}^{-1}$] and θ_{∞} is the saturation coverage [0.547]¹².

The theoretical values of the adsorbed amount are in agreement with the experimental adsorbed amount, but an extensive, quantitative validation of the parameters θ_{∞} and R_{eff} is still missing. The saturation coverage has been modelled by assuming proteins as hard disks. Using the random sequential adsorption (RSA) model and excluding diffusion of the proteins at the interface, this results in a saturation coverage at the jamming limit of 0.547 ¹². In case proteins can diffuse at the interface, the saturation coverage increases to 0.82 ¹³. As the likelihood for adsorption drastically decreases with increasing adsorbed amount¹⁴, the theoretical limit may indeed be close to 0.82 , whereas the experimental limit is probably lower. This is also supported by the fact that a saturation coverage of 0.547 could describe the experimental data (chapter 6). The effective radius has been described to be the sum of the protein radius and a contribution due to electrostatic repulsion¹⁵, but the contribution of the electrostatic repulsion has not been quantified. In chapter 6, the effective radius was described by equation 3.

$$R_{\text{eff}} = R_p - \frac{1}{2} \ln \left(\frac{U_{\text{driving}}}{2\pi\epsilon_0\epsilon_r R_p \Psi_0^2} \right) \kappa^{-1} \quad (3)$$

To further validate this equation, the effect of protein properties and system conditions on the effective radius of the protein could be determined. In addition, it would be of interest to determine the adsorbed amount at the oil-water interface in a direct way. In some studies, the adsorbed amount was estimated based on the protein concentration in the serum phase¹⁶. However, this method involves a number of steps that have been shown to affect

the measured value¹⁷. A more direct method, e.g. similar to ellipsometry used for air-water interfaces would be very interesting in this respect. However, at this moment no such techniques are available. Consequently, in this study the values obtained for the adsorbed amount at air-water interfaces are used as an indication for the adsorbed amount at oil-water interfaces. In both cases (i.e. air-water and oil-water), the adsorbed amount is expected to be determined by the size, charge and exposed hydrophobicity of the proteins. In addition, it has been mentioned that (partial) unfolding of proteins may occur upon adsorption. Since the experimental observations were described well by our calculations based on the adsorbed amount at air-water interfaces, it was concluded that the measurement of adsorbed amount at air-water interfaces is a good approximation of the values at the oil-water interface.

Eventually, the model can be applied to accurately predict the adsorbed amount of a globular proteins based on a single measurement of the radius of the protein (which can also be theoretically approximated) and the surface charge of the protein (as indicated by the zeta potential) by dynamic light scattering.

Adsorption rate (k_{adsorb})

Although in general a static measurement of the adsorption rate (i.e. ADT) is considered to be not representative for adsorption under turbulent flow (i.e. homogenization), such measurements do contain useful information. When the mass transport to the interface is considered, the two regimes distinguished by the concentration of protein in the sub-surface layer as a function of time. In the diffusion regime, this concentrations at $t = 0$ is considered 0 (when all the present proteins were adsorbed at the interface) and will slowly reach the value of the bulk concentration. In the convective regime, it may be considered that the protein concentration in the sub-surface layer is more constant in time and close to the bulk concentration. However, in both cases, proteins from the sub-surface layer need to adsorb at the interface. If it is considered that there is an energy barrier, this barrier will affect the adsorption in both regimes¹⁸. If two proteins, one with a high and one with a low barrier for adsorption are compared, it is expected that the protein with the low barrier will adsorb faster during tensiometry (diffusion regime) as well as during homogenization (convective regime). This is exactly what is experimentally observed for the results of the surface pressure in time of lysozyme and β -lactoglobulin (figure 3G, page 108) and those of the droplet size of these proteins as a function of concentration (figures 3A and B, page 120) (i.e. stabilization of droplets). If the energy barrier to adsorption would be negligible in the convection regime, one would expect a negligible difference between the droplet size obtained with these two proteins (i.e. the adsorption rate which is derived from the surface pressure in time would have been irrelevant). The observations, however, show a larger droplet size for the slow adsorbing protein (lysozyme) compared to that of the fast

adsorbing protein (i.e. β -lactoglobulin). Hence, we are of the opinion that the adsorption rate of the protein, measured by a diffusion based process, provides useful information on the ability of proteins to stabilize the oil-water interface (also in a convection process such as homogenization).

For succinylated patatin variants (chapter 5) and the different proteins (i.e. lysozyme, ovalbumin and β -lactoglobulin) (chapter 7), an increased hydrophobicity was shown to increase the rate of adsorption, and thereby the efficiency of emulsification. Therefore, it is of interest to also develop an equation to predict the rate of adsorption. The adsorption rate is described to depend on an energy barrier¹⁹. This energy barrier is affected by the protein charge (Ψ_0)^{20, 21}, the relative exposed hydrophobicity (Q_H)^{22, 23} and ionic strength (I)²¹. Qualitatively, the relation between these parameters and the adsorption rate can be described by equation 4.

$$k_{adsorb} \propto \frac{CQ_H I}{\Psi_0} \quad (4)$$

An increase of the adsorption rate enables more protein molecules to adsorb before droplets coalesce. It is, therefore, an indication of the efficiency of the protein to stabilize the interface. A quantitative description of the effect of these parameters on the adsorption rate (k_{adsorb}) would enable a more accurate description of the system and the efficiency of different proteins. Although the relevant parameters that determine the rate of adsorption were identified, the exact relationship to calculate k_{adsorb} was not established. However, under the system conditions studied in this thesis (i.e. constant ionic strength and pH), k_{adsorb} could be approximated by a term for the relative exposed hydrophobicity.

pH close to the iso-electric point

While comparing the model to experimental data, it was observed that data obtained around the pI of the protein could not be described by the surface coverage model (figure 1B). Based on equation 1, this is explained by the fact that the adsorbed amount around the iso-electric point is expected to increase. Unfortunately, no experimental data is available on the adsorbed amount around the pI. According to equation 2, a close-packed monolayer with a saturation coverage (θ_∞) of 0.82 and an effective radius equal to the radius of β -lactoglobulin would result in a maximum adsorbed amount of $\pm 3.25 \text{ mg m}^{-2}$. This increase from 1.62 mg m^{-2} for β -lactoglobulin ($\theta_\infty = 0.547$, $R_{eff} \neq R_p$) to 3.25 mg m^{-2} can, however, not explain the differences in figure 1B. Hence, the observation close to the pI cannot be explained by the formation of a close-packed monolayer the proteins. Consequently, the formation of a multilayer is expected with an adsorbed amount significantly larger than $\Gamma_{mono, theory}$. Multilayer formation has also been described for thin films of BSA at pH 5.7 (pI = 5.4)²⁴. As the repulsive interaction between the proteins is absent, proteins may ‘aggregate’ at the interface, similar as the observation of protein

aggregation in the continuous phase around the pI. Hence, the interface may act as a ‘black hole’ with an adsorbed amount approaching infinity. However, as an adsorbed layer of three close-packed monolayers results in a good agreement of the literature data and the expectations (figure 1C), the adsorbed amount is not expected to exceed ten times value of $\Gamma_{\text{mono, theory}}$. Nevertheless, this limits the applicability of protein-stabilized emulsions around the pI of the protein.

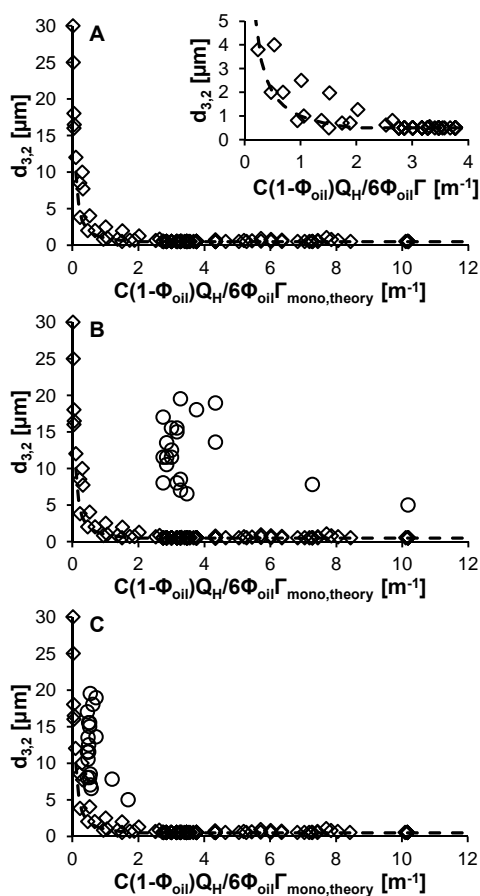


Figure 1. Master curve of the average droplet size ($d_{3,2}$) as function of $C(1-\Phi_{\text{oil}})Q_H/6\Phi_{\text{oil}}\Gamma_{\text{mono, theory}}$ for emulsions (A) at a pH away from the pI (\diamond), (B) as A and at a pH \approx pI (\circ) and (C) as B with correction of adsorbed amount to account for the formation of multilayers at the pI. The dashed lines in A-C represent the fit according to the surface coverage model (chapter 7). The data is a combination of the emulsions of chapters 3 and 7 and data reported in literature²⁵⁻³³.

These limitations to protein-stabilized emulsions around the pI were shown to be prevented by the glycation of the protein with a trisaccharide or larger (chapter 4). For stabilization at

increased ionic strength, the minimum theoretical degree of polymerization of the oligosaccharides was postulated to be 8. This stabilizing effect is attributed to the addition of a repulsive steric interaction. Hence, steric stabilization is concluded to be an effective method to stabilize emulsions under conditions where the non-modified protein cannot stabilize the emulsions efficiently. Steric stabilization can also originate from non-covalently bound carbohydrates or other polymer³⁴⁻³⁶. In the case of glycation, smaller carbohydrates may be preferred over larger polysaccharides as the glycation speed of smaller carbohydrates is higher than that of large ones. Since oligosaccharides are already sufficiently long to obtain steric stabilization, the use of longer polysaccharides seems redundant.

Proteins at the interface

Two discussions related to (globular) proteins at the (oil-water) interface are a recurring topic of discussion, namely the protein structure at the interface^{37, 38} and the fact whether excess protein adsorbs to form multilayers or that they do not adsorb and are therefore present in the continuous phase^{24, 39}. The results of this thesis yielded new insights on these topics which will be discussed below.

Protein structure

The stabilization of emulsions by the different proteins (β -lactoglobulin, patatin, ovalbumin and lysozyme) could be explained with the surface coverage model assuming a close-packed monolayer. This model does not include the conformation of the protein at the interface, although this is thought to influence the adsorbed amount. That the model still described the experimental data may be explained in two ways: (1) proteins do not unfold at the interface or (2) proteins do (partially) unfold at the interface, thereby not influencing the protein radius. While several approaches have been used in literature to measure the protein unfolding experimentally, these data seem to be insufficient to provide a final proof. Nevertheless, the results of this thesis indicate that proteins do not extensively unfold to a train-loop conformation at the interface as has been proposed in literature⁴⁰.

Multilayer formation

Based on the fact that the surface coverage model assuming monolayer coverage can be applied to describe the stability of an emulsion away from the pI (chapter 7), it is concluded that multilayers are not of important for emulsion stability. Whether the excess proteins adsorb to form multilayers or that these proteins are present in the bulk as non-adsorbed proteins becomes therefore irrelevant. Moreover, in contrast to the descriptions in literature^{24, 39}, even when multilayers are formed (such as around the pI), these multilayers do not stabilize the emulsion droplets (figure 1C).

Comparing protein aggregation and emulsion flocculation

The emulsion behaviour was described based on system conditions and molecular properties. It was surprising that these effects were due to the adsorption properties and saturation of adsorbed layers, rather than the interactions between the adsorbed protein layers on emulsion droplets. For the aggregation behaviour, it is at this moment not yet possible to come to a coherent model that describes the aggregation properties of the proteins based on their properties. Hence, it can still not be concluded whether both systems can be described by similar molecular properties. Interestingly there seems to be a correspondence between the qualitative size obtained for heat-induced aggregates and emulsion droplet flocs in the protein-poor regime under different system conditions (figure 2).

	Solution	Interface	
		Protein-poor regime	Protein-rich regime
$pI \ll pH \gg pI$ and low I			
$pI \ll pH \gg pI$ and high I			
$pH = pI$ and any I			

Figure 2. Proposed effect of electrostatic repulsion on protein aggregation in solution and aggregation of adsorbed protein layers at the oil-water interface (i.e. emulsion flocculation).

This thesis shows the importance of a comparison between proteins for the understanding of their behaviour. This understanding can then be applied to control the behaviour by modification of the proteins.

References

1. Lumry, R.; Eyring, H., Conformation changes of proteins. *J. Phys. Chem.* **1954**, 58, (2), 110-120.
2. Jahn, T. R.; Radford, S. E., Folding versus aggregation: polypeptide conformations on competing pathways. *Arch. Biochem. Biophys.* **2008**, 469, (1), 100-117.
3. Broersen, K.; Elshof, M.; De Groot, J.; Voragen, A. G. J.; Hamer, R. J.; De Jongh, H. H. J., Aggregation of β -lactoglobulin regulated by glycosylation. *J. Agric. Food Chem.* **2007**, 55, (6), 2431-2437.
4. Dobson, C. M., Protein folding and misfolding. *Nature* **2003**, 426, (6968), 884-890.
5. Nicolai, T.; Durand, D., Protein aggregation and gel formation studied with scattering methods and computer simulations. *Curr. Opin. Colloid Interface Sci.* **2007**, 12, (1), 23-28.
6. Visschers, R. W.; de Jongh, H. H. J., Disulphide bond formation in food protein aggregation and gelation. *Biotechnol. Adv.* **2005**, 23, (1), 75-80.
7. Burova, T. V.; Grinberg, N. V.; Visschers, R. W.; Grinberg, V. Y.; de Kruif, C. G., Thermodynamic stability of porcine β -lactoglobulin. *Eur. J. Biochem.* **2002**, 269, (16), 3958-3968.
8. Casterlain, C.; Genot, C., Conformational changes of bovine serum albumin upon its adsorption in dodecane-in-water emulsions as revealed by front-face steady-state fluorescence. *Biochim. Biophys. Acta, Gen. Subj.* **1994**, 1199, (1), 59-64.
9. Ward, A. F. H.; Tordai, L., Time-dependence of boundary tensions of solutions I. The role of diffusion in time-effects. *J. Chem. Phys.* **1946**, 14, (7), 453-461.
10. Guzman, R. Z.; Carbonell, R. G.; Kilpatrick, P. K., The adsorption of proteins to gas-liquid interfaces. *J. Colloid Interface Sci.* **1986**, 114, (2), 536-547.
11. Kotsmar, C.; Pradines, V.; Alahverdjiyeva, V. S.; Aksenenko, E. V.; Fainerman, V. B.; Kovalchuk, V. I.; Krägel, J.; Leser, M. E.; Noskov, B. A.; Müller, R., Thermodynamics, adsorption kinetics and rheology of mixed protein-surfactant interfacial layers. *Adv. Colloid Interface Sci.* **2009**, 150, (1), 41-54.
12. Talbot, J.; Tarjus, G.; Van Tassel, P. R.; Viot, P., From car parking to protein adsorption: an overview of sequential adsorption processes. *Colloids Surf., A* **2000**, 165, (1-3), 287-324.
13. Dickinson, E., Adsorbed protein layers at fluid interfaces: interactions, structure and surface rheology. *Colloids Surf., B* **1999**, 15, (2), 161-176.
14. Schaaf, P.; Talbot, J., Surface exclusion effects in adsorption processes. *J. Chem. Phys.* **1989**, 91, (7), 4401-4409.
15. Maranzano, B. J.; Wagner, N. J., The effects of interparticle interactions and particle size on reversible shear thickening: hard-sphere colloidal dispersions. *J. Rheo.* **2001**, 45, (5), 1205-1222.
16. Dickinson, E.; Matsumura, Y., Time-dependent polymerization of β -lactoglobulin through disulphide bonds at the oil-water interface in emulsions. *Int. J. Biol. Macromol.* **1991**, 13, (1), 26-30.
17. Tcholakova, S.; Denkov, N. D.; Sidzhakova, D.; Ivanov, I. B.; Campbell, B., Interrelation between drop size and protein adsorption at various emulsification conditions. *Langmuir* **2003**, 19, (14), 5640-5649.
18. Guzman, R. Z.; Carbonell, R. G.; Kilpatrick, P. K., The adsorption of proteins to gas-liquid interfaces. *J. Colloid Interface Sci.* **1986**, 114, (2), 536-547.
19. Wierenga, P. A.; Gruppen, H., New views on foams from protein solutions. *Curr. Opin. Colloid Interface Sci.* **2010**, 15, (5), 365-373.

20. Wierenga, P. A.; Meinders, M. B. J.; Egmond, M. R.; Voragen, A. G. J.; De Jongh, H. H. J., Quantitative description of the relation between protein net charge and protein adsorption to air-water interfaces. *J. Phys. Chem. B* **2005**, 109, (35), 16946-16952.
21. Song, K. B.; Damodaran, S., Influence of electrostatic forces on the adsorption of succinylated β -lactoglobulin at the air-water interface. *Langmuir* **1991**, 7, (11), 2737-2742.
22. Wierenga, P. A.; Meinders, M. B. J.; Egmond, M. R.; Voragen, A. G. J.; de Jongh, H. H. J., Protein exposed hydrophobicity reduces the kinetic barrier for adsorption of ovalbumin to the air-water interface. *Langmuir* **2003**, 19, (21), 8964-8970.
23. Damodaran, S.; Song, K. B., Kinetics of adsorption of proteins at interfaces: role of protein conformation in diffusional adsorption. *Biochim. Biophys. Acta, Protein Struct. Mol. Enzymol.* **1988**, 954, 253-264.
24. Dimitrova, T. D.; Leal-Calderon, F.; Gurkov, T. D.; Campbell, B., Disjoining pressure vs thickness isotherms of thin emulsion films stabilized by proteins. *Langmuir* **2001**, 17, (26), 8069-8077.
25. Hunt, J. A.; Dagleish, D. G., Heat stability of oil-in-water emulsions containing milk proteins: effect of ionic strength and pH. *J. Food Sci.* **1995**, 60, (5), 1120-1123.
26. Kulmyrzaev, A. A.; Schubert, H., Influence of KCl on the physicochemical properties of whey protein stabilized emulsions. *Food Hydrocolloids* **2004**, 18, (1), 13-19.
27. Schwenzfeier, A.; Helbig, A.; Wierenga, P. A.; Gruppen, H., Emulsion properties of algae soluble protein isolate from *Tetraselmis* sp. *Food Hydrocolloids* **2013**, 30, (1), 258-263.
28. Tcholakova, S.; Denkov, N. D.; Ivanov, I. B.; Campbell, B., Coalescence stability of emulsions containing globular milk proteins. *Adv. Colloid Interface Sci.* **2006**, 123-126, 259-293.
29. Gu, Y. S.; Decker, E. A.; McClements, D. J., Influence of pH and κ -carrageenan concentration on physicochemical properties and stability of β -lactoglobulin-stabilized oil-in-water emulsions. *J. Agric. Food Chem.* **2004**, 52, (11), 3626-3632.
30. Sarkar, A.; Goh, K. K. T.; Singh, H., Properties of oil-in-water emulsions stabilized by β -lactoglobulin in simulated gastric fluid as influenced by ionic strength and presence of mucin. *Food Hydrocolloids* **2010**, 24, (5), 534-541.
31. Gu, Y. S.; Decker, E. A.; McClements, D. J., Production and characterization of oil-in-water emulsions containing droplets stabilized by multilayer membranes consisting of β -lactoglobulin, κ -carrageenan and gelatin. *Langmuir* **2005**, 21, (13), 5752-5760.
32. van Koningsveld, G. A.; Walstra, P.; Voragen, A. G. J.; Kuijpers, I. J.; van Boekel, M. A. J. S.; Gruppen, H., Effects of protein composition and enzymatic activity on formation and properties of potato protein stabilized emulsions. *J. Agric. Food Chem.* **2006**, 54, (17), 6419-6427.
33. Guzey, D.; Kim, H. J.; McClements, D. J., Factors influencing the production of o/w emulsions stabilized by β -lactoglobulin-pectin membranes. *Food Hydrocolloids* **2004**, 18, (6), 967-975.
34. Dickinson, E., Mixed biopolymers at interfaces: competitive adsorption and multilayer structures. *Food Hydrocolloids* **2011**, 25, (8), 1966-1983.
35. Wooster, T. J.; Augustin, M. A., The emulsion flocculation stability of protein-carbohydrate diblock copolymers. *J. Colloid Interface Sci.* **2007**, 313, (2), 665-675.
36. Evans, M.; Ratcliffe, I.; Williams, P. A., Emulsion stabilisation using polysaccharide-protein complexes. *Curr. Opin. Colloid Interface Sci.* **2013**, 18, (4), 272-282.
37. Zhai, J.; Miles, A. J.; Pattenden, L. K.; Lee, T.-H.; Augustin, M. A.; Wallace, B. A.; Aguilar, M.-I.; Wooster, T. J., Changes in β -lactoglobulin conformation at the oil/water interface of emulsions studied by synchrotron radiation circular dichroism spectroscopy. *Biomacromolecules* **2010**, 11, (8), 2136-2142.
38. Freer, E. M.; Yim, K. S.; Fuller, G. G.; Radke, C. J., Shear and dilatational relaxation mechanisms of globular and flexible proteins at the hexadecane/water interface. *Langmuir* **2004**, 20, (23), 10159-10167.

39. Tcholakova, S.; Denkov, N. D.; Ivanov, I. B.; Campbell, B., Coalescence in β -lactoglobulin-stabilized emulsions: effects of protein adsorption and drop size. *Langmuir* **2002**, 18, (23), 8960-8971.
40. Damodaran, S., Protein stabilization of emulsions and foams. *J. Food Sci.* **2005**, 70, (3), R54-R66.

Summary

The aggregation of single proteins and flocculation of protein stabilized emulsions have often been related to colloidal interactions between the proteins or the adsorbed protein layers. Hence, these systems were expected to behave in a similar manner for all globular proteins.

Chapter 1 provides an overview of the different system conditions which are described to influence the aggregation and flocculation behaviour. As most studies were conducted with a single protein, information about the relation between molecular properties and the behaviour was still missing. Therefore, the aim of this thesis was to determine the main molecular properties determining the aggregation and flocculation behaviour of globular proteins. A secondary aim was to correlate the behaviour of proteins in solution with that of adsorbed protein layers at the interface.

To determine the main molecular properties affecting the aggregation behaviour, different proteins were studied under various system conditions (i.e. pH, ionic strength, temperature and concentration) (**chapter 2**). The main properties could, however, not be determined as a result of the complexity of the aggregation process. Consequently, the behaviour of one protein can only partly be extrapolated to that of another protein. Nevertheless, it was postulated that the aggregation rate was strongly influenced by the extent of unfolding (i.e. related to the structural stability of the protein). The formation of aggregates was shown to relate to the aggregation rate and the energy barrier for aggregate growth. With decreasing electrostatic repulsion, the aggregates of all proteins became larger and/or denser.

The flocculation behaviour of protein-stabilized emulsions is, similar as the aggregation behaviour, studied by comparing the behaviour of different proteins under various system conditions (**chapter 3**). This showed the importance of the protein exposed hydrophobicity as the extent of salt-induced flocculation decreased with increasing relative exposed hydrophobicity (Q_H). Furthermore, the addition of excess protein strongly increased the stability against salt-induced flocculation, which is not described by the colloidal interactions in the DLVO theory. Hence, it can be concluded that, in contrast to the general opinion of colloidal interactions, the flocculation behaviour of protein-stabilized emulsions cannot be explained based on electrostatic interactions.

Steric stabilization has been proposed to prevent emulsion flocculation. **Chapter 4** describes the effect of glycation on the flocculation behaviour of protein-stabilized emulsion. As steric interactions depend on the size of the molecule, the stabilizing effect was thought to be affected by the size of the carbohydrate moiety. Therefore, the stability of emulsions stabilized by patatin glycated with different mono- and oligosaccharides were compared. This showed that minimum length of a carbohydrate moiety to provide stability against pH-induced flocculation was a trisaccharide ($M_w > 500$ Da).

Besides glycation, the effect of succinylation on the flocculation behaviour was studied (**chapter 5**). This showed that succinylation resulted in (partial) unfolding of the secondary structure of patatin. The consequent increase of the Q_H resulted in an increase of the emulsion stability against salt-induced flocculation, as was also observed in **chapter 3**. This stabilizing effect was shown to be due to an increased affinity of the protein towards adsorption to the interface (i.e. increased adsorption rate). This results in a shift of the emulsion towards the protein-rich regime. This shows the importance of the adsorption behaviour on the emulsion stability.

As the adsorption behaviour was shown to be important for the emulsion stability, the effect of the molecular properties and system conditions on the adsorption rate and adsorbed amount at saturation was studied (**chapter 6**). This showed that the adsorption rate (k_{adsorb}) scales with the Q_H and ionic strength. Moreover, the adsorbed amount was shown to be dependent on the protein charge and the ionic strength. Based on these results, a model is proposed to predict the maximum adsorbed amount (Γ_{max}). The model approximates the maximum adsorbed amount as a close-packed monolayer using a hard-sphere approximation with an effective protein radius which depends on the electrostatic repulsion.

In **chapter 7**, an alternative for the colloidal model (i.e. emulsion stability is affected by colloidal interactions) was proposed. This model is based on the fact that emulsion stability depends on the coverage of the emulsion droplet, therefore referred to as the surface coverage model. The main parameters affecting the C_{cr} , which demarcates a stable from an unstable system, were the adsorbed amount and the adsorption rate as described by:

$$C_{\text{cr}} = \frac{F_s 6\Phi_{\text{oil}} \Gamma_{\text{mono,theory}}}{(1 - \Phi_{\text{oil}}) Q_H d_{3,2,\text{min}}} \quad (1)$$

The adsorbed amount was predicted with the model described in **chapter 6**. The adsorption rate was in this case approximated by Q_H . The model for the prediction of the critical protein concentration showed good correspondence with the experimental data, and was furthermore shown to be applicable to describe data obtained from literature. Hence, the surface coverage model can be applied to predict emulsion stability.

In **chapter 8**, the insights from the previous chapters are discussed in the light of commonly accepted views. In addition, the limitations of the proposed models are defined. These limitations can be used as indication for future research to extend the knowledge on the flocculation behaviour.

Summary

Samenvatting

Aggregatie van een eiwit en flocculatie van eiwit gestabiliseerde emulsies zijn vaak beschreven in relatie tot colloïdale interacties tussen de eiwitten of geadsorbeerde eiwitlagen. Dientengevolge werd verondersteld dat deze systemen zich voor alle globulaire eiwitten vergelijkbaar zouden gedragen.

Hoofdstuk 1 geeft een overzicht van de verschillende systeemcondities waarvan beschreven is dat ze invloed hebben op het aggregatie- en flocculatiegedrag van eiwitten. Omdat de meeste studies in literatuur zijn uitgevoerd met een enkel eiwit miste de informatie over hoe de moleculaire eigenschappen relateren aan het gedrag. Daarom was het doel van dit proefschrift om te bepalen welke moleculaire eigenschappen het belangrijkste waren voor het aggregatie- en flocculatiegedrag van globulaire eiwitten. Een secundair doel was om het gedrag van eiwit in oplossing te relateren aan dat van geadsorbeerde eiwitlagen aan het grensvlak.

Om te bepalen welke moleculaire eigenschappen het belangrijkste waren voor het aggregatiegedrag, werden verschillende eiwitten onder verschillende systeemcondities (i.e. pH, zoutsterkte, temperatuur en concentratie) bestudeerd (**hoofdstuk 2**). De belangrijkste eigenschappen konden door de complexiteit van het aggregatieproces echter niet worden geïdentificeerd. Daarom werd geconcludeerd dat het gedrag van een eiwit niet zomaar kan worden geëxtrapoleerd naar dat van een ander eiwit. Desondanks is het gesuggereerd dat de aggregatiesnelheid sterk beïnvloed wordt door de mate van ontvouwing (i.e. gerelateerd is aan eiwitstabiliteit). Verder, is aangetoond dat de vorming van aggregaten relateert aan de aggregatiesnelheid en de energie barrière voor aggregaat groei. Een afname van de elektrostatische afstoting resulteert in grotere en/of compactere aggregaten voor alle eiwitten.

Het flocculatiegedrag van eiwit gestabiliseerde emulsies is, net als het aggregatiegedrag, bestudeerd door het gedrag van verschillende eiwitten onder verschillende systeemcondities te vergelijken (**hoofdstuk 3**). Het belang van de hydrophobiciteit van het eiwit (Q_H) werd aangetoond door het feit dat een toename van de hydrophobiciteit de zout-geïnduceerde flocculatie verminderde. Daarnaast zorgde de toevoeging van een overmaat aan eiwit voor een forse toename van de stabiliteit tegen zout-geïnduceerde flocculatie. Volgens de DLVO theorie beïnvloedt de concentratie de colloïdale interacties echter niet. Daarom werd geconcludeerd dat het flocculatiegedrag van eiwit gestabiliseerde emulsies, in tegenstelling tot de algemene opinie op basis van colloïdale interacties, kan niet worden verklaard op basis van elektrostatische interacties.

Sterische stabilisatie is voorgesteld als een methode om emulsieflocculatie tegen te gaan. **Hoofdstuk 4** beschrijft het effect van glycatie op het flocculatiegedrag van eiwit gestabiliseerde emulsies. Omdat sterische interacties afhangen van de molecuulgrootte

werd verwacht dat de grootte van de suikergroep invloed had op het stabiliserende effect. Daarom werd de stabiliteit van emulsies vergeleken die werden gestabiliseerd door patatine geglyceerd met verschillende mono- en oligosachariden. Hiermee werd aangetoond dat een trisacharide ($M_w > 500$ Da) de minimulengte is van een suikergroep die kan zorgen voor stabiliteit tegen pH-geïnduceerde flocculatie.

Naast glycatie werd ook het effect van succinylatie op het flocculatiegedrag bestudeerd (**hoofdstuk 5**). Dit toonde aan dat succinylatie resulteerde in (gedeeltelijke) ontvouwing van de secundaire structuur van patatine. De daaruit voortvloeiende toename van Q_H resulteerde in een toename van de emulsiestabiliteit tegen zout-geïnduceerde flocculatie. Dit komt overeen met de observaties in **hoofdstuk 3**. Dit stabiliserende effect is toegewezen aan een toename van de affiniteit van het eiwit om te adsorberen aan het grensvlak (i.e. toegenomen adsorptiesnelheid). Dit resulteert in een verschuiving van de emulsies richting het eiwitrijke regime. Dit toont het belang van het adsorptiegedrag op emulsiestabiliteit aan.

Aangezien het adsorptiegedrag van belang bleek voor de emulsiestabiliteit, is het effect van moleculaire eigenschappen en systeemcondities op de adsorptiesnelheid en geadsorbeerde hoeveelheid bij verzadiging van het oppervlak bestudeerd (**hoofdstuk 6**). Dit liet zien dat de adsorptiesnelheid (k_{adsorb}) schaalte met Q_H en zoutsterkte. Daarnaast liet de geadsorbeerde hoeveelheid een verband zien met de eiwitlading en zoutsterkte. Op basis van deze resultaten werd een model voorgesteld om de maximale geadsorbeerde hoeveelheid (Γ_{max}) te voorspellen. Het model benadert Γ_{max} als een dicht gepakte monolaag gebruik makend van de aanname dat eiwitten zich gedragen als een harde bolletje met een effectieve straal die afhangt van de elektrostatiche afstoting.

In **hoofdstuk 7**, wordt een alternatief voor het colloïdale model (i.e. de emulsiestabiliteit hangt af van colloïdale interacties) geboden. Dit model is gebaseerd op het feit dat emulsiestabiliteit afhangt van de bedekkingsgraad van een emulsiedruppel. Daarom wordt dit aangeduid als grensvlakbedekkingsmodel. Hiermee kan voor elk eiwit een kritische concentratie eiwit (C_{cr}) worden berekend, die de grens vormt tussen een stabiel van een onstabiel systeem. De waarde wordt voornamelijk beïnvloed door de geadsorbeerde hoeveelheid en de adsorptiesnelheid zoals beschreven in:

$$C_{cr} = \frac{F_s 6\Phi_{oil}\Gamma_{mono,theory}}{(1 - \Phi_{oil})Q_H d_{3,2,min}} \quad (1)$$

De geadsorbeerde hoeveelheid werd voorspeld met het in **hoofdstuk 6** beschreven model. De adsorptiesnelheid werd in dit geval benaderd door Q_H . Het model om de kritische eiwitconcentratie te voorspellen beschreef de experimentele data goed en kon daarnaast ook worden gebruikt om literatuurdata te beschrijven. De conclusie was daarom dat het

Samenvatting

grensvlakbedekkingsmodel kan worden toegepast voor het voorspellen van de emulsiestabiliteit.

In **hoofdstuk 8**, werden de inzichten verkregen in de voorgaande hoofdstukken bediscussieerd in het licht van algemeen aangenomen denkbeelden. Daarnaast werden de limitaties van de voorgestelde modellen gedefiniëerd. Deze limitaties kunnen een bron vormen voor toekomstig onderzoek om de kennis over het flocculatiegedrag uit te breiden.

Acknowledgements

Acknowledgements

Mensen die me kennen weten dat het sociale aspect rondom het werk belangrijk voor mij is. Daarom wil ik iedereen in mijn omgeving bedanken, en sommigen in het bijzonder.

Henk, zonder jouw ‘zetje’ was ik op dit moment waarschijnlijk (nog) niet in de positie geweest waarin ik nu ben. Jouw vertrouwen (ondanks de ‘high-risk, high-potential’ stempel) heeft er mede voor gezorgd dat ik voldoende vertrouwen in mezelf kreeg om me op dit project storten.

Maar een PhD verkrijg je niet in je eentje, daarom wil ik Peter bedanken voor alle discussies, gerelateerd of niet gerelateerd aan hetgene waar ik mee bezig was. Meermaals hebben je verfrissende ideeën geleid tot nieuwe plannen, inzichten of gewoonweg meer discussies. Wat dit betreft zitten we volledig op een lijn en ik vind dat we samen een goed team vormden. Harry, ondanks je altijd kritische noot denk ik dat iedereen uiteindelijk wel moet toegeven dat je opmerkingen vaak terecht waren. Dank je voor alle tijd die je hebt geïnvesteerd om de puntjes op de i te zetten.

Marco en Neleke, jullie industriële kijk op het geheel heeft ervoor gezorgd dat het niet een puur fundamenteel onderzoek is geworden. Het linken van eiwiteigenschappen aan het functionele gedrag heeft geleid tot een aantal verrassende inzichten.

De belangrijkste persoon is vaak de persoon die je niet zo opmerkt: Jolanda. Ondanks de vele vragen (ook van mij) blijf je altijd vriendelijk en vrolijk en ben je tussendoor ook in voor een babbeltje, natuurlijk met de klassiekers van Arrow of Veronica rock radio op de achtergrond.

Daarnaast wil ik Paul Venema en Harry Baptist van Fysica en Fysische Chemie van Levensmiddelen, Renko de Vries en Remko Fokkink van Fysische Chemie en Kolloïdkunde, Adrie Westphal van Biochemie en Jos Sewalt van Levensmiddelenproceskunde ook graag bedanken voor het meedenken over de problemen die ik tegenkwam en voor de ondersteuning bij het wegnemen van bepaalde hordes.

Arthur en Manuel, bedankt voor jullie bijdrage aan en enthousiasme voor het aardappel(eiwit)onderzoek. Onderbewust hebben de soms opmerkelijke uitkomsten van jullie afstudeervakken mijn gedachten en ideeën over emulsies sterk beïnvloed.

Of course I would like to thank all colleagues from Food Chemistry for all the coffee breaks, trips and other activities. I always really enjoyed to be around the lab/office. Thanks again! Special thanks to all the roomies from the Biotechnion and the ‘new place’. Exchanging ideas, fighting together to finish our (first) papers and growing plants together. I always had a good time, and enjoyed my time in the offices. Lab mates from our spacious lab in the Biotechnion or the cosy one in the ‘new place’, thanks for the small chats and discussions about one of our strange/unexpected observations. And of course thanks for accepting me as I am (singing or whistling along with the music from the radio).

Thank you protein colleagues for the nice time, discussions and drinks we had together. Special thanks to Frederik and Surrender for brainstorming about possible causes and actions to come to new ideas and plans for even more Friday afternoon experiments. Claire, thanks for all the help during completion of the thesis, your expertise helped me a lot.

Marijntje, ik waardeer het heel erg dat jij mijn paranimf wilt zijn op deze, voor mij, bijzondere dag. Met jou als lab- en later als kantoorgenootje heb ik altijd veel plezier beleefd. En als ik weer eens een wrak was, kon ik mijn frustratie/gedachten altijd bij jou kwijt. Dank je voor de fijne tijd!

Surrender, thank you for being my paranimf! I really appreciate that you always had or otherwise made time for your colleague who again passed by with yet another question. And of course all our discussions about proteins or completely other things. But more importantly, just the fun and relax time outside work. Thanks a lot!

Danny, Martijn en alle andere ski- en klimmaatjes. Bedankt voor alle mooie, eenzame tochten die we samen hebben ondernomen. De bergen hebben een speciale plaats in al onze harten. Ik kan nu al niet wachten op ons volgende trip!

Mam, pap, Robbie en Harry. Ze zeggen wel eens dat het leven een mens maakt. Ondanks dat niet alle momenten altijd even gemakkelijk waren en dat we over sommige dingen van mening verschillen zou ik het zonder jullie steun nooit zo ver hebben kunnen schoppen. Ik waardeer het altijd heel erg als we samen zijn. Dank!

Roy

Acknowledgements

About the author

Curriculum vitae

Roy Jozef Bernard Marie Delahaije was born on March 7th, 1986 in Heerlen, The Netherlands. After finishing secondary school (Sint-Janscollege, Hoensbroek) in 2004, he started his study Food Technology at Wageningen University. His BSc degree was completed with a thesis project on the fractionation of okra pectin after enzyme treatment at the Laboratory of Food Chemistry. His MSc degree in Food Technology, with a specialisation in Product Functionality, was completed with a thesis on the synthesis and characterization of oligosaccharide fatty acid esters at the Laboratory of Physics and Physical Chemistry of Foods, followed by an internship at Givaudan Schweiz AG, Dübendorf, Switzerland on the enthalpy relaxation of carbohydrate matrices for flavour encapsulation.



After graduating in 2009, he started the presented PhD thesis work. During his PhD work, he also worked on a six month research project at the Laboratory of Food Chemistry in collaboration with Danone on distinguishing whey protein structures. Currently, he is working on a Post-doc project to elaborate on the work presented in this thesis.

List of publications

Kool, M.M.; Schols, H.A.; **Delahaije, R.J.B.M.**; Sworn, G.; Wierenga, P.A.; Gruppen, H. The influence of the primary and secondary xanthan structure on the enzymatic hydrolysis of the xanthan backbone. *Carbohydr. Polym.* **2013**, 97, (2), 368-375.

Delahaije, R.J.B.M.; Wierenga, P.A.; van Nieuwenhuijzen, N.H.; Giuseppin, M.L.F.; Gruppen, H. Protein concentration and protein-exposed hydrophobicity as dominant parameters determining flocculation of protein-stabilized oil-in-water emulsions. *Langmuir* **2013**, 29, (37), 11567-11574.

Delahaije, R.J.B.M.; Gruppen, H.; van Nieuwenhuijzen, N.H.; Giuseppin, M.L.F.; Wierenga, P.A. Effect of glycation on the flocculation behavior of protein-stabilized oil-in-water emulsions. *Langmuir* **2013**, 29, (49), 15201-15208.

Delahaije, R.J.B.M.; Wierenga, P.A.; Giuseppin, M.L.F.; Gruppen, H. Improved emulsion stability by succinylation of patatin is caused by partial unfolding rather than charge effects. *J. Colloid Interface Sci.* **2014**, 430, 69-77.

Delahaije, R.J.B.M.; Wierenga, P.A.; Giuseppin, M.L.F.; Gruppen, H. Comparison of heat-induced aggregation of globular proteins. *Submitted for publication.*

Delahaije, R.J.B.M.; Gruppen, H.; Giuseppin, M.L.F.; Wierenga, P.A. Quantitative description of the parameters affecting the adsorption behaviour of globular proteins. *Submitted for publication.*

Delahaije, R.J.B.M.; Gruppen, H.; Giuseppin, M.L.F.; Wierenga, P.A. Quantitative description of the parameters resulting in stability of protein-stabilized emulsions. *To be submitted for publication.*

Overview of completed training activities

Discipline specific activities

Courses

Advanced Food Analysis (VLAG), Wageningen, The Netherlands, 2010[†]

Industrial Food Proteins (VLAG), Wageningen, The Netherlands, 2013[†]

Conferences

ECIS (Max Planck Institute of Colloids and Interfaces), Berlin, Germany, 2011[†]

Food Colloids (University of Copenhagen), Copenhagen, Denmark, 2012[†]

BRM day (FOM/DPI), Utrecht, The Netherlands, 2013

Gums and stabilizers for the food industry (Food Hydrocolloid Trust), Wrexham, UK, 2013[†]

General courses

VLAG PhD introduction week (VLAG), 2010

Scientific writing (WGS), 2011

Interpersonal communication for PhD students (WGS), 2012

Mobilising your –scientific- network (WGS), 2013

Career orientation (WGS), 2013

Additional activities

Preparation PhD project proposal

PhD trip Food Chemistry to Switzerland and Italy, 2010[‡]

PhD trip Food Chemistry to Singapore and Malaysia, 2012[‡]

BSc and MSc thesis presentations, 2009-2014

PhD presentations Food Chemistry 2009-2014

[†] Poster; [‡] Poster and oral presentation; VLAG: Graduate School for Nutrition, Food Technology, Agrobiotechnology and Health Sciences; WGS: Wageningen Graduate Schools

This study was carried out at the Laboratory of Food Chemistry of Wageningen University, the Netherlands and financially supported by AVEBE, Veendam, the Netherlands.

This thesis was printed by Gildeprint drukkerijen, Enschede, The Netherlands.

Edition: 300 copies.

Cover design: Roy Delahaije.

Roy J.B.M. Delahaije, 2014.